

For Reference

NOT TO BE TAKEN FROM THIS ROOM

Ex LIBRIS
UNIVERSITATIS
ALBERTAENSIS





Digitized by the Internet Archive
in 2023 with funding from
University of Alberta Library

<https://archive.org/details/McGinnis1972>

THE UNIVERSITY OF ALBERTA

MULTIVARIABLE CONTROL OF A BINARY DISTILLATION COLUMN

BY



R. GLENN MCGINNIS

A THESIS

SUBMITTED TO THE FACULTY OF GRADUATE STUDIES AND RESEARCH
IN PARTIAL FULFILMENT OF THE REQUIREMENTS FOR THE DEGREE
OF MASTER OF SCIENCE

DEPARTMENT OF CHEMICAL AND PETROLEUM ENGINEERING

EDMONTON, ALBERTA

FALL, 1972

UNIVERSITY OF ALBERTA

FACULTY OF GRADUATE STUDIES AND RESEARCH

The undersigned certify that they have read, and recommend to the Faculty of Graduate Studies and Research, for acceptance, a thesis entitled MULTIVARIABLE CONTROL OF A BINARY DISTILLATION COLUMN submitted by R. Glenn McGinnis, B.Eng., in partial fulfilment of the requirements for the degree of Master of Science.

ABSTRACT

This thesis is concerned with the development of a model of an eight tray distillation column and subsequent use of this model for simulation and experimental testing of a multivariable control system.

The first portion of this work is a literature survey of distillation modelling techniques and of distillation column control strategies. A description and a discussion of many of the more common assumptions used in modelling are presented. The models appearing in the technical literature are considered with special attention being given to the assumptions that have been utilized and application of the models to control studies. Many of the control strategies which appear in the technical literature are presented, compared and evaluated on the basis of the necessity of a model and also if any experimental verification exists.

The twentieth-order linear state space model of the pilot scale distillation column is derived by using the transient mass and energy balances about each stage in linear perturbation form. The changes in internal liquid flows are included as a first order function of time. The states in this model are the stage enthalpies and the liquid flows from each stage. Experimental evaluation indicates good agreement between the behavior of the model and the pilot scale equipment. Two model reduction techniques are presented and applied to the model to obtain a low order model for control studies. A fourth-order and a second-order model are obtained and the latter is selected for the control application.

Multiloop control studies indicate that the selected product control loops exhibit interactive effects, and so a multivariable control

approach is applicable. The second-order model, with the states being the product enthalpies is used to derive a multivariable control law. It is found that measurement noise and time delays in the bottoms composition measurement from the gas chromatograph system cause instability in the bottom enthalpy control loop. Simulation studies on an adjusted feedback and a feedback-feedforward control system indicate moderately good controlled behavior, with the bottoms composition exhibiting sustained oscillations. Subsequent experimental runs verify the applicability of the control schemes and the results predicted by the simulation studies.

ACKNOWLEDGEMENTS

The author is greatly indebted to his thesis supervisor, Dr. R. K. Wood for his guidance and assistance in this project.

Grateful acknowledgement is due to the staff of the Data Acquisition, Control, and Simulation Centre in the Department of Chemical and Petroleum Engineering for their assistance and the use of their computing facilities.

The author also acknowledges his fellow graduate students for their aid and advice during the completion of this study.

Financial support was generously given by the National Research Council.

Finally, the author expresses great appreciation for the support and encouragement of his wife, Mary.

TABLE OF CONTENTS

	Page
CHAPTER I INTRODUCTION	1
CHAPTER II LITERATURE SURVEY	3
2.1 Introduction	3
2.2 Survey of Distillation Modelling Techniques	3
2.3 Survey of Model Reduction Techniques	10
2.4 Survey of Distillation Column Control Methods	11
CHAPTER III MODEL DEVELOPMENT	16
3.1 Introduction	16
3.2 Tray Model	17
3.3 Condenser Model	21
3.4 Reboiler Model	21
3.5 Matrix-Vector Representation	24
3.6 Enthalpy Linearization	25
3.7 Liquid Flow Dynamics	27
3.8 Augmented State Space Model	29
3.9 Disturbance-Control Vector	30
CHAPTER IV MODEL EVALUATION	32
4.1 Introduction	32
4.2 Solution to the State Equation	32
4.3 Experimental Studies	40
4.3-1 Experimental Equipment	40
4.3-2 Open-loop Tests	41
4.4 Comparison of Simulated and Experimental Results	42
4.4-1 Feed Flow Disturbances	45
4.4-2 Reflux Flow Disturbances	49
4.4-3 Steam Flow Disturbances	49

TABLE OF CONTENTS (continued)

	Page
CHAPTER V MODEL REDUCTION	55
5.1 Introduction	55
5.2 Marshall's Method	55
5.2-1 Reduction Theory	55
5.2-2 Reduction Results	58
5.3 Anderson's Method	62
5.3-1 Reduction Method	62
5.3-2 Reduction Results	65
5.4 Conclusions	66
CHAPTER VI CONTROL STUDIES	76
6.1 Introduction	76
6.2 Single Loop Control	77
6.2-1 Simulation Studies	77
6.2-2 Top Product Composition Control	81
6.2-3 Bottom Product Composition Control	87
6.3 Multiloop Control	90
6.3-1 Simulation Results	90
6.3-2 Experimental Results	90
6.4 Multivariable Control	94
6.4-1 Multivariable and Multiloop Control	94
6.4-2 Multivariable Control Laws	95
6.4-3 Simulation of Feedback Control Behaviour	96
6.4-4 Experimental Feedback Control Behaviour	107
6.4-5 Simulation of Feedback-Feedforward Control Behaviour	111

TABLE OF CONTENTS (continued)

	Page
6.4-6 Experimental Feedback-Feedforward Control Behaviour	113
6.5 Comparison with Previous Control Studies	113
CHAPTER VII DISCUSSION AND CONCLUSIONS	120
CHAPTER VIII RECOMMENDATIONS	123
References	125
APPENDIX A NOMENCLATURE	130
APPENDIX B MATRIX REPRESENTATION OF BALANCE EQUATIONS	135
APPENDIX C EXPERIMENTAL CONDITIONS AND SAMPLE MODEL PARAMETERS	140
APPENDIX D COMPUTER PROGRAMS	168

LIST OF TABLES

TABLE	TITLE	Page
2.2-1	Typical Assumptions in Distillation Modelling	5
2.2-2	Survey of Distillation Column Models	7
4.4-1	Comparison of Experimental and Simulated Final Steady State Overhead Enthalpy Values for Various Step Input Disturbances	43
4.4-2	Comparison of Experimental and Simulated Final Steady State Bottom Enthalpy Values for Various Step Input Disturbances	44
5.2-1	Sample Model Eigenvalues	63
6.4-1	Constants for Simulation Tests	103

LIST OF FIGURES

Figure	Title	Page
3.1-1	Schematic Representation of Distillation Column	18
3.2-1	Schematic Representation of a Tray	20
3.3-1	Schematic Representation of the Total Condenser	22
3.4-1	Schematic Representation of the Reboiler	23
4.4-1	Comparison of Model and Experimental Overhead Enthalpy Response to a Positive Feed Flow Step Change	46
4.4-2	Comparison of Model and Experimental Overhead Enthalpy Response to a Negative Feed Flow Step Change	47
4.4-3	Comparison of Model and Experimental Bottoms Enthalpy Response to a Positive Feed Flow Step Change	48
4.4-4	Comparison of Model and Experimental Overhead Enthalpy Response to a Positive Reflux Flow Step Change	50
4.4-5	Comparison of Model and Experimental Overhead Enthalpy Response to a Negative Reflux Flow Step Change	51
4.4-6	Comparison of Model and Experimental Overhead Enthalpy Response to a Positive Steam Flow Step Change	52

LIST OF FIGURES (continued)

Figure	Title	Page
4.4-7	Comparison of Model and Experimental Overhead Enthalpy Response to a Negative Steam Flow Step Change	53
5.2-1	Comparison of Twenty and Four State Models for a Feed Flow Step Change	59
5.2-2	Comparison of Twenty and Four State Models for a Reflux Flow Step Change	60
5.2-3	Comparison of Twenty and Four State Models for a Steam Flow Step Change	61
5.3-1	Reduced Model	67
5.3-2	Comparison of Twenty and Two State Models for a Feed Flow Step Change	68
5.3-3	Comparison of Twenty and Two State Models for a Reflux Flow Step Change	69
5.3-4	Comparison of Twenty and Two State Models for a Steam Flow Step Change	70
5.4-1	Experimental and Two State Model Bottom Enthalpy Responses to a Positive Feed Flow Step Change	71
5.4-2	Experimental and Two State Model Overhead Enthalpy Responses to Feed Flow Step Changes	72
5.4-3	Experimental and Two State Model Overhead Enthalpy Responses to Reflux Flow Step Changes	73
5.4-4	Experimental and Two State Model Overhead Enthalpy Responses to Steam Flow Step Changes	74

LIST OF FIGURES (continued)

Figure	Title	Page
6.2-1	Simulated Open Loop Behaviour - Positive Feed Flow Step Disturbance	78
6.2-2	Simulated Overhead Enthalpy Control Behaviour ($K_{pT} = 22$)	79
6.2-3	Simulated Bottom Enthalpy Control Behaviour ($K_{pB} = -330$)	80
6.2-4	Simulated Open Loop Behaviour - Filtered Noise Included in Bottom Composition Measurement ($\alpha = 0.8$)	82
6.2-5	Simulated Overhead Enthalpy Control Behaviour - Measurement Noise Included ($\alpha = 0.8$, $K_{pT} = 20$)	83
6.2-6	Simulated Bottom Enthalpy Control Behaviour - Measurement Noise Included ($\alpha = 0.8$, $K_{pB} = -300$)	84
6.2-7	Experimental Overhead Enthalpy Control Behaviour; +5% Feed Flow Step ($\alpha = 0.8$, $K_{pT} = 10$)	85
6.2-8	Experimental Overhead Enthalpy Control Behaviour; -5% Feed Flow Step ($\alpha = 0.8$, $K_{pT} = 10$)	86
6.2-9	Experimental Bottom Enthalpy Control Behaviour; +5% Feed Flow Step ($\alpha = 0.8$, $K_{pB} = -50$)	88
6.2-10	Experimental Bottom Enthalpy Control Behaviour; -5% Feed Flow Step ($\alpha = 0.8$, $K_{pB} = -50$)	89
6.3-1	Simulated Multiloop Control Behaviour - Measurement Noise Included ($\alpha = 0.8$, $K_{pT} = 15$, $K_{pB} = -150$)	91

LIST OF FIGURES (continued)

Figure	Title	Page
6.3-2	Experimental Multiloop Control Behaviour; +5% Feed Flow Step ($\alpha = 0.8$, $K_{pT} = 10$, $K_{pB} = -50$)	92
6.3-3	Experimental Multiloop Control Behaviour; -5% Feed Flow Step ($\alpha = 0.8$, $K_{pT} = 10$, $K_{pB} = -50$)	93
6.4-1	Model and Control Law	97
6.4-2	Simulated Multivariable Feedback Control Behaviour - Positive Feed Flow Step Disturbance	99
6.4-3	Simulated Multivariable Feedback Control Behaviour - Filtered Noise in Bottom Composi- tion Measurement Included ($\alpha = 0.8$)	100
6.4-4	Simulated Multivariable Feedback Control Behaviour with Modified Control Matrix and Measurement Noise ($\alpha = 0.8$)	101
6.4-5	Simulated Multivariable Feedback Control Behaviour with Time Delay and Measurement Noise Included ($\alpha = 0.8$, $\tau_D = 6$)	104
6.4-6	Simulated Multivariable Feedback Control Behaviour with Measurement Noise Included ($\alpha = 0.5$)	105
6.4-7	Simulated Multivariable Feedback Control Behaviour with Time Delay and Measurement Noise Included ($\alpha = 0.5$, $\tau_D = 4$)	106

LIST OF FIGURES (continued)

Figure	Title	Page
6.4-8	Experimental Multivariable Feedback Control Behaviour - No Disturbance ($\alpha = 0.5$)	108
6.4-9	Comparison of Experimental Open Loop and Multivariable Feedback Control Behaviour; +5% Feed Flow Step ($\alpha = 0.5$)	109
6.4-10	Comparison of Experimental Open Loop and Multivariable Feedback Control Behaviour; -5% Feed Flow Step ($\alpha = 0.5$)	110
6.4-11	Simulated Multivariable Feedback-Feedforward Control Behaviour with Time Delay and Measurement Noise Included ($\alpha = 0.5$, $\tau_D = 4$)	112
6.4-12	Comparison of Experimental Open Loop and Multivariable Feedback-Feedforward Control Behaviour; +5% Feed Flow Step ($\alpha = 0.5$)	114
6.4-13	Comparison of Experimental Open Loop and Multivariable Feedback-Feedforward Control Behaviour; -5% Feed Flow Step ($\alpha = 0.5$)	115
6.5-1	Comparison of Ratio and Noninteracting Control Systems as Implemented by Berry [6]; +15% Feed Flow Step	117
6.5-2	Comparison of Ratio and Noninteracting Control Systems as Implemented by Berry [6]; -15% Feed Flow Step	118

CHAPTER I

INTRODUCTION

The approach to control systems most extensively used in the process industries has been through the use of pneumatic or electronic controllers in a multiloop configuration. This approach has been used despite the problems of control variable selection and control loop interaction because of the inherent complexity of many processes. This complexity has been coupled with the liberal design of processing equipment to remove the need for exacting control systems. However, the recent increase in the number of industrial real time computers and advances in process modelling have increased the feasibility of multi-variable control system applications.

The usual objective of a control system applied to a distillation column is to maintain product compositions within specific limits as dictated by downstream processes or required product specifications, despite input disturbances. In the case of a column with no sidestream drawoff a typical multiloop product control system could include:

- i) Bottom product composition control by manipulation of heat input to the reboiler.
- ii) Top product composition control by manipulation of reflux flowrate.

However, the simultaneous application of both control loops can lead to a deterioration in control of both compositions due to the interaction between the two loops. This interaction arises from the effects of the manipulated variable of one loop on the controlled variable of the other loop. The presence of this interaction indicates that the control of a distillation column is an ideal situation for the application of a

multivariable control scheme.

However, for the design of a multivariable control system, it is necessary to be able to predict the interactive effects. This, in general, requires a process model which includes the effects of all disturbances as well as these interactive effects. Two general approaches to the dynamic modelling of distillation columns which have been found successful are:

- i) The application of the governing differential equations to yield a model comprised of a system of coupled first order differential equations.
- ii) The application of experimental transient data to yield an approximate transfer function model.

For the pilot-scale distillation column located in the Department of Chemical and Petroleum Engineering at the University of Alberta, the latter approach has been successfully applied to modelling and to the subsequent design of control systems [56,57]. The objective of this study will be to use the former approach to obtain a process model, and to apply that model to the design of a multivariable control system. The distillation column referred to above will be used in this study to experimentally evaluate the control system.

CHAPTER II

LITERATURE SURVEY

2.1 Introduction

The control of the compositions of products from a distillation column has been shown to be quite difficult. Rosenbrock [42] has presented a general discussion of problems encountered, and Davison [13] has extensively studied one of these problems, that of control loop interaction. The development of control strategies for distillation systems has received extensive discussion in the technical literature. The more recent design of control strategies has hinged on the development and application of a process model, and so this has also received attention in the technical literature. This chapter will attempt to outline several approaches to modelling and subsequent control which have been applied.

2.2 Survey of Distillation Modelling Techniques

In the technical literature, two general approaches to distillation modelling can be distinguished. The first of these methods involves the application of the dynamic mass, component and energy balances which apply to sections of the system. These equations are then simplified by the application of certain assumptions and by the knowledge of specific physical property data for the system involved. The second approach to modelling involves the use of experimental data from a specific system to obtain an approximate transfer function relationship between the relevant variables. In this section, several models developed from the two different approaches will be compared and discussed with specific attention being paid to application and model

testing.

In an early series of articles, Rosenbrock [39-41] has presented the general form of the transient balance relationships. He also discusses, at some length, several simplifying assumptions, methods of solving the resulting equations, and the development of computer programs for this purpose. Subsequent to this series of articles, review articles by Archer and Rothfus [3] in 1961 and by Williams [49] in 1963 have discussed the progress that has been made and have given an evaluation of the specific modelling approaches proposed.

In recent years, several theoretically based models, established using various different assumptions have been presented in the literature. A brief description of some typical assumptions and some remarks on their significance are presented in Table 2.2-1. A number of models which have been proposed are classified in Table 2.2-2, with some brief remarks on the type of model, its application and specific assumptions made in the derivation. It should be noted that in the case of results of specific groups of workers, for example the University of Delaware and the University of Florida groups, several papers have been presented together.

Svrcek [46] has presented a complicated model solution, which shows very good agreement with experimental data. In many cases [4,5,45, 26,20,50,51,52] the binary system used was chosen to enable several simplifying assumptions to be made. The most common choice is two components with similar heats of vapourization, allowing the assumption of equimolar overflow to be made. Davison [12] has attempted to define the problem in terms of pressure variations but many simplifying assumptions and approximations were necessary in order to obtain a feasible model. Several other authors have proposed similar models [1,22], but those

TABLE 2.2-1: TYPICAL ASSUMPTIONS IN DISTILLATION MODELLING		
Number	Basic Assumption	Remarks
1	Negligible vapour a) holdup b) dynamics	- Both assumptions may be approximately true and greatly simplify the dynamic equations.
2	Liquid holdup constant a) molar b) mass c) volume	- The specific assumption chosen depends on the binary system used, and on the extent of simplification desired.
3	Liquid dynamics a) instantaneous b) negligible c) some function of time	- This set of assumptions deals with the liquid flow from a stage as a function of the flow in and possibly the holdup. The choice of assumption depends on the liquid dynamic time relative to the overall transient time.
4	Well mixed liquid and/or vapour phase in each stage	- This assumption removes the problem of an 'average' composition and temperature. Each stage is then considered to be an ideal mixer-settler.
5	Constant pressure operation	- This assumption allows the use of stage temperature measurements to indicate composition, in a binary mixture. It also simplifies equilibrium and enthalpy relations.
6	a) Adiabatic operation b) Constant heat losses c) Heat loss as some function of composition	- These assumptions are usually applied in the determination of initial steady state compositions by an iterative approach.

TABLE 2.2-1 Continued

Number	Basic Assumption	Remarks
7	Efficiency: a) constant b) some function of composition and/or flowrate	- The first of these assumptions allows great simplification and is usually introduced by the application of a "pseudo-equilibrium" relation for each stage. It is a good assumption when only small changes are expected. The second assumption requires a detailed knowledge of the system and prior experimental study.
8	Linear equilibrium and enthalpy relations a) over entire range b) about steady state on each stage	- These assumptions are usually applied to remove vapour composition and enthalpy terms by expressing them in terms of the corresponding liquid properties.
9	Thermal equilibrium in each stage	- This assumption can be applied to allow both phase compositions to be found from temperature data, in a binary system at known pressure (see Ref. [50]).
10	Only small excursions from steady state will be experienced	- This permits the application of linearized perturbation techniques to simplify the problem.
11	Feed a) saturated liquid b) subcooled liquid c) superheated liquid	- These assumptions affect the heat input to the system, and consequently the extent to which changes in feed flow effect the vapour and liquid flows.

TABLE 2.2-2: SURVEY OF DISTILLATION COLUMN MODELS

Author(s)	Year of Pub. [Ref]	Model Description	Assumptions per Table 2.2-1	Remarks
Lamb Pigford Rippin	1961 [25]	mass and component balances	1a, 3a, 4, 7a, 8b, 10, 11	-constant relative volatility -first order liquid dynamics -analogue solution -no experimental verification -discussion of a general case
Baber Gerster Edwards Harper Witte Sproul Luyben Verneuil	1961 [4] 1962 [5] 1963 [45] 1964 [26]	mass and component balances	1a, 1b, 3c, 4, 7a, 8a, 10, 11	-liquid dynamics as a first order lag -reflux subcooling -perturbation in input flows -shows time lag introduced by downcomer holdup to be negligible -analogue solution -special consideration given to reboiler and condenser systems -compared to experimental data showing good agreement
Williams Hammond	1966 [51] 1967 [20] 1968 [50]	mass and component balances	1a, 1b, 2c, 3b, 4, 8, 11b	-no changes in vapour or liquid flows -ethanol-water system - similar latent heats -matrix-vector equation -good agreement with experimental transients for small changes

TABLE 2.2-2 Continued

Author(s)	Year of Pub. [Ref]	Model Description	Assumptions per Table 2.2-1	Remarks
Distefano May Huckaba Franke	1963 [23] 1964 [15] 1967 [16]	mass and component balances	1a, 3b, 4, 5, 6a, 7b, 8b, 11	-methanol-tertiary butyl alcohol -holdup as a function of flowrates -efficiency as a linear function of composition -transport delays in downcomers found to be negligible -reboiler duty as a function of steam temperature and reboiler liquid composition -experimental verification shows good agreement
Davison	1967 [12] 1970 [13]	mass, energy and component balances	1a, 2b, 3a, 4, 7a, 8b, 11a	-energy balances used to give pressure equation -very complicated derivation with many simplifying assumptions -matrix-vector equation -no experimental verification
Sargent Mah Michaelson	1962 [30] 1963 [43]	mass, energy and component balances	1b, 3b, 4, 8	-discussion of general multicomponent case -a relationship for molar holdup in each phase is required -numerical iterative solution

TABLE 2.2-2 Continued

Author(s)	Year of Pub. [Ref.]	Model Description	Assumptions per Table 2.2-1	Remarks
Svrcek	1967 [46]	mass, energy and component balances	1a, 2c, 3a, 4, 5, 6c, 7	<ul style="list-style-type: none"> -reboiler model by using average heat transfer coefficient -efficiency as a linear function of composition -numerical solution calculating all variables at each time interval -experimental evaluation shows very good agreement with open loop tests

presented in Table 2.2-2 represent the best documented and tested models.

The other approach to distillation column modelling has been through the use of experimental data, and often the use of pulse test data. Janis [24] and Wood and Pacey [56] have used pulse data, analyzed by the use of Fourier transforms to arrive at a Bode plot. An arbitrary form of transfer function is then employed to represent the data. Wood and Pacey [56] indicate good agreement between experimental transients and transfer functions of the first order plus time delay form. Chanh [10] has presented and compared several techniques for the time and frequency domain fitting of experimental data. He and Berry [6] have applied time domain methods and indicate good agreement with experimental data for simple transfer function forms.

2.3 Survey of Model Reduction Techniques

The problem of reducing a state space model involves the removal of specific states because they are unmeasurable or don't contribute greatly to the overall transient solution. Several methods have been proposed in the literature to accomplish this end. Marshall [31] and Davison and Chadha [14] have each presented methods based on a modal analysis of the system. The difference between the two methods is in the approximation used to account for the dynamics of the states to be removed. Wilson et. al. [53] have discussed these methods at some length, and extended each case to the discrete form of the model. Anderson [2] has presented a different method which is actually a least squares regression fit of the desired states. These methods will be discussed and compared further in the chapter of this work dealing specifically with this topic.

2.4 Survey of Distillation Column Control Methods

Historically distillation column control problems have been simplified by the use of an over-designing policy for process equipment so that utilization of simple control systems gave adequate results. However, with the increase in knowledge of distillation system behavior, and the development of on-line analysis techniques and control systems, more stringent design and control methods are being applied.

Because of the problems which occur in trying to measure compositions on a continuing basis, the use of temperature as a composition indicator has been widely used. Its application is based on the assumption that a mixture composition can change only slightly without affecting the mixture temperature, even in a multicomponent mixture, where this is not necessarily the case. Williams [50] has outlined the estimation of compositions from temperature measurements in a binary system, and presents some problems encountered in its application to control. The use of product temperature as the controlled variable has been shown to yield poor control [47]. In order to minimize product composition changes, an intermediate tray temperature has been suggested as a controlled variable. An early analysis by Boyd [8,9] indicates several possible control schemes utilizing intermediate tray temperatures. Similar analyses have been presented by Tivy [47] and by Pyle [34]. All authors indicate that the temperature sensor used in a control loop should be placed between the feed tray and the end of the column where the composition is being controlled. Furthermore the sensor should be placed on the tray where a steady state analysis of the column temperature gradient, indicates the largest slope. However, the sensor should also be as close to the end of the column as possible in order to minimize the

time lag between the measured temperature change and the expected product composition change. Wood [55] follows a similar approach to sensor location but extends the problem to include pressure control by controlling the temperature difference between the top tray and an intermediate tray. Chanh [10] has studied extensively the problem of sensor location with special consideration given to sensitivity and steady state error. He presents simulation results from two distillation systems and subsequent experimental results from one of these systems. In general, the approach of using an intermediate tray temperature has the advantage that a control system can be designed without a process model and using only steady state temperature data. However, many problems can arise as indicated by several of the above authors.

As indicated in Section 2.1, the major problem encountered in a two point control problem, that is, simultaneous control of both end product compositions, is the interaction between control loops. Several authors, Luyben [28] and Zalkind [59,60] have proposed methods to compensate for this interaction. Niederlinski [33] has presented an analysis and a criterion to indicate whether this decoupling is advantageous. The decoupling method entails the use of a process model to design "interaction compensators" for the control loops. Berry [6] has applied this approach to the design of a noninteracting control system for the distillation column used in this study, using a transfer function model derived from pulse test data. He reports a vast improvement from the simple multiloop interacting case to the noninteracting case. Berry [6] has also applied a method suggested by Rijnsdorp and van Kampen [36-38] which has a decoupling effect. The method is based on controlling the ratio of the reflux flow rate to overhead vapour flow rate. The actual ratio

used is varied according to measured composition changes. This ratio control tends to remove the effect of boil-up rate on the overhead control loop thus removing part of the interaction. Berry reports that this control scheme also gave improved control performance, being approximately the same as the noninteracting case. This method also has an advantage over the previous method in that no process model is required for compensator design.

The control schemes discussed thus far have been, in general, some form of feedback control, that is correcting for changes in the controlled variable and not accounting for any disturbances which may enter the system. This latter action is designated as feedforward compensation, and its inclusion usually improves control performance since no change in controlled variable need occur before some corrective action is taken. However, it has the added requirement that some knowledge of the effect of each disturbance on the behavior of the system is needed. One method of accomplishing feedforward control which has been suggested by Luyben [27] is by manipulation of the feed inlet location. A subsequent experimental study has been reported by Speicher and Luyben [44]. These workers used feed plate manipulation to account for feed composition changes. The steady state effects of feed plate location and of feed composition were investigated and this information used in the design of a control strategy. They report moderately good control results, however, it was found necessary to introduce a time lag into the control action. They also point out that the option of using several different trays as the feed tray is required in order to prevent over-compensation.

Distefano [16] describes the modelling and subsequent feedforward

control of a distillation column, with overhead composition being the controlled variable. His model [15,16] was modified slightly to yield a form which could be used for control studies. The reflux flow rate was used as a control variable to compensate for feed composition changes. The required reflux flow rate as a function of time was calculated beforehand for a given feed composition change, and then manually set during a corresponding experimental test. He reports good control of the system but some discrepancy between the simulated and experimental controlled transients, which he attributes to reboiler modelling errors.

Janis [24] has conducted a brief study of feedforward controllers derived from different models of a distillation column. He used a model derived from experimental pulse data and a model from linearized perturbation equations. He compares the models and controllers but presents no experimental evaluation of the control systems. The use of a feedback-feedforward control law derived from a transfer function model of a column has been described by Wood and Pacey [56]. The model was derived from pulse data. The data were fit in the frequency domain to a first order plus time delay function. The controllers derived from these transfer functions were used to control overhead product composition when the column was subject to feed flow disturbances. The reported experimental results indicate good control performance, when feedforward action is included.

A great deal of effort has recently been spent on the control and optimization of systems of the linear time invariant state space form. Newell [32] has outlined to some extent the derivation of such optimal control laws and their application to the process industry. Brasilow and Handley [9] have presented the optimal feedback case for a

quadratic performance index as the solution to the matrix Ricatti equation. The model used was obtained by linearizing the balance equations about the steady state operating point. The experimental tests presented used temperature as a composition indicator, and the controlled transients demonstrate good control and only small offsets for step load changes. Hu [22] has presented an extensive review of control strategies for distillation columns. He has applied dynamic programming to the optimization of a linearized balance model and presents simulation results to demonstrate and compare the control laws.

CHAPTER III

MODEL DEVELOPMENT

3.1 Introduction

In order to obtain a model of any process which can be mathematically solved, it is usually necessary to make simplifying assumptions, which hopefully can be justified by the physical system, and also will not restrict the solution. The assumptions which will be applied in the development of the distillation column model used in this study are:

- 1) The vapour dynamics are negligible compared to the liquid dynamics.
- 2) For small changes in steam rate to the reboiler, the changes in vapour flows are negligible.
- 3) The liquid and vapour phases in each stage are each well mixed, and so are homogeneous in composition and temperature.
- 4) The time rate of change of vapour mass holdup is small.
- 5) The heat losses from each stage are constant with time.
- 6) The pressure throughout the column is constant.
- 7) The fluctuations in time dependent variables are small so that linearized perturbations can be used.

The above assumptions are based either on the physical system or on the observations of other workers. The sixth assumption is justified by the presence of a pressure controller on the condenser using the cooling water flow as the control variable. The last assumption allows the time varying properties to be expressed in the form:

$$G = \bar{G} + G'$$

where G = any general time varying property

\bar{G} = the "steady state" value of G

G' = the deviation in G from the "steady state" value

Since the perturbations are assumed to be small, the terms involving products of perturbation terms can be neglected.

A schematic diagram of the distillation column being considered in this study is shown in Figure 3.1-1. The column has eight bubble-cap trays, a basket-type steam reboiler, and a total condenser. The feed is introduced onto the fourth tray under flow and temperature control. The product streams are drawn off under level control on the appropriate vessel. The dynamic equations describing each stage are outlined in the following sections, and the nomenclature used is presented in Appendix A.

3.2 Tray Model

The trays of a distillation column represent a group of stages which have the same set of governing equations and so a general set of equations can be derived. Figure 3.2-1 shows a schematic representation of a tray, designated as stage i . The unsteady state total mass and energy balances on this general stage yield:

$$W_i = W_{Li} + W_{Gi}$$

$$\frac{dW_i}{dt} = V_{i-1} + L_{i+1} - V_i - L_i$$

$$\frac{d}{dt} (W_{Li} h_i + W_{Gi} H_i) = V_{i-1} H_{i-1} + L_{i+1} h_{i+1} - V_i H_i - L_i h_i - Q_i$$

These expressions can be transformed by applying the steady state relations, and the perturbation relations of the form:

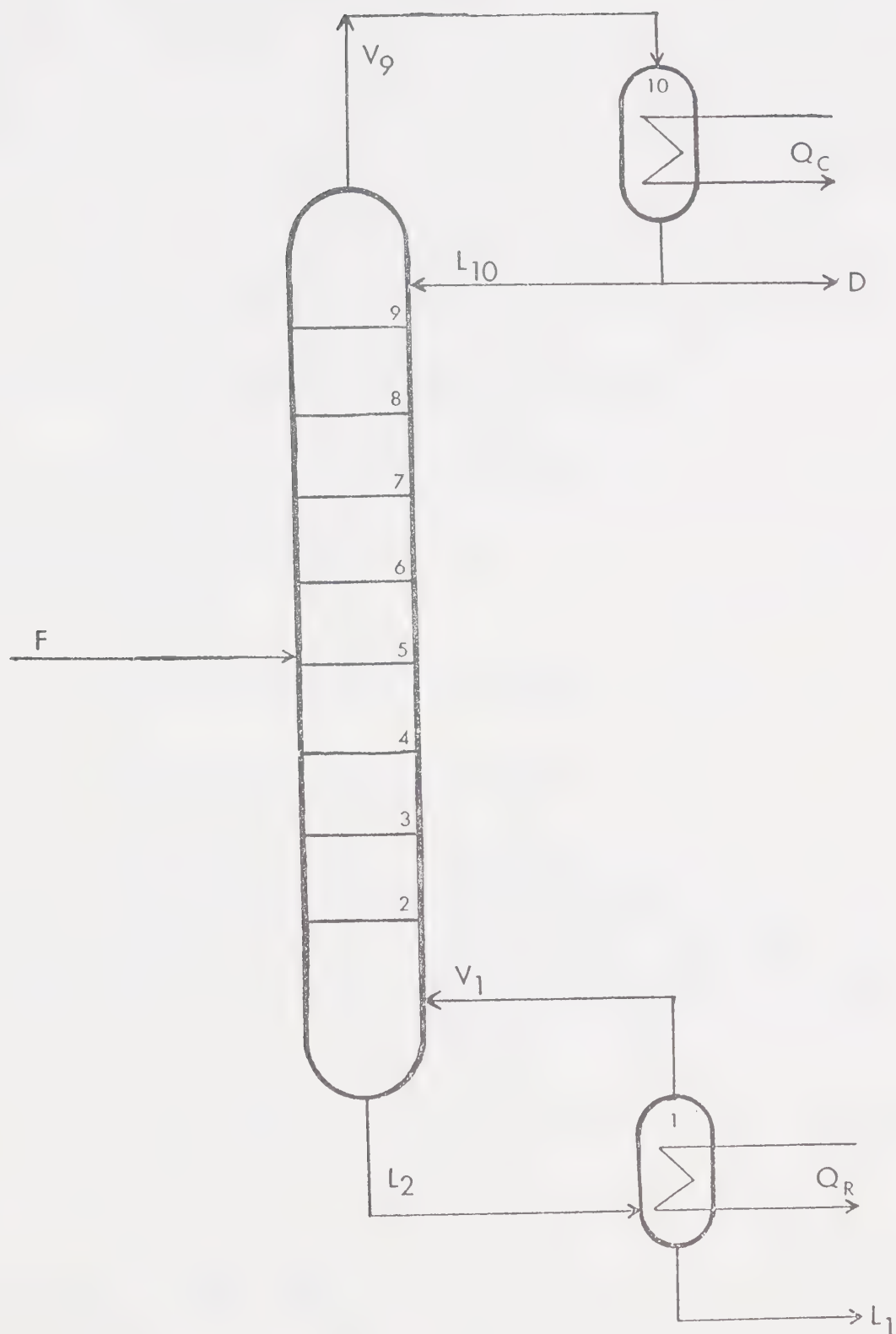


FIGURE 3.1-1: SCHEMATIC REPRESENTATION OF DISTILLATION COLUMN

$$W_i = \bar{W}_i + \dot{W}_i'$$

and

$$\bar{V}_{i-1} + \bar{L}_{i+1} = \bar{V}_i + \bar{L}_i$$

$$\bar{V}_{i-1}\bar{H}_{i-1} + \bar{L}_{i+1}\bar{h}_{i+1} = \bar{V}_i\bar{H}_i + \bar{L}_i\bar{h}_i + \bar{Q}_i$$

The unsteady state balances then simplify to yield:

$$\dot{W}_{Li}' + \dot{W}_{Gi}' = V_{i-1}' + L_{i+1}' - V_i' - L_i' \quad (3.2-1)$$

$$\begin{aligned} & \bar{W}_{Li}\dot{h}_i' + \bar{h}_i\dot{W}_{Li}' + \bar{W}_{Gi}\dot{H}_i' + \bar{H}_i\dot{W}_{Gi}' \\ &= \bar{V}_{i-1}H_{i-1}' + \bar{H}_{i-1}V_{i-1}' + \bar{L}_{i+1}h_{i+1}' + \bar{h}_{i+1}L_{i+1}' \\ & \quad - \bar{V}_iH_i' - \bar{H}_iV_i' - \bar{L}_ih_i' - \bar{h}_iL_i' \end{aligned} \quad (3.2-2)$$

These equations apply to each tray in the distillation column except the feed tray, where terms must be added for the mass and energy inputs of the feed stream. The equations which apply to the feed tray (stage 5) are:

$$\dot{W}_{L5}' + \dot{W}_{G5}' = V_4' + L_6' - L_5' - V_5' + F' \quad (3.2-3)$$

and

$$\begin{aligned} & \bar{W}_{L5}\dot{h}_5' + \bar{h}_5\dot{W}_{L5}' + \bar{W}_{G5}\dot{H}_5' + \bar{H}_5\dot{W}_{G5}' \\ &= \bar{V}_4H_4' + \bar{H}_4V_4' + \bar{L}_6h_6' + \bar{h}_6L_6' - \bar{V}_5H_5' \\ & \quad - \bar{H}_5V_5' - \bar{L}_5h_5' - \bar{h}_5L_5' + \bar{F}h_f' + \bar{h}_fF' \end{aligned} \quad (3.2-4)$$

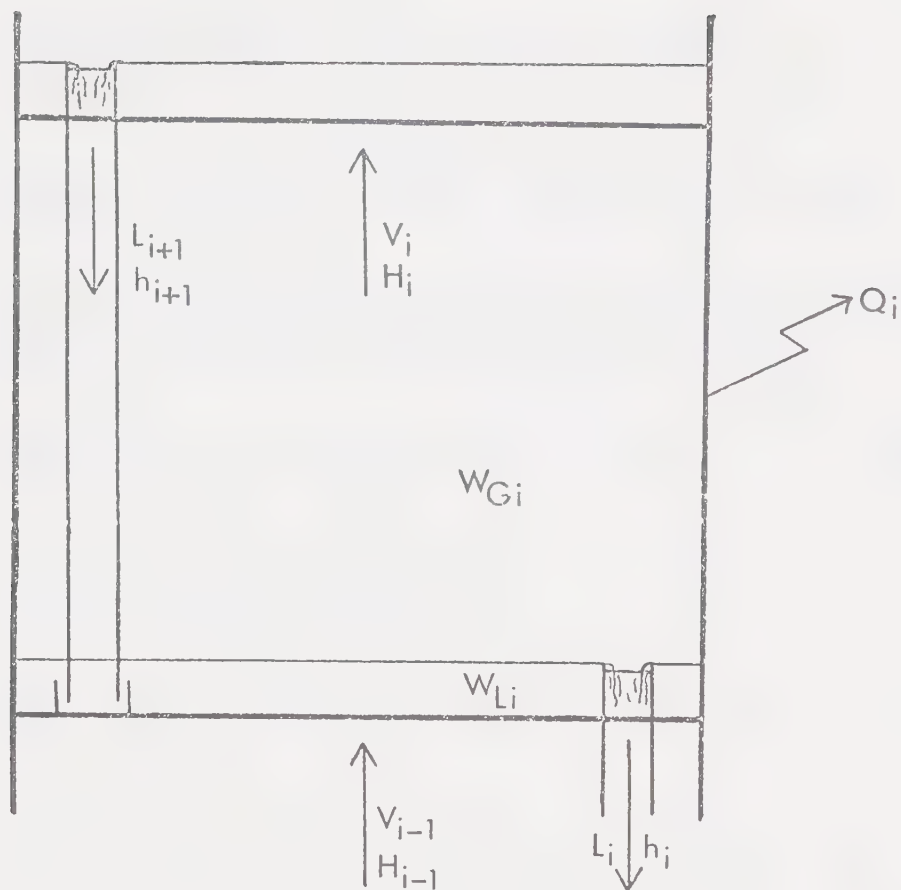


FIGURE 3.2-1: SCHEMATIC REPRESENTATION OF A TRAY

3.3 Condenser Model

The condenser on the equipment under study is the total condenser shown schematically in Figure 3.3-1. The heat removed from the condenser by the cooling water is designated as Q_c and is a load variable in the model. The total mass and energy balances yield:

$$\frac{d}{dt} (W_{L10} + W_{G10}) = V_9 - L_{10} - D$$

$$\frac{d}{dt} (W_{L10}h_{10} + W_{G10}H_{10}) = V_9H_9 - L_{10}h_{10} - Dh_{10} - Q_c - Q_{10}$$

Substitution of the perturbation expressions and the steady state mass and energy balance relationships yields the following equations:

$$\dot{W}'_{G10} + \dot{W}'_{L10} = V'_9 - L'_{10} - D' \quad (3.3-1)$$

$$\begin{aligned} & \bar{W}_{G10}\dot{H}'_{10} + \bar{H}_{10}\dot{W}'_{G10} + \bar{W}_{L10}\dot{h}'_{10} + \bar{h}_{10}\dot{W}'_{L10} \\ &= \bar{V}_9H'_9 + \bar{H}_9V'_9 - \bar{h}_{10}(L'_{10} + D') - h'_{10}(\bar{L}_{10} + \bar{D}) - Q'_c \end{aligned} \quad (3.3-2)$$

3.4 Reboiler Model

The reboiler used in this study is a basket type reboiler, shown schematically in Figure 3.4-1. The mass and energy balances about this stage yield the following expressions:

$$\frac{d}{dt} (W_{L1} + W_{G1}) = L_2 - V_1 - L_1$$

$$\frac{d}{dt} (W_{L1}h_1 + W_{G1}H_1) = L_2h_2 - V_1H_1 - L_1h_1 + Q_R - Q_1$$

Application of the linearized perturbation and steady state relations yields:

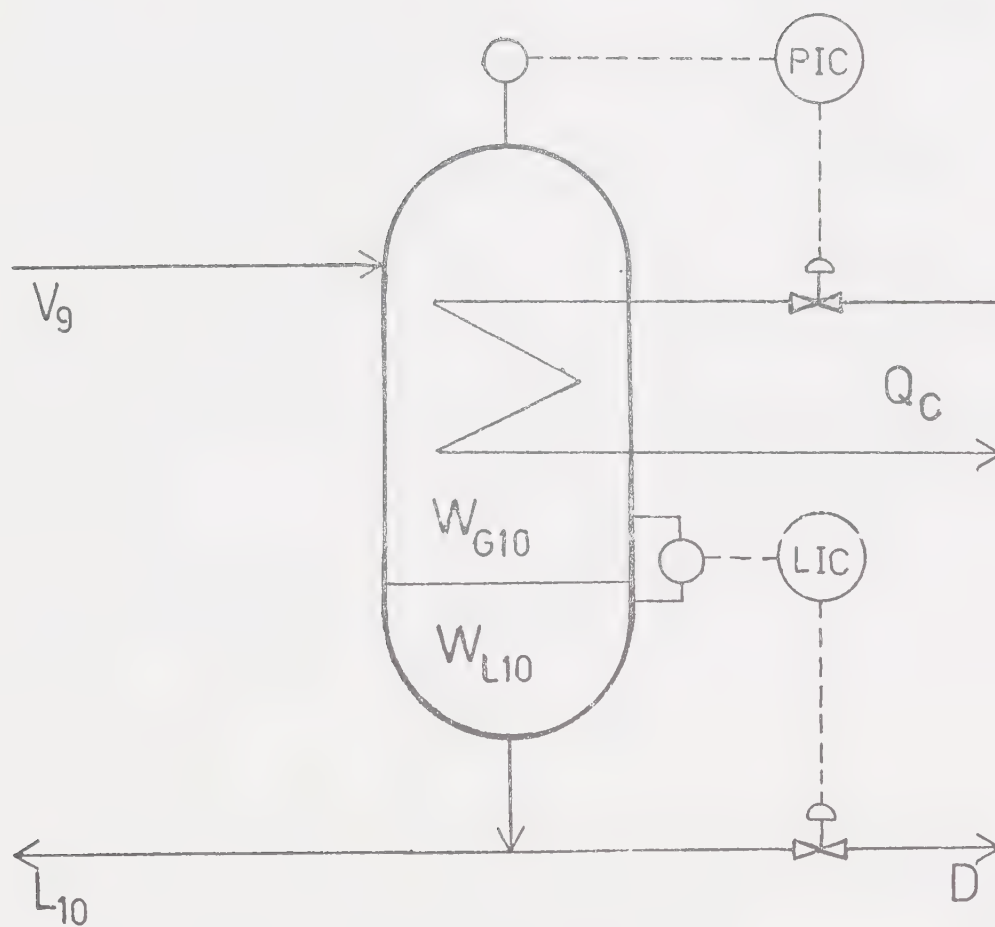


FIGURE 3.3-1: SCHEMATIC REPRESENTATION OF THE TOTAL CONDENSER

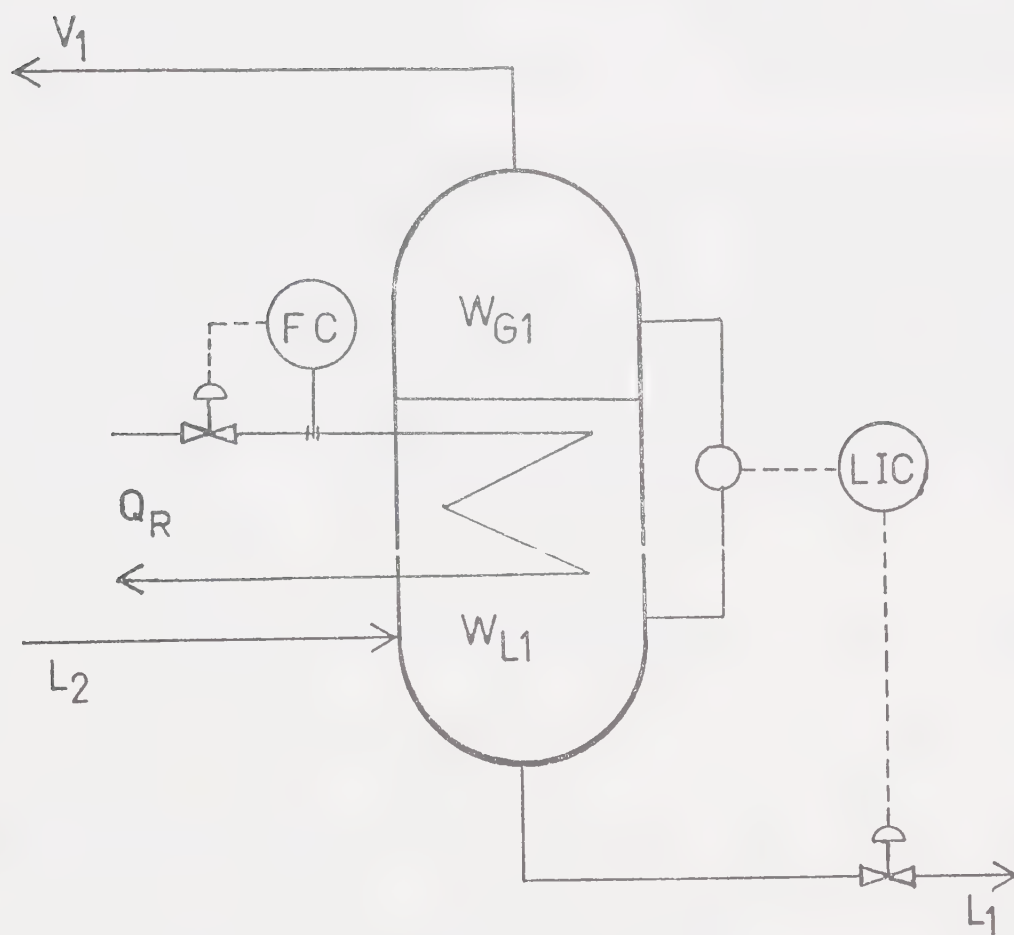


FIGURE 3.4-1: SCHEMATIC REPRESENTATION OF THE REBOILER

$$\dot{W}_{L1} + \dot{W}_{G1} = L_2' - V_1' - L_1' \quad (3.4-1)$$

$$\begin{aligned} \bar{W}_{L1} \dot{h}_1' + \bar{h}_1 \dot{W}_{L1} + \bar{W}_{G1} \dot{H}_1' + \bar{H}_1 \dot{W}_{G1} \\ = \bar{L}_2 h_2' + \bar{h}_2 L_2' - \bar{V}_1 H_1' - \bar{H}_1 V_1' - \bar{L}_1 h_1' - \bar{h}_1 L_1' + Q_R' \end{aligned} \quad (3.4-2)$$

3.5 Matrix-Vector Representation

The linearized perturbation balance expressions presented in the previous sections represent two sets of ten simultaneous differential equations, one set derived from the total mass balance, the other from the energy balances. These expressions can be written as two matrix-vector equations as outlined in detail in Appendix B. These equations are:

$$\dot{\underline{M}}_L + \dot{\underline{M}}_G = \underline{A} \underline{L} + \underline{B} \underline{V} + \underline{C}_1 \underline{D} \quad (3.5-1)$$

and

$$\begin{aligned} \underline{W}_G \dot{\underline{H}} + \underline{\bar{H}} \dot{\underline{M}}_G + \underline{W}_L \dot{\underline{h}} + \underline{\bar{h}} \dot{\underline{M}}_L \\ = \underline{A} [\underline{\bar{L}} \underline{h} + \underline{\bar{h}} \underline{L}] + \underline{B} [\underline{\bar{V}} \underline{H} + \underline{\bar{H}} \underline{V}] + \underline{C}_2 \underline{D} \end{aligned} \quad (3.5-2)$$

where \underline{W}_G , \underline{W}_L , $\underline{\bar{H}}$, $\underline{\bar{h}}$, $\underline{\bar{L}}$, $\underline{\bar{V}}$ are diagonal matrices of steady state values; \underline{A} , \underline{B} , \underline{C}_1 , \underline{C}_2 are appropriate coefficient matrices, and the vectors consist of perturbation terms. An analysis of these equations indicate that there are 20 scalar relationships in 60 time dependent unknowns. If it is assumed that:

- 1) the vapour dynamics are negligible compared to the liquid dynamics,

- 2) for small changes in steam rate to the reboiler, the changes in vapour flow are negligible,

then the following simplifications can be applied.

$$\begin{aligned} \text{i) } \dot{\underline{M}}_{\underline{G}} &= \underline{0} \\ \text{ii) } \underline{V} &= \underline{0} \end{aligned}$$

Substitution of these approximations into Equations (3.5-1) and (3.5-2) and the subsequent elimination of the vector $\dot{\underline{M}}_{\underline{L}}$ yields:

$$\underline{W}_{\underline{G}} \dot{\underline{H}} + \underline{W}_{\underline{L}} \dot{\underline{h}} = \underline{A} \underline{\bar{L}} \underline{h} + [\underline{A} \underline{\bar{h}} - \underline{\bar{h}} \underline{A}] \underline{L} + \underline{B} \underline{\bar{V}} \underline{H} + [\underline{C}_2 - \underline{\bar{h}} \underline{C}_1] \underline{D} \quad (3.5-3)$$

By applying these assumptions and substitutions the problem has been reduced to one of ten equations in 30 unknowns. Therefore, in order to solve the system of equations, 20 auxiliary equations are required. Since \underline{H} and \underline{h} are the vectors of enthalpies in each stage, it can be assumed that they are related by some form of pseudo-equilibrium relationship. The vector \underline{L} is composed of the liquid flow perturbations, and so should be related in some way to the input liquid flow disturbances. These two simplifying assumptions are pursued in the following sections to yield the relationships required to allow solution of the equations.

3.6 Enthalpy Linearization

Since in a binary system, with pressure constant, or specified, there is only one degree of freedom, it seems reasonable to assume that the vapour and liquid enthalpies should be related. If the assumption that the "tray efficiency" is constant is made, then it is possible to express a linearized enthalpy relationship as:

$$H = b_1 h + b_2$$

From this, the perturbation form can be expressed as:

$$H' = b_1 h'$$

This can be shown as follows:

$$\text{In general} \quad H = f_1(y, T)$$

$$h = f_2(x, T)$$

Furthermore, the assumption of a constant efficiency allows the use of 'pseudo-equilibrium' relations of the form:

$$y = f_3(T)$$

$$x = f_4(T)$$

So that the enthalpies can be expressed as:

$$H = f_5(y)$$

$$h = f_6(x)$$

For small perturbations in the variables, the term b_1 can be expressed as:

$$b_1 = \left. \frac{\Delta H}{\Delta h} \right|_{s.s.}$$

If a pseudo-equilibrium relationship of the form:

$$y = f_7(x)$$

is used, then b_1 can be expressed as:

$$b_1 = \left[\frac{df_5}{dy} \cdot \frac{df_7}{dx} \middle/ \frac{df_6}{dx} \right] \bigg|_{s.s.}$$

This term, b_1 , the enthalpy linearization factor, can be evaluated for each stage, knowing the steady state values and the form of the enthalpy and 'equilibrium' functions. Sample calculations of this factor are presented in Appendix C. When all stages are being considered, the enthalpy linearization can be written as a vector-matrix form:

$$\underline{H} = \underline{B_1} \underline{h} \quad (3.6-1)$$

where $\underline{B_1}$ is a diagonal matrix of the enthalpy linearization factors.

3.7 Liquid Flow Dynamics

Several authors [40-42, 3-5, 25,26] have stated that the dynamics of the liquid flow rates within a distillation column can be significant. In general, the liquid flowrate from a tray is dependent on the tray design, the liquid and vapour flows to that tray, and the fluid properties. As several workers have outlined [4,5,25,26], the liquid flow dynamics can be expressed as a first order equation. This approach was used in this study, to express the liquid flow perturbations in the form:

$$L_i' = L_{i+1}' K_i [1 - e^{-t/\tau_i}] \quad (3.7-1)$$

The τ_i is a liquid flow time constant and K_i accounts for different flowrate changes on each tray.

Equation (3.7-1) can be expressed as the following differential equation:

$$\dot{L}'_i = \frac{1}{\tau_i} [L'_{i+1} K_i - L'_i] \quad (3.7-2)$$

This expression relates the flow out of a stage to the flow into that stage as a function of time. It must, however, be modified for the feed tray, to account for changes in feed flow. The equation for the feed tray is:

$$\dot{L}'_5 = \frac{1}{\tau_5} [L'_6 K_5 + F' K_{F5} - L'_5] \quad (3.7-3)$$

where K_{F5} accounts for different changes in F and L_5 .

The vector \underline{L} also includes a perturbation term for changes in distillate flow since changes in this variable are observed for changes in feed and reflux flowrates. The response of distillate flow to feed flow changes can be written as:

$$D' = F' K_{FD} [1 - e^{-t/\tau_D}] \quad (3.7-4)$$

The response to reflux flow changes is slightly more complicated, since the distillate is withdrawn under condenser level control. A step change in reflux flow will produce an immediate equal and opposite step in distillate flow followed by a gradual response to a final steady state value. This can be expressed mathematically as:

$$D' = -L'_{10} + L'_{10} K_{RD} [1 - e^{-t/\tau_D}] \quad (3.7-5)$$

If the τ_D terms in equations (3.7-4) and (3.7-5) are assumed to be approximately the same, the overall equation can be written as:

$$D' = -L'_{10} + L'_{10} K_{RD} [1 - e^{-t/\tau_D}] + F' K_{FD} [1 - e^{-t/\tau_D}]$$

This can be expressed as a differential equation in the form:

$$\dot{\underline{D}}' = \frac{1}{\tau_D} [\underline{F}' K_{FD} + \underline{L}'_{10} K_{RD} - \underline{D}' - \underline{L}'_{10}] \quad (3.7-6)$$

Applying equation (3.7-2) to the appropriate stages and combining these with equations (3.7-3) and (3.7-6), the following matrix-vector differential equation can be written:

$$\dot{\underline{L}} = \underline{M} \underline{L} + \underline{N} \underline{D} \quad (3.7-7)$$

where the vector \underline{D} includes feed and reflux flow disturbances, and \underline{M} and \underline{N} are appropriate coefficient matrices.

3.8 Augmented State Space Model

In the previous sections several expressions which can be used to simplify equation (3.5-3) have been presented. Each of these equations is rewritten below:

$$\underline{W}_G \dot{\underline{H}} + \underline{W}_L \dot{\underline{h}} = \underline{A} \underline{L} \underline{h} + [\underline{A} \underline{h} - \underline{h} \underline{A}] \underline{L} + \underline{B} \underline{V} \underline{H} + [\underline{C}_2 - \underline{h} \underline{C}_1] \underline{D} \quad (3.5-3)$$

$$\underline{H} = \underline{B}_1 \underline{h} \quad (3.6-1)$$

$$\dot{\underline{L}} = \underline{M} \underline{L} + \underline{N} \underline{D} \quad (3.7-7)$$

Substitution of equation (3.6-1) into equation (3.5-3) and simplification yields:

$$\dot{\underline{h}} = \hat{\underline{A}} \underline{h} + \hat{\underline{B}} \underline{L} + \hat{\underline{C}} \underline{D} \quad (3.8-1)$$

where

$$\hat{\underline{A}} = \underline{P}^{-1} [\underline{A} \underline{L} + \underline{B} \underline{V} \underline{B}_1]$$

$$\hat{\underline{B}} = \underline{P}^{-1} [\underline{A} \underline{h} - \underline{h} \underline{A}]$$

$$\hat{\underline{C}} = \underline{P}^{-1} [\underline{C}_2 - \underline{h} \underline{C}_1]$$

$$\underline{P} = [\underline{W}_L + \underline{W}_G \underline{B}_1]$$

Equation (3.7-7) can now be combined with equation (3.8-1) to give the augmented state space equation:

$$\begin{bmatrix} \dot{\underline{h}} \\ \dot{\underline{L}} \end{bmatrix} = \begin{bmatrix} \hat{\underline{A}} & \hat{\underline{B}} \\ \underline{0} & \underline{M} \end{bmatrix} \begin{bmatrix} \underline{h} \\ \underline{L} \end{bmatrix} + \begin{bmatrix} \hat{\underline{C}} \\ \underline{N} \end{bmatrix} \underline{D} \quad (3.8-2)$$

where the submatrices are as defined previously and $\underline{0}$ is a 10 x 10 null matrix. This equation can be expressed in the form:

$$\dot{\underline{x}} = \underline{G} \underline{x} + \underline{H} \underline{D} \quad (3.8-3)$$

and as such is a general state space representation of the distillation column.

Equation (3.8-3) represents a matrix-vector differential equation of order 20. There are 20 states or time varying unknowns and 5 inputs. These inputs appear in the vector \underline{D} which comprises a control/disturbance vector. The model in the form of equation (3.8-3) can be solved for a specific \underline{D} to yield the time domain response of each variable or state.

3.9 Disturbance-Control Vector

The possible disturbance and control variables for the distillation column have been introduced into the model by the vector \underline{D} . This vector contains the following perturbation inputs:

$$\underline{D}^T = [F' \quad L'_{10} \quad Q'_R \quad Q'_C \quad h'_f]$$

The disturbances which can enter by the feed stream are feed flow and feed enthalpy. Since the cooling water flow is used to control the pressure in the condenser, its effect as a load or disturbance variable must enter into the model and is included as Q'_C , a change in condenser heat duty. The two control variables most often used, and used in this study are reflux flow and steam flow (reboiler duty Q'_R) and these enter into the vector \underline{D} . This formulation allows the disturbance and control variables to be isolated from each other, and from the state variables.

CHAPTER IV

MODEL EVALUATION

4.1 Introduction

Before a process model can be accepted as representative of a process, its ability to predict the effect of disturbances on the process must be verified. The simplest form of disturbance to utilize is a step disturbance since it is easily obtained experimentally and analytically. The approach adopted in this study is to obtain the time domain solution to the linearized state space model for a step disturbance. This time domain solution is then compared to the experimental response to the same step disturbance. This testing procedure, and the solution to the state equation are outlined in the following sections.

4.2 Solution to the State Equation

The general state space equation, in differential form, can be written as:

$$\dot{\underline{x}} = \underline{G} \underline{x} + \underline{H} \underline{D} \quad (4.2-1)$$

where \underline{x} is an $n \times 1$ state vector

\underline{G} is an $n \times n$ matrix

\underline{D} is an $m \times 1$ disturbance-control vector

\underline{H} is an $n \times m$ matrix

The solution to this matrix differential equation can be found in standard texts on state space techniques and has been outlined by Newell [32]. The solution can be written as:

$$\underline{x}(t_1) = \underline{f}(t_1) \underline{x}(t_0) + \int_0^{t_1} \underline{f}(t_1 - \tau) \underline{H} \underline{D}(\tau) d\tau \quad (4.2-2a)$$

where $\underline{f}(t)$ is a matrix function defined as

$$\underline{f}(\alpha) = \exp(\underline{G} \alpha) \quad (4.2-2b)$$

If the vector \underline{D} is assumed to be constant over the interval $\{t; t_0 \leq t \leq t_1\}$, then equation (4.2-2a) can be written as:

$$\underline{x}(t_1) = \underline{\phi} \underline{x}(t_0) + \underline{\Delta} \underline{D}(t_0) \quad (4.2-3)$$

where

$$\begin{aligned} \underline{\phi} &= \exp [\underline{G} t_1] \\ \underline{\Delta} &= \int_0^{t_1} \exp[\underline{G}(t_1 - \tau)] \underline{H} d\tau \end{aligned}$$

This formulation gives an exact solution to equation (4.2-1) and can be used to yield the time domain solution. This approach can be programmed for a digital computer and a series approach used. However, if the model is of a large order the computational time can be quite large. An alternate approach whereby a trapezoidal approximation is used will be outlined below and the resulting solution compared to the exact solution obtained by solving equation (4.2-3).

Consider a time interval of duration T and an incremental time Δt such that:

$$T = k \Delta t$$

If \underline{D} can be considered constant over a time interval $\{t; t_0 \leq t \leq t_0 + T\}$, then within this interval:

$$\underline{D}(t) = \underline{D}(t_0) = \underline{D}$$

Also from equation (4.2-1) several general expressions can be written:

$$\dot{\underline{x}}(t) = \underline{G} \underline{x}(t) + \underline{H} \underline{D}(t) \quad (4.2-4a)$$

and
$$\dot{\underline{x}}(t_0) = \underline{G} \underline{x}(t_0) + \underline{H} \underline{D}(t_0) \quad (4.2-4b)$$

However in the interval $\{t; t_0 < t < t_0 + T\}$, \underline{D} is constant and for $\ell < k$ and $t_0 = 0$, equation (4.2-4a) can be written as:

$$\dot{\underline{x}}(\ell\Delta t) = \underline{G} \underline{x}(\ell\Delta t) + \underline{H} \underline{D}$$

and for the following interval:

$$\dot{\underline{x}}([\ell+1]\Delta t) = \underline{G} \underline{x}([\ell+1]\Delta t) + \underline{H} \underline{D}$$

Also if $\underline{x}(\ell\Delta t)$ is known, $\underline{x}([\ell+1]\Delta t)$ can be calculated from the mean value theorem as

$$\underline{x}([\ell+1]\Delta t) = \underline{x}(\ell\Delta t) + \Delta t \underline{\eta} \quad (4.2-5)$$

where $\underline{\eta} = \dot{\underline{x}}(\alpha)$

and $\ell\Delta t \leq \alpha \leq [\ell+1]\Delta t$

The trapezoidal approximation that:

$$\underline{\eta} = \frac{1}{2} [\dot{\underline{x}}([\ell+1]\Delta t) + \dot{\underline{x}}(\ell\Delta t)]$$

can be made to simplify the solution.

Application of this approximation and substitution into equation (4.2-5) yields:

$$\underline{x}([\ell+1]\Delta t) = \underline{x}(\ell\Delta t) + \frac{\Delta t}{2} [\underline{G} \underline{x}(\ell\Delta t) + \underline{x}([\ell+1]\Delta t) + 2 \underline{H} \underline{D}]$$

This equation can be rearranged to yield:

$$[\underline{I} - \frac{\Delta t}{2} \underline{G}] \underline{x}([\ell+1]\Delta t) = [\underline{I} + \frac{\Delta t}{2} \underline{G}] \underline{x}(\ell\Delta t) + \Delta t \underline{H} \underline{D}$$

where \underline{I} is an $n \times n$ identity matrix. This equation can be rewritten in the form:

$$\underline{x}([\ell+1]\Delta t) = \underline{\phi} \underline{x}(\ell\Delta t) + \underline{\Delta} \underline{D} \quad (4.2-6a)$$

where

$$\underline{\phi} = [\underline{I} - \frac{\Delta t}{2} \underline{G}]^{-1} [\underline{I} + \frac{\Delta t}{2} \underline{G}] \quad (4.2-6b)$$

$$\underline{\Delta} = [\underline{I} - \frac{\Delta t}{2} \underline{G}]^{-1} \underline{H} \Delta t \quad (4.2-6c)$$

These equations can be used to obtain an approximate solution and the difference between this solution and the exact solution will decrease as Δt is decreased or as k is increased. It can be shown that, for a given input disturbance, the final steady state predicted by equations (4.2-6a) and (4.2-1) are identical. From equation (4.2-6a) the final value is obtained by setting:

$$\underline{x}([\ell+1]\Delta t) = \underline{x}(\ell\Delta t) = \underline{x}_f$$

yielding:

$$\underline{x}_f = [\underline{I} - \underline{\phi}]^{-1} \underline{\Delta} \underline{D} \quad (4.2-7a)$$

From equation (4.2-1), if the system is stable, that is if the real parts of the eigenvalues of \underline{G} are negative, the final steady state can be obtained by setting

$$\dot{\underline{x}} = \underline{0}$$

yielding

$$\underline{x}_f = -\underline{G}^{-1} \underline{H} \underline{D} \quad (4.2-7b)$$

The equivalence of these final values can be shown as follows:

$$\text{Let } \underline{\underline{A}} = [\underline{\underline{I}} - \frac{\Delta t}{2} \underline{\underline{G}}]^{-1}$$

$$\underline{\underline{B}} = [\underline{\underline{I}} + \frac{\Delta t}{2} \underline{\underline{G}}]$$

so that

$$\underline{\underline{\phi}} = \underline{\underline{A}} \underline{\underline{B}}$$

$$\underline{\underline{\Delta}} = \underline{\underline{A}} \underline{\underline{H}} \underline{\underline{D}} \Delta t$$

Further

$$[\underline{\underline{I}} - \underline{\underline{\phi}}]^{-1} \underline{\underline{\Delta}} \underline{\underline{D}} = [\underline{\underline{I}} - \underline{\underline{A}} \underline{\underline{B}}]^{-1} \underline{\underline{A}} \underline{\underline{H}} \underline{\underline{D}} \Delta t$$

also

$$\begin{aligned} [\underline{\underline{I}} - \underline{\underline{A}} \underline{\underline{B}}]^{-1} \underline{\underline{A}} &= \{\underline{\underline{A}}^{-1} [\underline{\underline{I}} - \underline{\underline{A}} \underline{\underline{B}}]\}^{-1} \\ &= [\underline{\underline{A}}^{-1} - \underline{\underline{B}}]^{-1} \end{aligned}$$

However, from the definition of $\underline{\underline{A}}$ and $\underline{\underline{B}}$:

$$[\underline{\underline{A}}^{-1} - \underline{\underline{B}}]^{-1} = [-\Delta t \underline{\underline{G}}]^{-1}$$

so that

$$\begin{aligned} [\underline{\underline{I}} - \underline{\underline{\phi}}]^{-1} \underline{\underline{\Delta}} \underline{\underline{D}} &= [-\Delta t \underline{\underline{G}}]^{-1} \underline{\underline{H}} \underline{\underline{D}} \Delta t \\ &= -\underline{\underline{G}}^{-1} \underline{\underline{H}} \underline{\underline{D}} \end{aligned}$$

This result is the same as in equation (4.2-7b) indicating that the final steady state values are identical.

The equations (4.2-6a, b, c) represent an approximate solution to equation (4.2-1). The exact solution is as given in equations

(4.2-2a, b). The similarities and differences between the two solutions can be shown, and so some criterion for the choice of Δt given. The following is a presentation of this in scalar form for simplicity, and with the extension to the vector-matrix form.

For the scalar case:

$$\dot{x} = g x + h d$$

the exact solution is

$$x(t_1) = e^{gt_1} x_0 + \int_0^{t_1} e^{g(t_1-\tau)} h d \, d\tau \quad (4.2-8)$$

An approximate solution, by analogy to equations (4.2-6a, b, c) is given by

$$x(t_1) = a x_0 + b d \quad (4.2-9a)$$

where

$$a = \left(1 - \frac{t_1}{2} g\right)^{-1} \left(1 + \frac{t_1}{2} g\right) \quad (4.2-9b)$$

$$b = \left(1 - \frac{t_1}{2} g\right)^{-1} t_1 h \quad (4.2-9c)$$

The time difference t_1 in this case is analogous to the Δt term defined for the matrix case.

By the binomial expansion:

$$\left(1 - \frac{t_1}{2} g\right)^{-1} = 1 + \frac{t_1 g}{2} + \frac{t_1^2 g^2}{4} + \dots + \frac{t_1^k g^k}{2^k}$$

So the terms in equation (4.2-9) can be redefined as:

$$a = 1 + t_1 g + \frac{t_1^2 g^2}{2} + \frac{t_1^3 g^3}{4} + \dots + \frac{t_1^k g^k}{2^{(k-1)}} \quad (4.2-10a)$$

$$b = t_1 h + \frac{g h t_1^2}{2} + \frac{g^2 h t_1^3}{4} + \dots + \frac{g^k h t_1^{(k+1)}}{2^k} \quad (4.2-10b)$$

However, the coefficients as defined in equation (4.2-8) can also be expressed in series form as:

$$e^{g t_1} = 1 + t_1 g + \frac{t_1^2 g^2}{2} + \frac{t_1^3 g^3}{6} + \dots + \frac{t_1^k g^k}{k!} \quad (4.2-10c)$$

$$\begin{aligned} \int_0^{t_1} e^{g(t_1-\tau)} h \, d\tau &= \int_0^{t_1} h [1 - g(t_1-\tau) + \frac{g^2}{2}(t_1-\tau)^2 + \dots] d\tau \\ &= h t_1 + \frac{g h t_1^2}{2} + \frac{h g^2 t_1^3}{6} + \dots + \frac{g^{(k-1)} h t_1^k}{k!} \end{aligned} \quad (4.2-10d)$$

By comparing equations (4.2-10a, b, c, d) it can be seen that:

$$a - e^{g t_1} \approx \frac{t_1^3 g^3}{12}$$

and

$$b - \int_0^{t_1} h e^{g(t_1-\tau)} d\tau \approx \frac{t_1^3 g^2 h}{12}$$

At this point, a criterion can be selected for the choice of t_1 , the time interval used. A convenient form, which expresses the error in the approximation as a fraction of the previous term in the expansion is to let:

$$\left| \frac{t_1^3 g^3}{12} \right| \leq \alpha \left| \frac{t_1^2 g^2}{2} \right| \quad \text{or} \quad \left| \frac{t_1 g}{6} \right| \leq \alpha \quad (4.2-11a)$$

and

$$\left| \frac{t_1^2 g^2 h}{12} \right| \leq \beta \left| \frac{t_1^2 h g}{2} \right| \quad \text{or} \quad \left| \frac{t_1 g}{6} \right| \leq \beta \quad (4.2-11b)$$

where α and β are selected constants. Since equations (4.2-11a, b) are essentially the same, a criterion can be selected in the form.

$$\left| \frac{t_1 g}{6} \right| \leq \alpha \quad (4.2-12)$$

where α is a measure of the goodness of the approximation.

This criterion applies to the scalar case and the extension to the matrix-vector case is based on the definition of an eigenvalue. If the original equation (4.2-1) is diagonalized by the similarity transform:

$$\underline{x} = \underline{M} \underline{z}$$

to yield

$$\dot{\underline{z}} = \underline{\Lambda} \underline{z} + \underline{\theta} \underline{d}$$

then each canonical state can be expressed in the form of a scalar equation. So for each canonical state a criterion of the form of equation (4.2-12) can be written. The logical choice of a Δt is therefore to select the smallest one as given by:

$$\max \left[\left| \frac{\Delta t}{6} \operatorname{Re} (\lambda_i) \right| \right] \leq \alpha \quad (4.2-13)$$

where the λ_i are the eigenvalues of the matrix \underline{G} .

The time base of $\underline{\phi}$ and $\underline{\Delta}$ as in equation (4.2-3) is then Δt .

The time base or sample interval can be changed to any time T if

$$T = k \Delta t$$

by the relations:

$$\begin{aligned} \underline{\phi}_T &= \underline{\phi}^k \\ \underline{\Delta}_T &= \sum_{j=0}^{k-1} \underline{\phi}^j \underline{\Delta} \end{aligned}$$

to give the discrete form with time base T as:

$$\underline{x}(t+T) = \underline{\phi}_T \underline{x}(t) + \underline{\Delta}_T \underline{D}(t)$$

4.3 Experimental Studies

4.3.1 Experimental Equipment

The distillation column used in this study is located in the Department of Chemical and Petroleum Engineering at the University of Alberta. The glass column is nine inches in diameter and has eight trays, each fitted with four 2-1/4 x 1-7/8 inch diameter bubble caps, 1-1/2 inch diameter inlet and outlet wiers and a 1 inch diameter down-comer. The vapour is condensed in a glass total condenser fitted with stainless steel cooling coils. The reboiler is a 7 inch nominal diameter basket type reboiler using 70 psi steam.

The column is instrumented with conventional local analog controllers as well as being interfaced to an IBM 1800 process control computer. The present configuration allows the computer to act in a supervisory capacity by varying the setpoints of the local controllers for feed, steam and reflux flow rates. The computer also acts in a data gathering and logging capacity by sensing many other variables. Details of the column and its instrumentation have been adequately presented by Svrcek [46] and by Berry [6].

The condenser outlet fluid composition is continually monitored by means of an in-line capacitance analyzer. The details of this apparatus have been presented by Svrcek [46]. The reboiler bottoms composition is monitored by the use of an on-line gas chromatograph operating under computer supervision. The separation and analysis is done on a 150 second cycle. The computer collects the data and analyzes it to calculate the composition. The values are also collected in a computer disk file for data logging purposes.

The feed is pumped onto the fourth tray (from the bottom) under flowrate control. It is preheated by a steam preheater, under temperature control. The bottom product is withdrawn under reboiler level control while the top product is withdrawn under condenser level control. The reflux is preheated by a steam preheater before returning to the top tray, and it is maintained close to its boiling point.

4.3-2 Open-Loop Tests

Experimental transient data for use in the evaluation of the proposed model was gathered by carrying out several 'open-loop' step tests on the column. These tests were open-loop in that the effect of a step change in one variable on the product compositions was investigated

with other variables maintained at their steady state values. For example, if a step in feed flowrate was used, steam and reflux flowrates, column pressure, reboiler and condenser levels, and feed and reflux temperatures were controlled at their steady state values.

The step input disturbances were implemented by introducing a step change in the setpoint of the appropriate local controller by means of the IBM direct digital control (DDC) system. The transient data was then gathered using the data accumulation algorithm in the DDC system. The data was stored in disk files and so could be plotted or punched onto cards for future use.

4.4 Comparison of Simulated and Experimental Results

The discrete form of the model, as represented by equation (4.2-6a) was used to calculate the transient model response to given inputs. The time base was taken as one minute for convenience. The disturbances, as calculated from the average of initial and final values were input to the model. In general, one of feed, steam and reflux flow was perturbed by a step in flowrate, and the others held constant. Since the cooling water flow was used to control column pressure, the condenser heat duty varied, and so was another disturbance input to the model.

The overhead and bottom product enthalpies were calculated from the transient composition data. The bottom product analyzer, the process gas chromatograph, gave results with appreciable noise. An exponential filter was used to smooth the data. This, coupled with the measurement time lag, made a comparison of bottom enthalpies difficult.

The following sections detail the transients for various forms of step disturbances. Table 4.4-1 indicates the final values of the overhead enthalpy perturbations for the steps considered. Table 4.4-2

TABLE 4.4-1
COMPARISON OF EXPERIMENTAL AND SIMULATED FINAL STEADY STATE OVERHEAD
ENTHALPY VALUES FOR VARIOUS STEP INPUT DISTURBANCES

Type of Step Disturbance	Magnitude (%)	Final Perturbation Values Exp.	Final Perturbation Values Sim.	Figure
Feed flow	+5.6	-.072	-.089	4.4-1
Feed flow	-5.7	+.119	+.090	4.4-2
Reflux flow	+4.8	-.099	-.123	4.4-4
Reflux flow	-8.7	+.337	+.315	4.4-5
Steam flow	+4.0	+.284	+.287	4.4-6
Steam flow	-4.0	-.133	-.135	4.4-7

TABLE 4.4-2

COMPARISON OF EXPERIMENTAL AND SIMULATED FINAL STEADY STATE BOTTOM
ENTHALPY VALUES FOR VARIOUS STEP INPUT DISTURBANCES

Type of Step Disturbance	Magnitude (%)	Final Perturbation Values Exp.	Sim.
Feed flow	+5.6	-.021	-.020
Feed flow	-5.7	.007	.020
Reflux flow	+4.8	-.042	-.024
Reflux flow	-8.7	.096	.060
Steam flow	+4.0	+.900	+.700
Steam flow	-4.0	-.620	-.328

presents the same information for the bottoms enthalpy perturbations. In most cases the bottoms enthalpy transients are not presented, due to inaccurate measurements as described above.

4.4-1 Feed Flow Disturbances

The ability of the model to adequately predict the effect of a feed flow disturbance on the experimental system was studied. The magnitude of the step changes used and the final steady state perturbations obtained are indicated in Tables 4.4-1 and 4.4-2. The model and experimental responses of the overhead enthalpy for feed changes are presented in Figures 4.4-1 and 4.4-2. A similar set of data for the bottoms enthalpy is presented in Figure 4.4-3. These data are presented as a fraction of the total change complete, relative to the final model steady state.

In the case of the positive feed flow step, the tendency is to increase the overhead composition. This tends to force the composition into the equilibrium curve pinch area. The change observed is therefore smaller than that predicted by the linearized model. The model responds slightly faster also, and a delay is observed between the time of disturbance and the experimental response. Figure 4.4-3 shows the bottoms enthalpy response to the same feed flow disturbance. The experimental points illustrate the amount of measurement noise in the filtered signal from the gas chromatograph system. The final steady states, as indicated in Table 4.4-2 show moderate agreement, but the transients do not agree very well.

The overhead enthalpy response to a negative feed flow step are presented in Figure 4.4-2. The model predicts a smaller change than experimentally observed, as the composition moved away from the

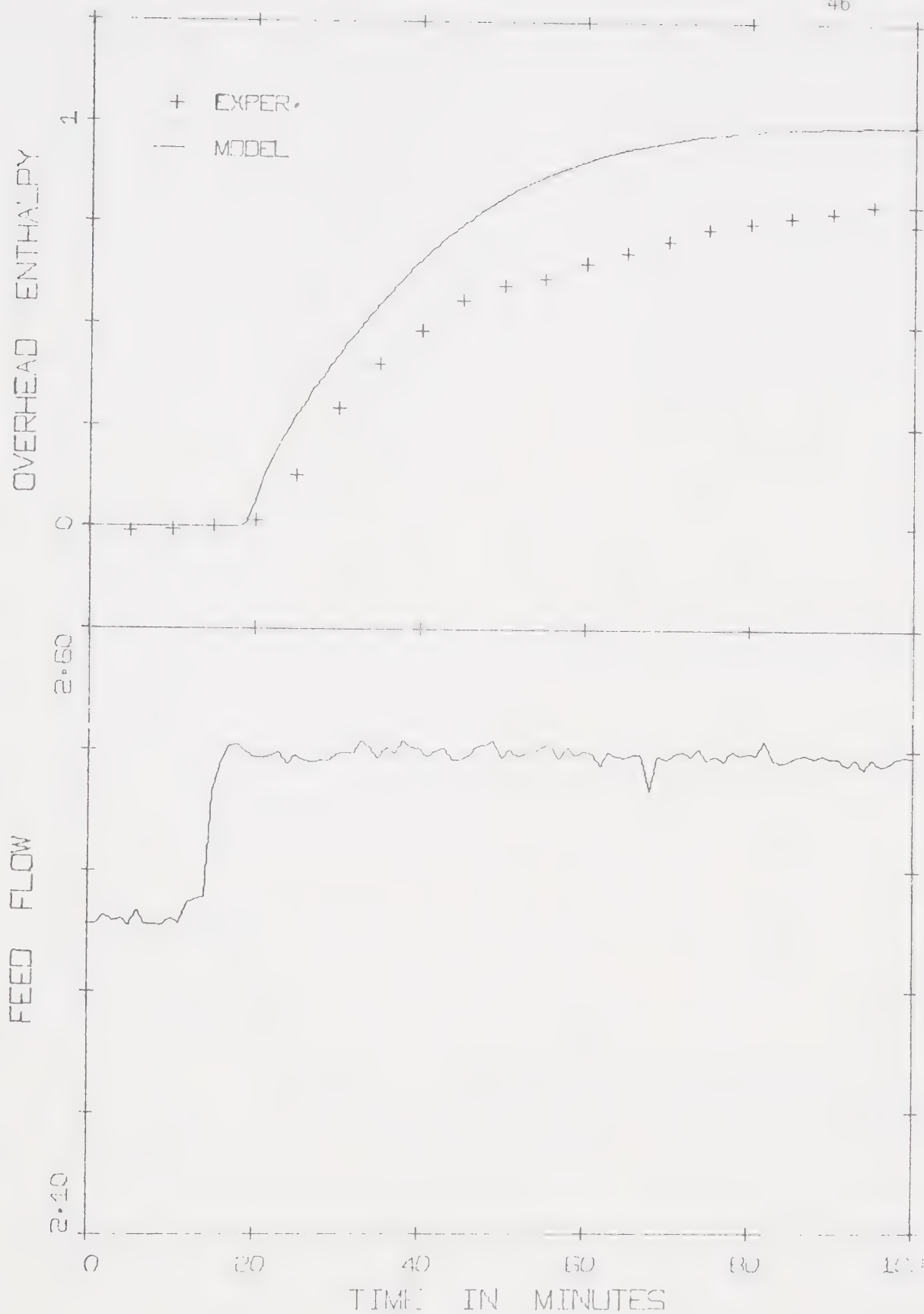


FIGURE 4.4-1: COMPARISON OF MODEL AND EXPERIMENTAL OVERHEAD ENTHALPY RESPONSE TO A POSITIVE FEED FLOW STEP CHANGE

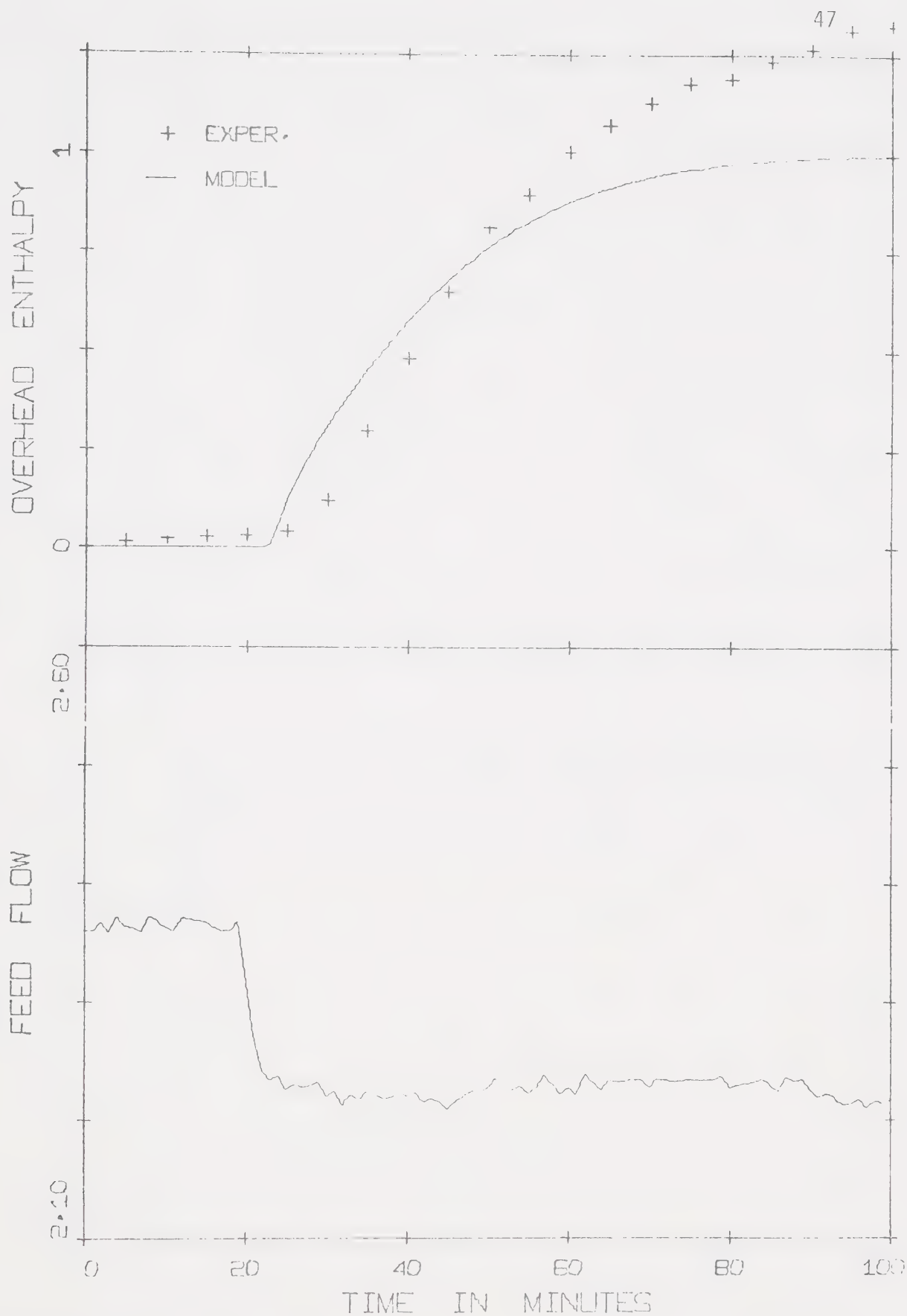


FIGURE 4.4-2: COMPARISON OF MODEL AND EXPERIMENTAL OVERHEAD ENTHALPY RESPONSE TO A NEGATIVE FEED FLOW STEP CHANGE

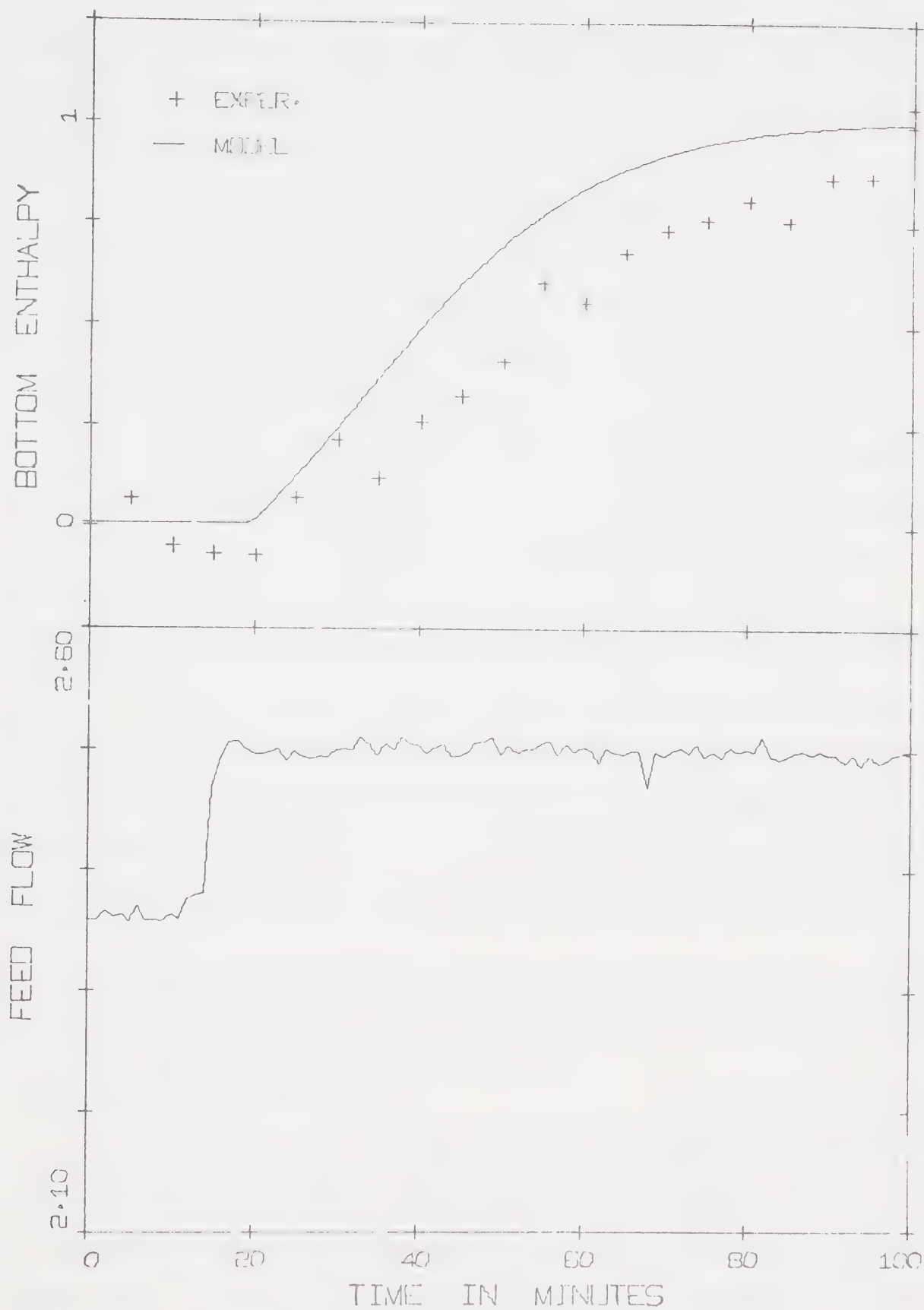


FIGURE 4.4-3: COMPARISON OF MODEL AND EXPERIMENTAL BOTTOMS ENTHALPY RESPONSE TO A POSITIVE FEED FLOW STEP CHANGE

equilibrium curve pinch area. It can be seen that, again, the experimental curve exhibits a short time lag.

4.4-2 Reflux Flow Disturbances

The ability of the model to predict the open loop response to reflux flow changes was tested next. The magnitude of the step changes are presented in Table 4.4-1. Figures 4.4-4 and 4.4-5 indicate the transients obtained in each case. The figures indicate the overhead product enthalpy as a fraction of the final model steady state value.

In the case of a positive flow change, the tendency is toward an increase in product composition. This drives the composition toward the pinch area of the equilibrium curve so the model predicts a larger perturbation than was actually observed. The model also exhibits an initial time lag behind the experimental curve, but it is not very large.

For the case of a negative step in reflux flow as indicated in Figure 4.4-5, the agreement is quite good. The final value predicted by the model is slightly below the experimental one, as the composition moved away from the pinch area. Again the model responds slightly slower initially, so the model response lies entirely below the experimental one.

The final values of the bottoms enthalpy perturbations for the two cases above are presented in Table 4.4-2.

4.4-3 Steam Flow Disturbances

The experimental response of the overhead enthalpy perturbations to steam flow changes are indicated in Figures 4.4-6 and 4.4-7. The responses are presented as a fraction complete, relative to the final model value. The step in steam flow caused a step in reboiler duty which in each case was accompanied by a change in condenser duty of the same

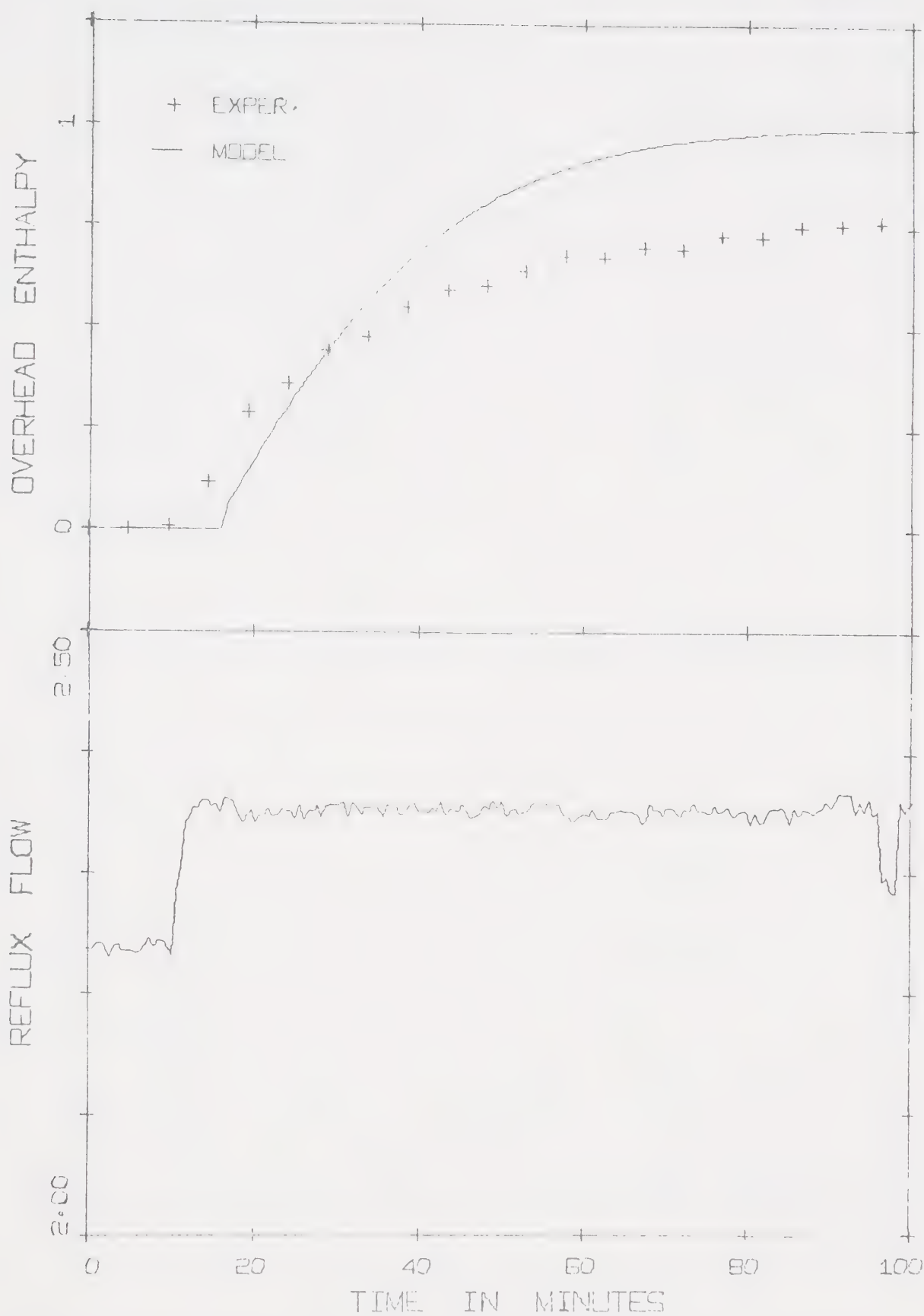


FIGURE 4.4-4: COMPARISON OF MODEL AND EXPERIMENTAL OVERHEAD ENTHALPY RESPONSE TO A POSITIVE REFLUX FLOW STEP CHANGE

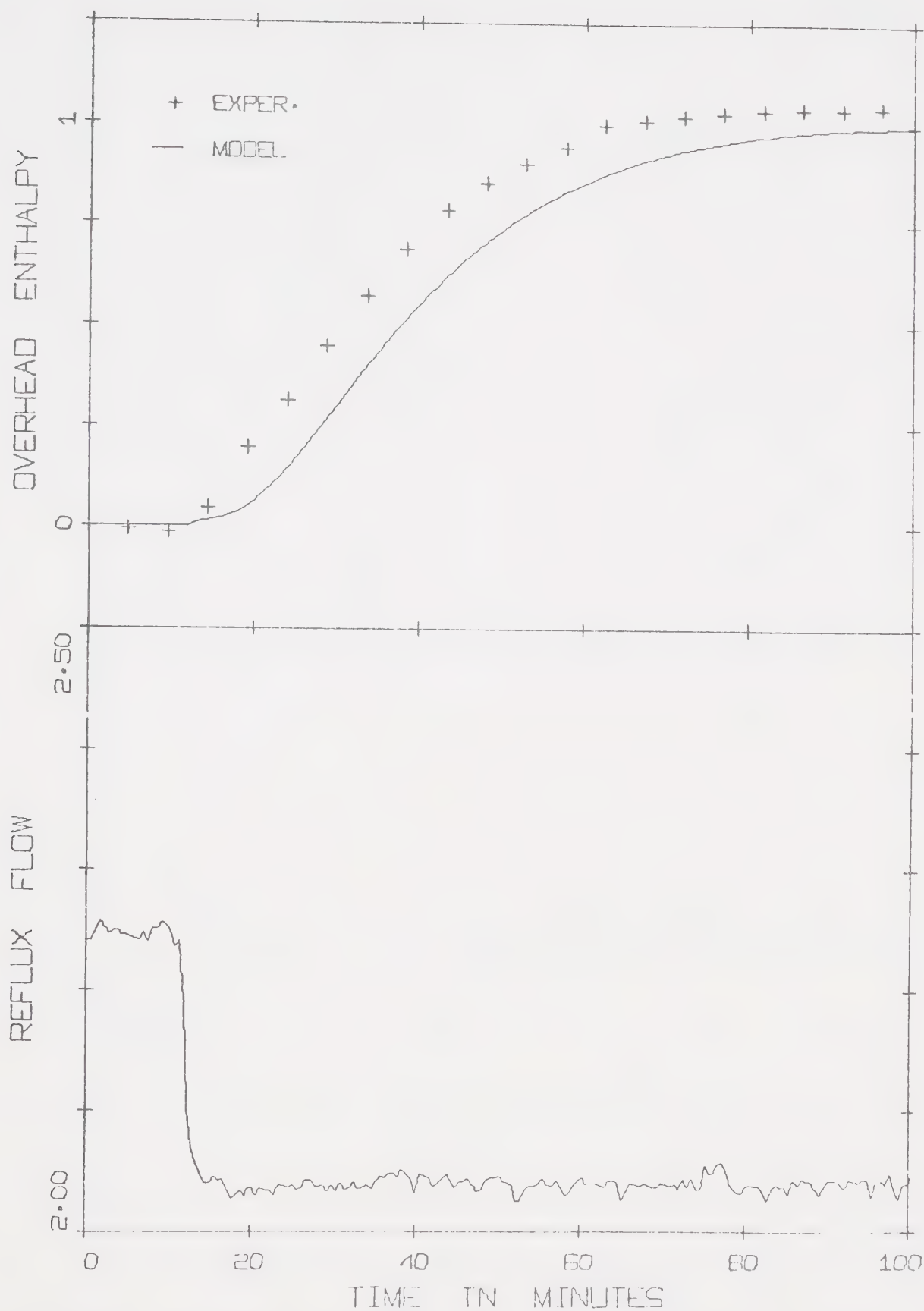


FIGURE 4.4-5: COMPARISON OF MODEL AND EXPERIMENTAL OVERHEAD ENTHALPY RESPONSE TO A NEGATIVE REFLUX FLOW STEP CHANGE

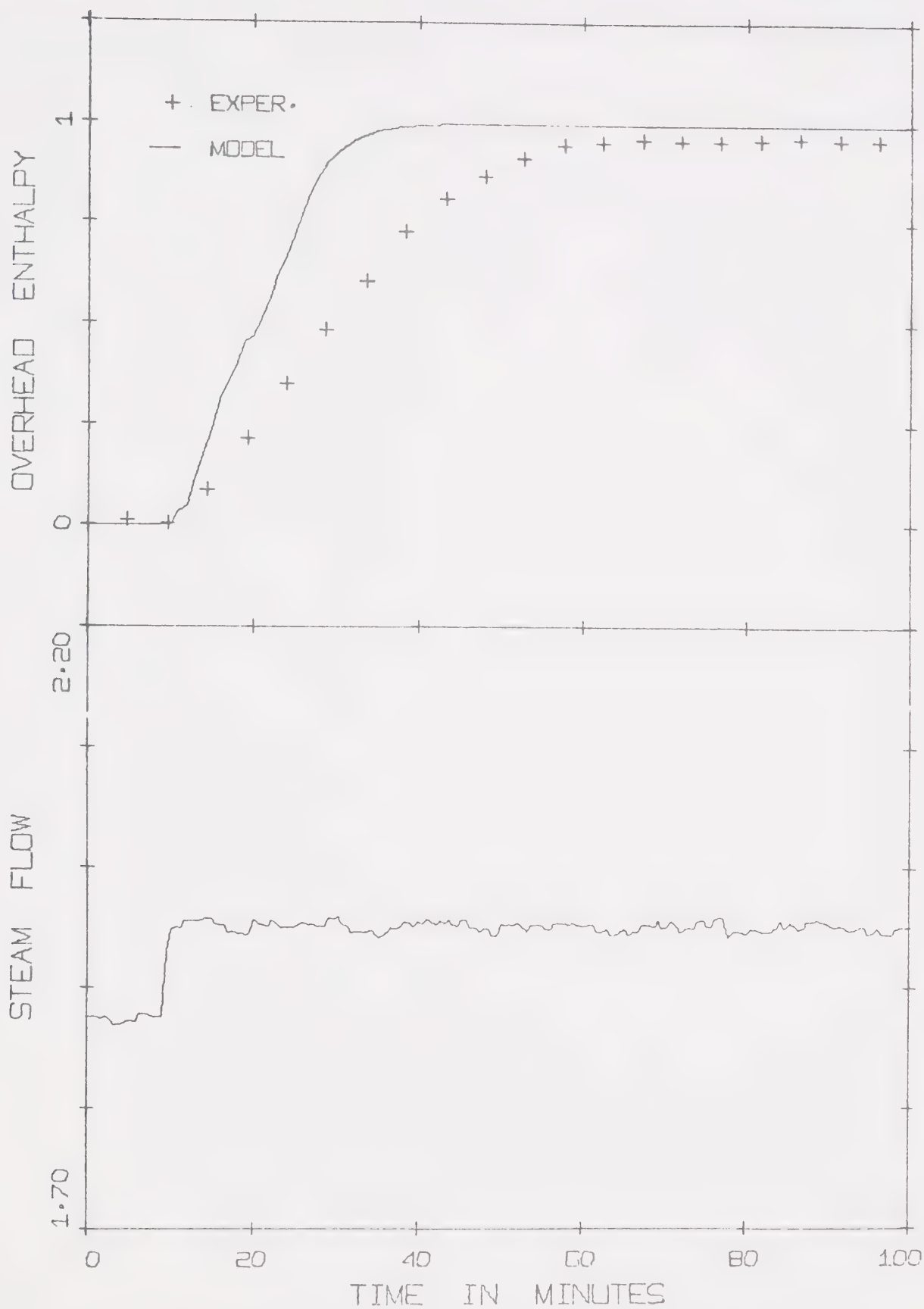


FIGURE 4.4-6: COMPARISON OF MODEL AND EXPERIMENTAL OVERHEAD ENTHALPY RESPONSE TO A POSITIVE STEAM FLOW STEP CHANGE

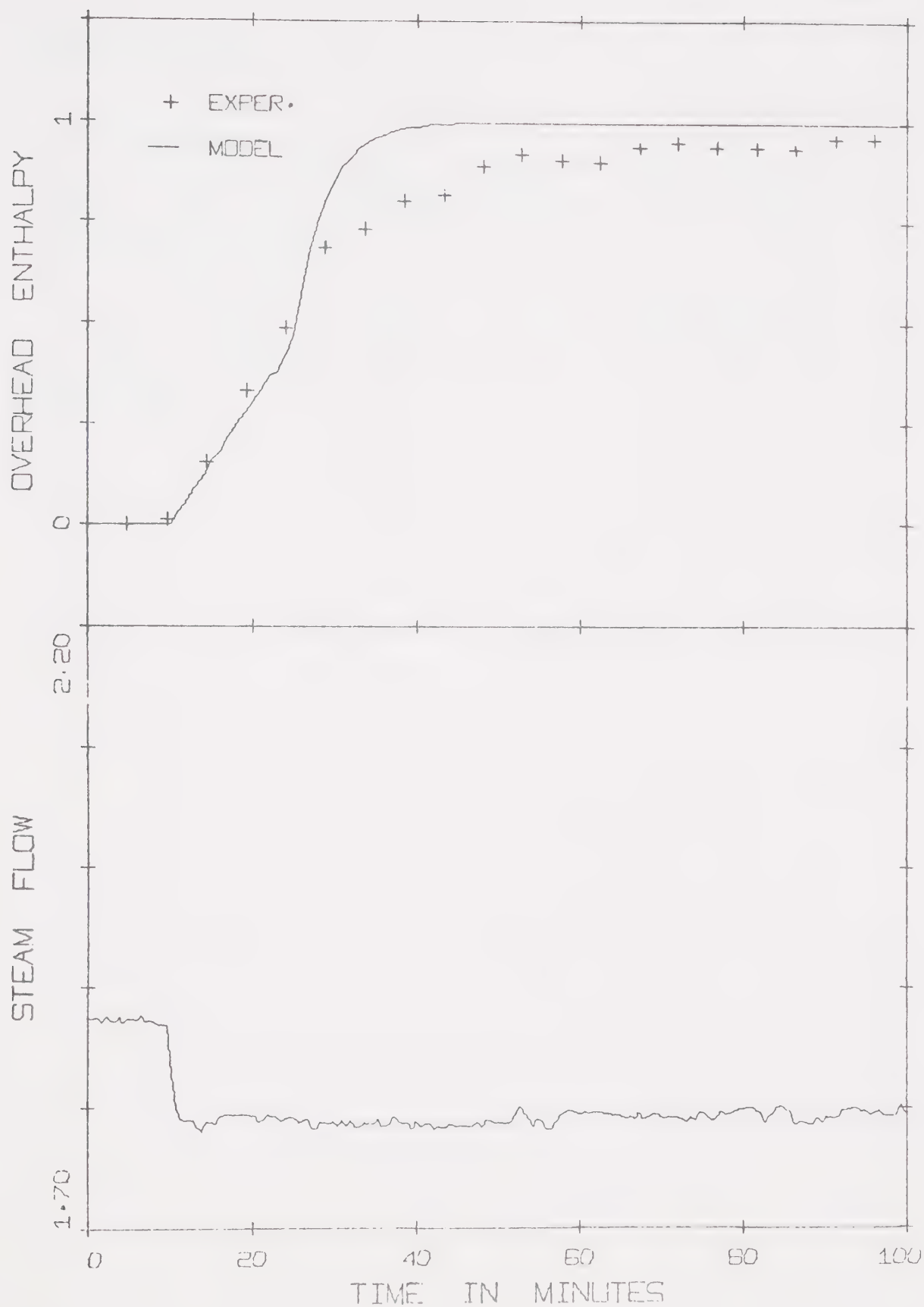


FIGURE 4.4-7: COMPARISON OF MODEL AND EXPERIMENTAL OVERHEAD ENTHALPY RESPONSE TO A NEGATIVE STEAM FLOW STEP CHANGE

order of magnitude.

For both the positive and negative step changes, the model response compares very well with the experimental one. The model reaches a final value quite rapidly, probably due to the assumption of no vapour flow changes.

Again, the final values of the bottoms enthalpy perturbations for these step inputs are presented in Table 4.4-2, but the transients are not shown.

CHAPTER V: MODEL REDUCTION

5.1 Introduction

The model of the distillation system under study as formulated in Chapter III of this work is of order 20. In general, the order of such a model will be $2(N+2)$, where N is the number of trays in the distillation column. For a control study on a large system, the size of the problem thus becomes prohibitive. Also the usual control strategies require values for all states, and in general, many of the states in this model cannot be directly measured. So the feasibility of model reduction was considered. Two approaches were considered and their results compared to the original models and to each other, as outlined in the following sections.

5.2 Marshall's Method

5.2-1 Reduction Theory

This method is the so-called "modal approach" outlined by Marshall [31]. The method has been further studied by Wilson et al [53] and extended to the case of a discrete model. The continuous method, as implemented in the GEMSCOPE system [54] was used in this study.

The method revolves around the partitioning of the states into fast and slow mode states. The reduced order model is comprised of the slow states, and an instantaneous response is assumed for the fast canonical states. The method reduces a model of order n of the form:

$$\dot{\underline{x}} = \underline{A} \underline{x} + \underline{B} \underline{u} \quad (5.2-1)$$

to the reduced model:

$$\dot{\underline{x}}_1 = \underline{A}_R \underline{x}_1 + \underline{B}_R \underline{u} \quad (5.2-2)$$

where \underline{x}_1 are the states to be 'retained', and \underline{A}_R and \underline{B}_R are derived from \underline{A} and \underline{B} as will be indicated below.

Equation (5.2-1) can be rewritten in a partitioned form:

$$\begin{bmatrix} \dot{\underline{x}}_1 \\ \dot{\underline{x}}_2 \end{bmatrix} = \begin{bmatrix} \underline{a}_1 & \underline{a}_2 \\ \underline{a}_3 & \underline{a}_4 \end{bmatrix} \begin{bmatrix} \underline{x}_1 \\ \underline{x}_2 \end{bmatrix} + \begin{bmatrix} \underline{b}_1 \\ \underline{b}_2 \end{bmatrix} \underline{u} \quad (5.2-1a)$$

where \underline{x}_1 are the states to be retained, and \underline{x}_2 are those to be eliminated. An $n \times n$ matrix \underline{M} exists which will transform equation (5.2-1) into the Jordan canonical form [53] by using the similarity transform:

$$\begin{bmatrix} \underline{x}_1 \\ \underline{x}_2 \end{bmatrix} = \begin{bmatrix} \underline{m}_1 & \underline{m}_2 \\ \underline{m}_3 & \underline{m}_4 \end{bmatrix} \begin{bmatrix} \underline{z}_1 \\ \underline{z}_2 \end{bmatrix} \quad (5.2-3)$$

where \underline{z} is the canonical state vector. If the states \underline{x}_1 are to be the 'slow mode' states, matrix \underline{M} is arranged so that its columns are ordered from left to right, in order of decreasing significance of the corresponding eigenvalue of the matrix \underline{A} . When equation (5.2-3) is introduced into equation (5.2-1a), the Jordan canonical form results:

$$\begin{bmatrix} \dot{\underline{z}}_1 \\ \dot{\underline{z}}_2 \end{bmatrix} = \begin{bmatrix} \underline{\alpha}_1 & \underline{0} \\ \underline{0} & \underline{\alpha}_2 \end{bmatrix} \begin{bmatrix} \underline{z}_1 \\ \underline{z}_2 \end{bmatrix} + \begin{bmatrix} \underline{\beta}_1 \\ \underline{\beta}_2 \end{bmatrix} \underline{u} \quad (5.2-4)$$

where $\underline{\alpha}$ which is a block diagonal matrix, and $\underline{\beta}$ are defined by:

$$\underline{\alpha} = \begin{bmatrix} \underline{\alpha}_1 & 0 \\ 0 & \underline{\alpha}_2 \end{bmatrix} = \underline{P} \underline{A} \underline{M} \quad (5.2-5a)$$

$$\underline{\beta} = \begin{bmatrix} \underline{\beta}_1 \\ \underline{\beta}_2 \end{bmatrix} = \underline{P} \underline{B} \quad (5.2-5b)$$

$$\underline{P} = \underline{M}^{-1} = \begin{bmatrix} \underline{p}_1 & \underline{p}_2 \\ \underline{p}_3 & \underline{p}_4 \end{bmatrix} \quad (5.2-5c)$$

From equation (5.2-1a), the following can be written:

$$\dot{\underline{x}}_1 = \underline{a}_1 \underline{x}_1 + \underline{a}_2 \underline{x}_2 + \underline{b}_1 \underline{u} \quad (5.2-6)$$

An expression for \underline{x}_2 can be obtained from equation (5.2-3) and (5.2-5c), yielding:

$$\underline{x}_2 = \underline{p}_4^{-1} [\underline{z}_2 - \underline{p}_3 \underline{x}_1] \quad (5.2-7)$$

Since the \underline{z}_2 canonical states are assumed to correspond to the fast modes, assume that:

$$\dot{\underline{z}}_2 = \underline{\alpha}_2 \underline{z}_2 + \underline{\beta}_2 \underline{u} = 0$$

so that

$$\underline{z}_2 = - \underline{\alpha}_2^{-1} \underline{\beta}_2 \underline{u}$$

This expression is then substituted into equation (5.2-7) to yield:

$$\underline{x}_2 = \underline{p}_4^{-1} [-\underline{\alpha}_2^{-1} \underline{\beta}_2 u - \underline{p}_3 \underline{x}_1]$$

This can then be substituted into equation (5.2-6) to yield:

$$\dot{\underline{x}}_1 = \underline{A}_R \underline{x}_1 + \underline{B}_R u \quad (5.2-8a)$$

where

$$\underline{A}_R = [\underline{a}_1 - \underline{a}_2 \underline{p}_4^{-1} \underline{p}_3] \quad (5.2-8b)$$

$$\underline{B}_R = [\underline{b}_1 - \underline{a}_2 \underline{p}_4^{-1} \underline{\alpha}_2^{-1} \underline{\beta}_2] \quad (5.2-8c)$$

For the extension of the above method to the discrete model case, and for equivalent forms of the \underline{A}_R matrix see Wilson et al [53].

5.2-2 Reduction Results

Marshall's reduction method as implemented in the GEMSCOPE system [54] was used in an attempt to reduce the 20 state distillation model, to one which could be used for a control study. This reduction method permits the choice of which states and which eigenvalues to retain in the reduced model. Several combinations of states and eigenvalues were tried, in an attempt to obtain a valid reduced model. The problem was assumed to be one of removing all unmeasurable states, i.e. internal liquid flows, and as many enthalpies as possible. The models obtained were compared to the original one for a given disturbance and thus accepted or rejected. No acceptable two state model was found.

One of the better models obtained was a fourth order model in which the states were the enthalpies in the first, fourth, sixth and tenth stages. Figures 5.2-1 to 5.2-3 compare the end product enthalpy perturbation transients in normalized form as predicted by the four and twenty state models, for various step inputs.

In Figure 5.2-1 the responses to a feed flow disturbance are

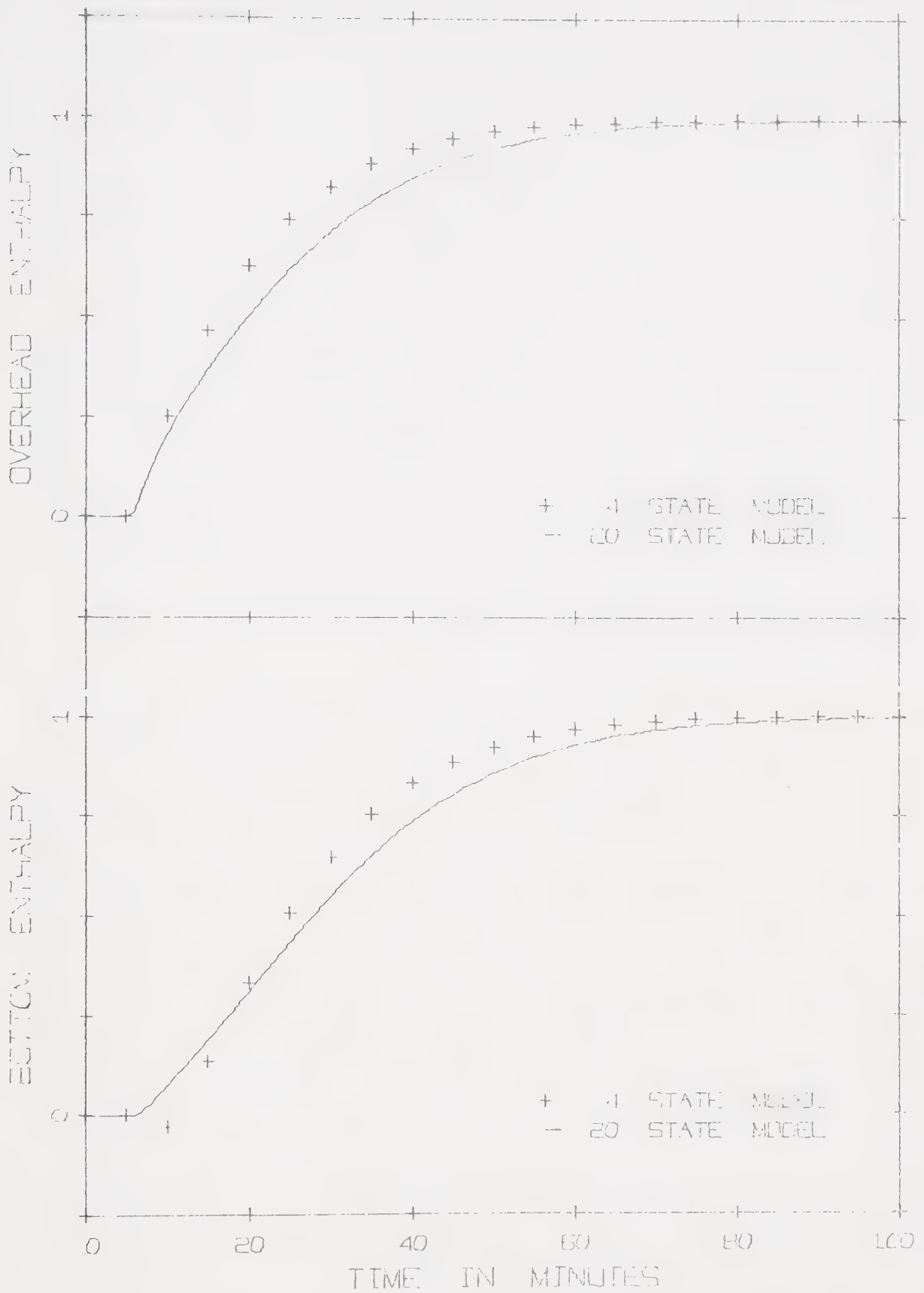


FIGURE 5.2-1: COMPARISON OF TWENTY AND FOUR STATE MODELS FOR A FEED FLOW STEP CHANGE

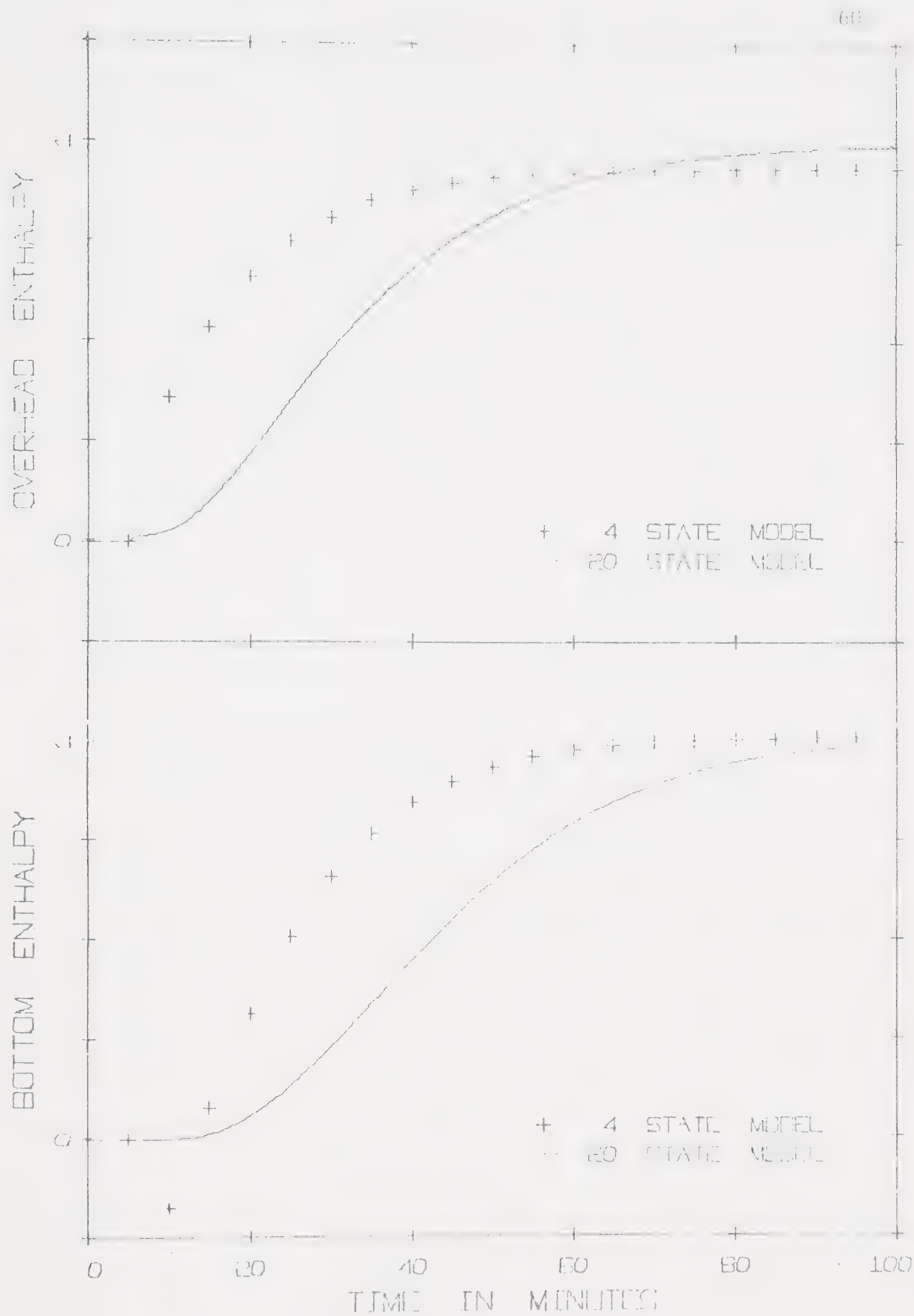


FIGURE 5.2-2: COMPARISON OF TWENTY AND FOUR STATE MODELS FOR A REFLUX FLOW STEP CHANGE

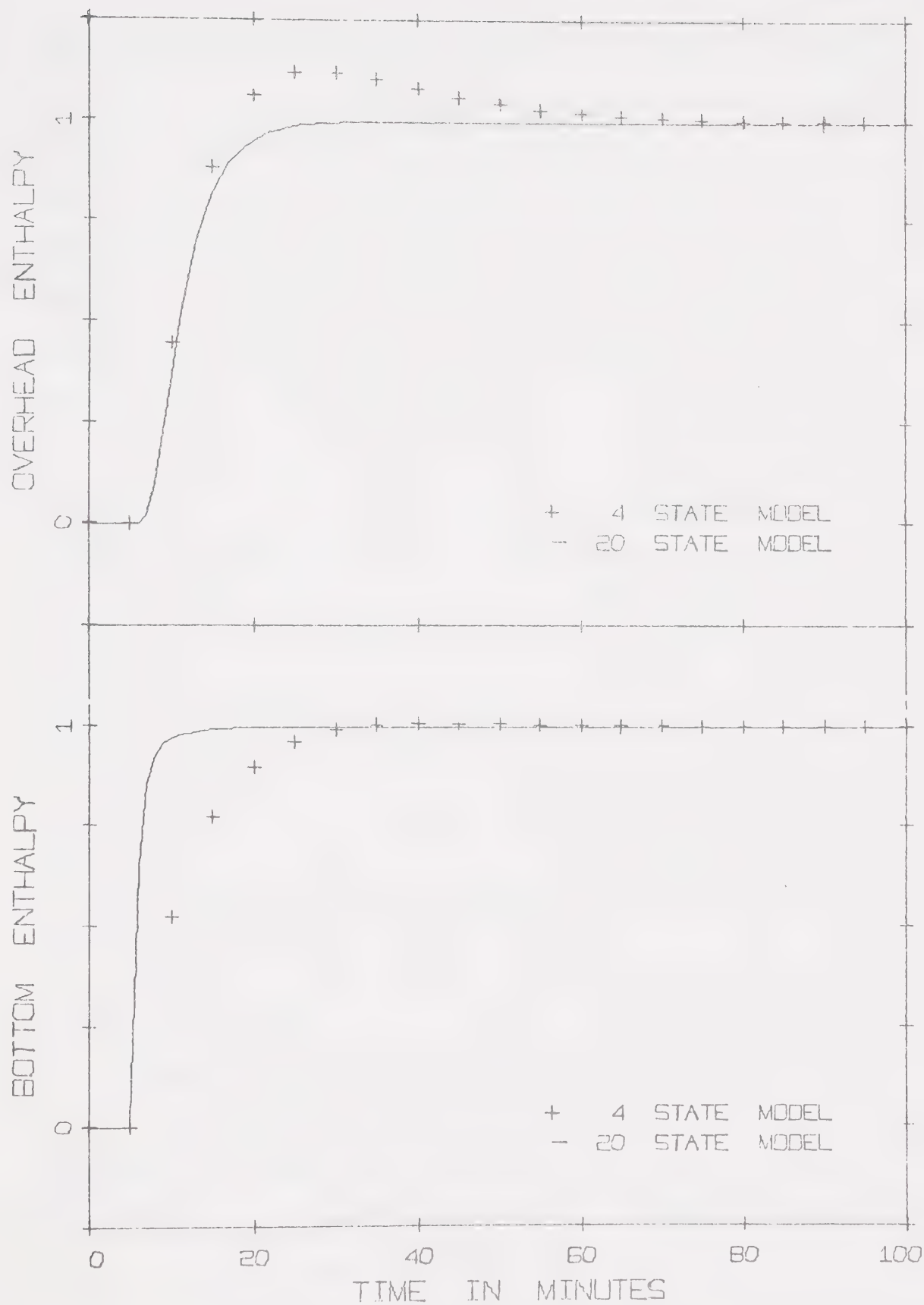


FIGURE 5.2-3: COMPARISON OF TWENTY AND FOUR STATE MODELS FOR A STEAM FLOW STEP CHANGE

shown, and good agreement between the models is observed. In the case of a reflux flow step, illustrated in Figure 5.2-2 the four state model exhibits a response that is appreciably faster than the original large model. For the reboiler duty disturbance, illustrated in Figure 5.2-3, both models exhibit rapid responses, with the four state model exhibiting some overshoot. In all cases, the final steady state values are comparable since the reduction method preserves the final steady state values, for step input disturbances.

As stated earlier, several combinations of states and eigenvalues were tried, in an attempt to obtain an adequate model. Many problems were encountered in these attempts to reduce the model, such as "instant" responses and "infinite" final steady state values. It is thought that these problems stem from the grouping of eigenvalues, and from selecting some from each group. Table 5.2-1 presents a tabulation of a sample set of eigenvalues of the 20 state model.

Because of these problems, and the desirability of a two state model, in which only the product enthalpies appear, it was decided to attempt another, more analytical reduction method. This method is outlined in the following sections.

5.3 Anderson's Method

5.3-1 Reduction Method

This method is a 'least-squares approach' to model reduction. The method has been outlined by Anderson [2] and is used to find a reduced discrete model which approximates the response of a larger model.

Given a discrete model of the form:

$$\underline{x}(k+1) = \underline{\phi} \underline{x}(k) + \underline{\Delta} \underline{u}(k) \quad (5.3-1)$$

TABLE 5.2-1: Sample Model Eigenvalues

i	λ_i	i	λ_i
1	-.0990	11	-.333
2	-.100	12	-1.05
3	-.101	13	-1.33
4	-.123	14	-2.51
5	-.125	15	-3.18
6	-.126	16	-4.49
7	-.200	17	-5.71
8	-.250	18	-6.95
9	-.256	19	-7.89
10	-.260	20	-15.9

a reduced model:

$$\underline{x}_1(k+1) = \underline{\phi}_R \underline{x}_1(k) + \underline{\Delta}_R \underline{u}(k) \quad (5.3-2)$$

can be found, which approximates the response of the original model for the states to be retained, designated as \underline{x}_1 , the first r states.

The method requires the values for the states and disturbances for a number of time intervals, say $(\ell+1)$, where ℓ is the number of points to be fit. Form the vector:

$$\underline{b}_q^T = [x_q(T) : x_q(2T) : \dots : x_q((\ell+1)T)]$$

where T is the discrete model time interval, and q refers to a specific state. Also the vector \underline{c}_q can be formed of the elements of $\underline{\phi}_R$ and $\underline{\Delta}_R$ to be determined as:

$$\underline{c}_q^T = [\phi_{q1} : \phi_{q2} : \dots : \phi_{qr} \Delta_{q1} \dots \Delta_{qm}]$$

If the matrices $\hat{\underline{B}}$ and $\hat{\underline{C}}$ are formed from these vectors, such that

$$\hat{\underline{B}} = [\underline{b}_1 : \underline{b}_2 : \dots : \underline{b}_r]$$

and
$$\hat{\underline{C}} = [\underline{c}_1 : \underline{c}_2 : \dots : \underline{c}_r]$$

where the first r states are to be retained.

Also, definition of a set of vectors of the form:

$$\underline{m}_{i+1} = [x_1(iT) : x_2(iT) \dots x_r(iT) : u_1(iT) : \dots : u_m(iT)]$$

allows the formation of a matrix $\hat{\underline{m}}$ such that:

$$\hat{\underline{\underline{m}}} = \begin{bmatrix} \underline{\underline{m}}_1^T \\ \underline{\underline{m}}_2^T \\ \vdots \\ \underline{\underline{m}}_{\ell+1}^T \end{bmatrix}$$

By inspection of matrices $\hat{\underline{\underline{B}}}$, $\hat{\underline{\underline{C}}}$ and $\hat{\underline{\underline{m}}}$ it can be seen that the time domain solution of the first r states is:

$$\hat{\underline{\underline{B}}} = \hat{\underline{\underline{m}}} \hat{\underline{\underline{C}}} \quad (5.3-3)$$

and that $\hat{\underline{\underline{C}}}$ will yield $\underline{\underline{\phi}}_R$ and $\underline{\underline{\Delta}}_R$ since:

$$\hat{\underline{\underline{C}}} = [\underline{\underline{\phi}}_R : \underline{\underline{\Delta}}_R] \quad (5.3-4)$$

Anderson [2] has indicated that the solution does exist and also minimizes a quadratic error index of the least squares type.

The solution to Equation (5.3-3) cannot be directly obtained and a pseudo-inverse approach is needed. This approach yields:

$$\hat{\underline{\underline{C}}}^T = [\underline{\underline{\phi}}_R : \underline{\underline{\Delta}}_R] = \hat{\underline{\underline{B}}}^T \hat{\underline{\underline{m}}} (\hat{\underline{\underline{m}}}^T \hat{\underline{\underline{m}}})^{-1}$$

5.3-2 Reduction Results

The reduction method outlined in the previous section is essentially one of fitting a set model form to transient data generated for a set disturbance by a least squares technique. The simplest form of disturbance to use is a step disturbance, so this form of forcing was used. However, only one step could be used at a time or the matrix $[\hat{\underline{\underline{m}}}^T \hat{\underline{\underline{m}}}]$ would be singular. Because of this, each disturbance was fit in turn, so five reduced state transition matrices ($\underline{\underline{\phi}}_R$) and the five

vectors δ_{Ri} , the columns of Δ_R were obtained. Since the distillation column responds differently for various disturbances, the five state transition matrices obtained are different.

The matrices corresponding to the feed flow, reflux flow and feed enthalpy disturbances were all quite similar. The matrices corresponding to reboiler and condenser duty were similar to one another but were quite different from the other three. Since one matrix ϕ_R must be used, one very similar to the former three was chosen, and the columns of the matrix Δ_R manipulated to give the same final steady states as the original reduced models. The effect of this approximation is to slightly slow down the responses to condenser and to reboiler duty changes, while keeping the responses to the other three disturbances essentially the same as the original model. The resulting reduced model is presented in Figure 5.3-1, with a sample interval of one minute.

The responses of this two state model to several disturbances are compared to those of the twenty state model in Figures 5.3-2 to 5.3-4. The responses to a feed flow step are very much alike, as indicated in Figure 5.3-2. The responses to a reflux flow step are shown in Figure 5.3-3 and it can be seen that the reduced model responds faster than the original model and does not exhibit an initial lag. Figure 5.3-4 compares the responses to reboiler duty changes and it can be seen that the reduced model is appreciably slower than the original model. The application of this reduced model, therefore, has the effect of slowing down the response to a steam flow change.

5.4 Conclusions

The reduced models described in the previous sections both

$$\underline{x}_R(k+1) = \underline{\phi}_R \underline{x}_R(k) + \underline{\Delta}_R \underline{u}(k)$$

$$\begin{bmatrix} h_1^i(k+1) \\ h_{10}^i(k+1) \end{bmatrix} = \begin{bmatrix} 0.955 & -.00610 \\ 0.0130 & 0.950 \end{bmatrix} \begin{bmatrix} h_1^i(k) \\ h_{10}^i(k) \end{bmatrix} + \begin{bmatrix} -.0198 & -.0126 & .00260 & 0.0 & .000200 \\ -.0972 & -.0795 & .00120 & -.00150 & .00280 \end{bmatrix}$$

$$\begin{bmatrix} F^i \\ L_{10}^i \\ Q_R^i \\ Q_C^i \\ h_c^i \end{bmatrix}$$

FIGURE 5.3-1: REDUCED MODEL

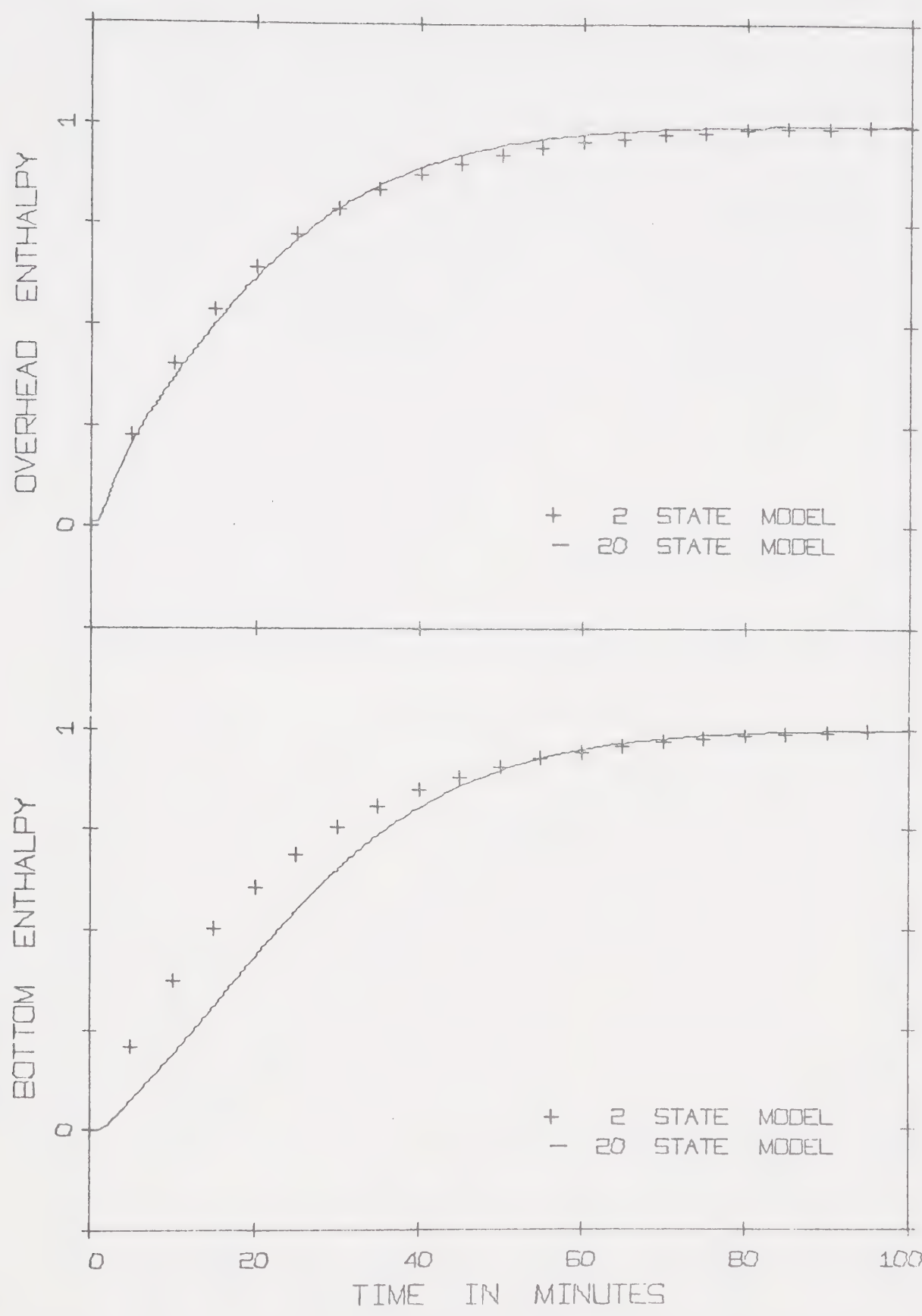


FIGURE 5.3-2: COMPARISON OF TWENTY AND TWO STATE MODELS FOR A FEED FLOW STEP CHANGE

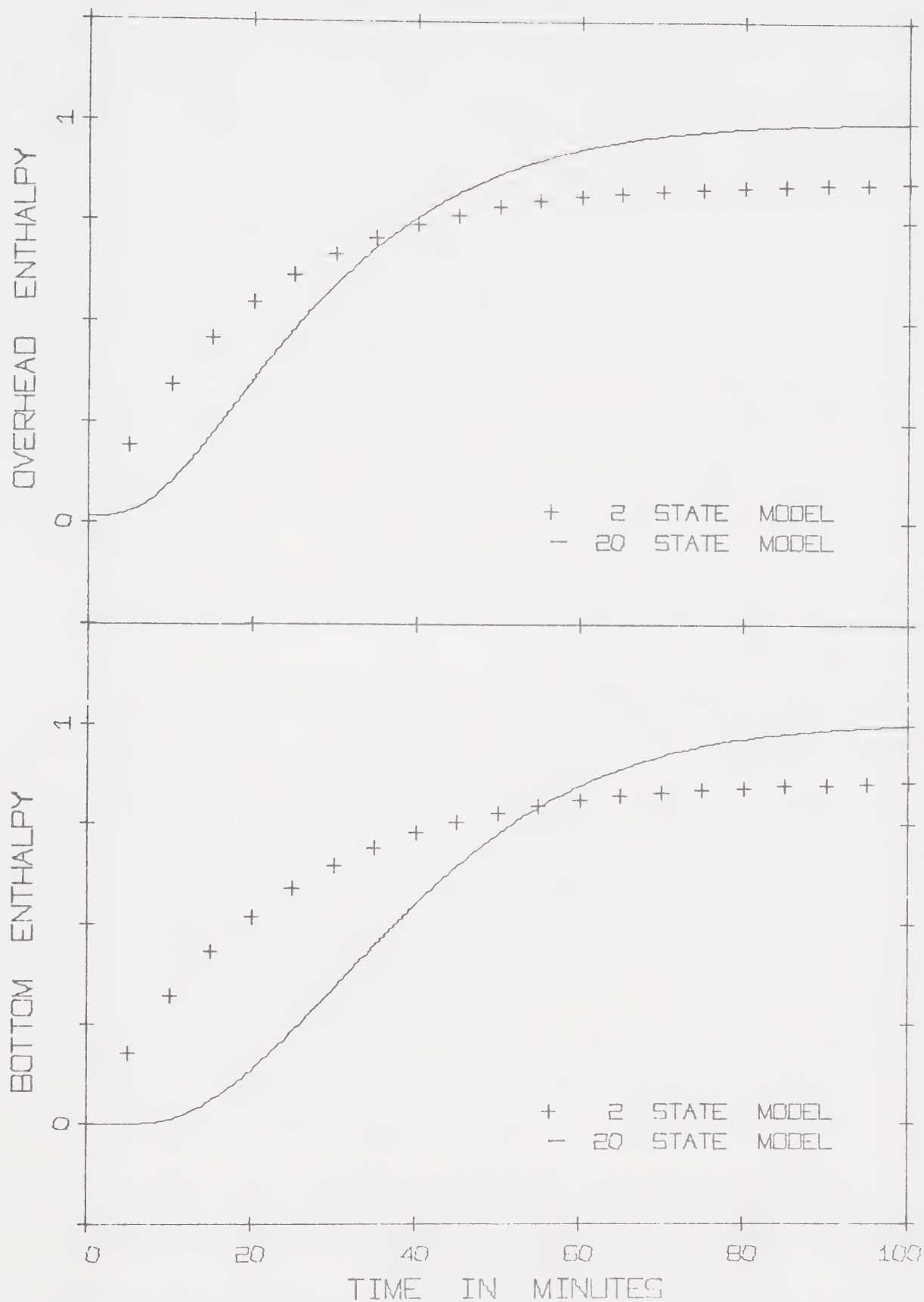


FIGURE 5.3-3: COMPARISON OF TWENTY AND TWO STATE MODELS FOR A REFLUX FLOW STEP CHANGE

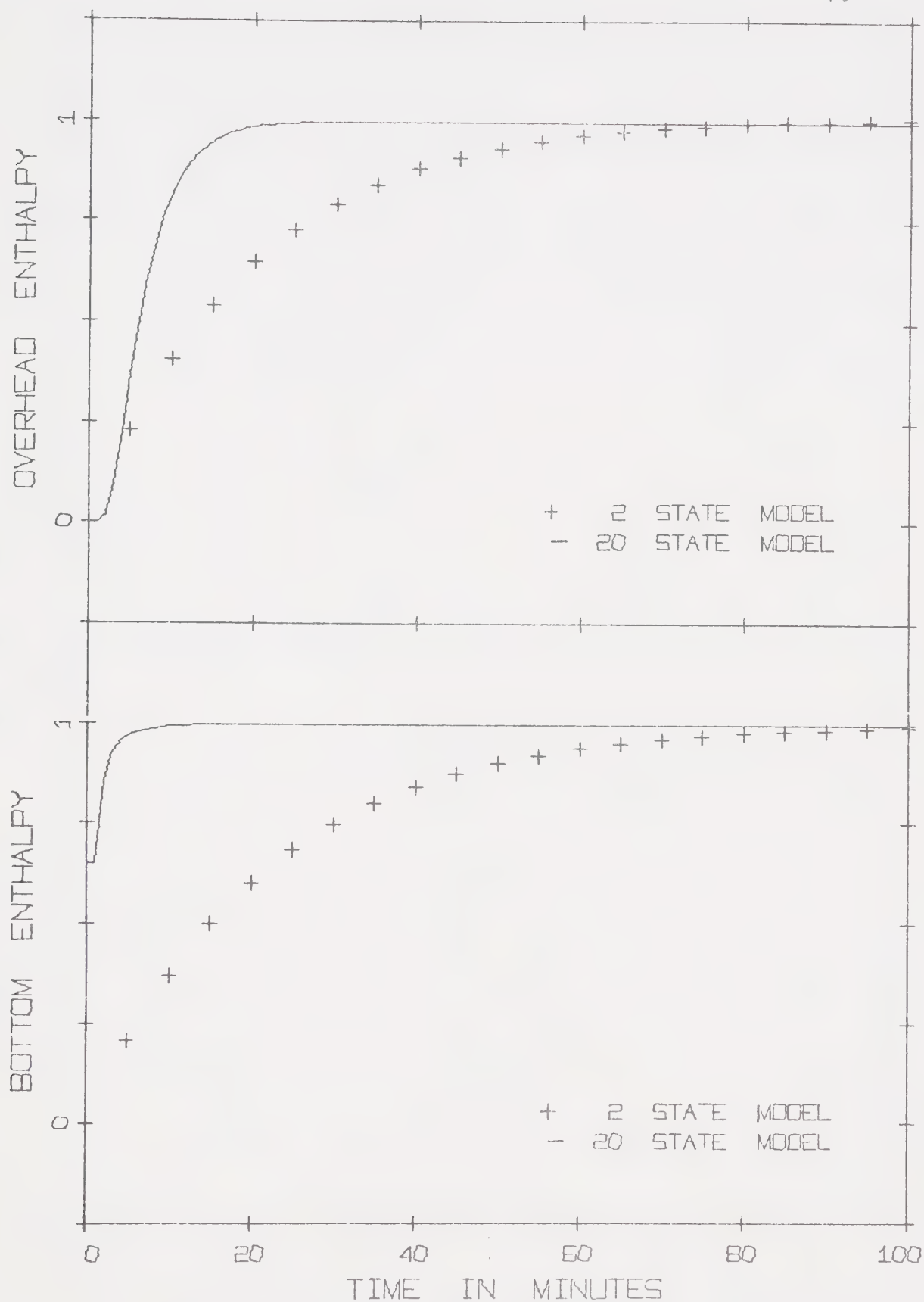


FIGURE 5.3-4: COMPARISON OF TWENTY AND TWO STATE MODELS FOR A STEAM FLOW STEP CHANGE

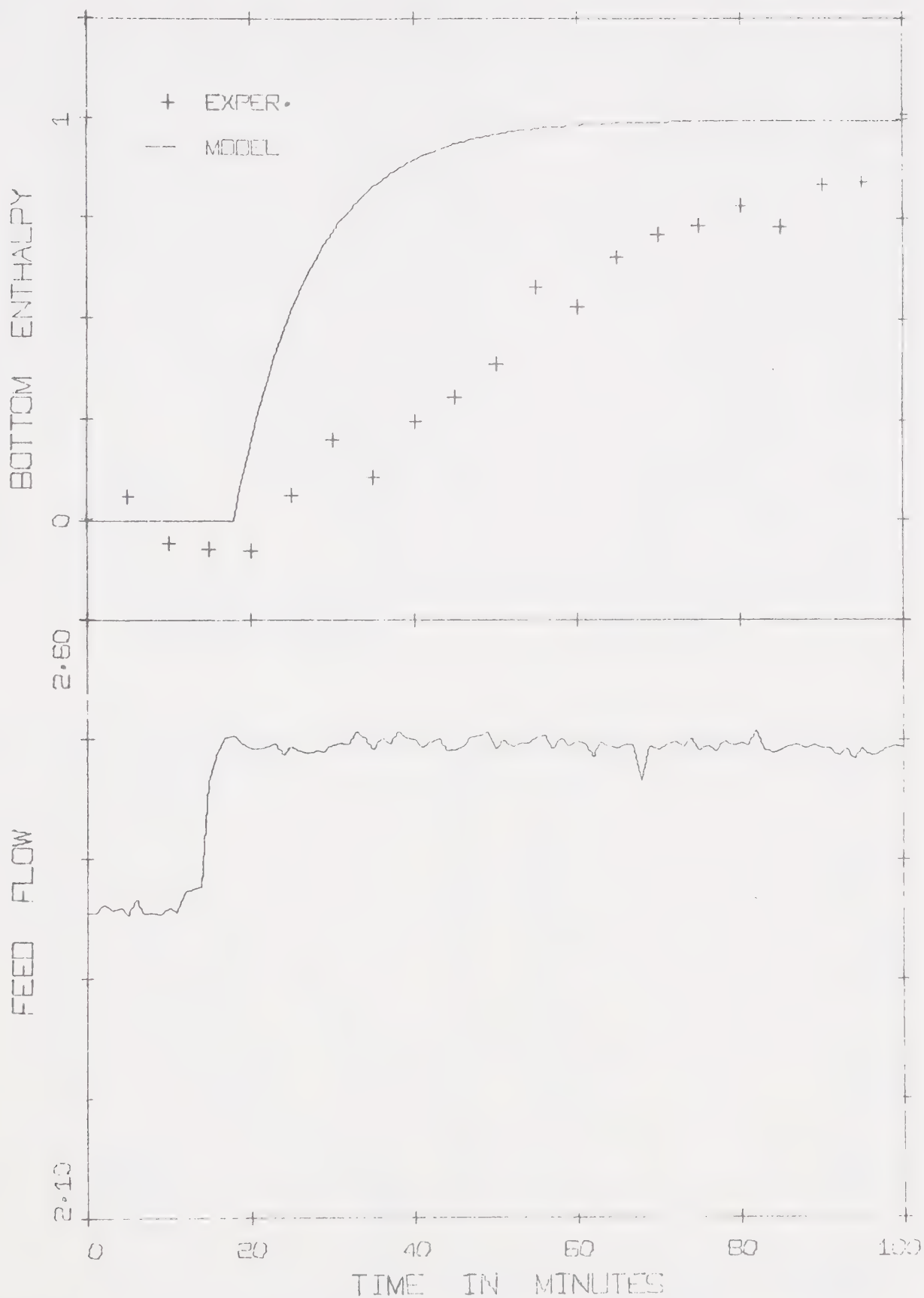


FIGURE 5.4-1: EXPERIMENTAL AND TWO STATE MODEL BOTTOM ENTHALPY RESPONSES TO A POSITIVE FEED FLOW STEP CHANGE

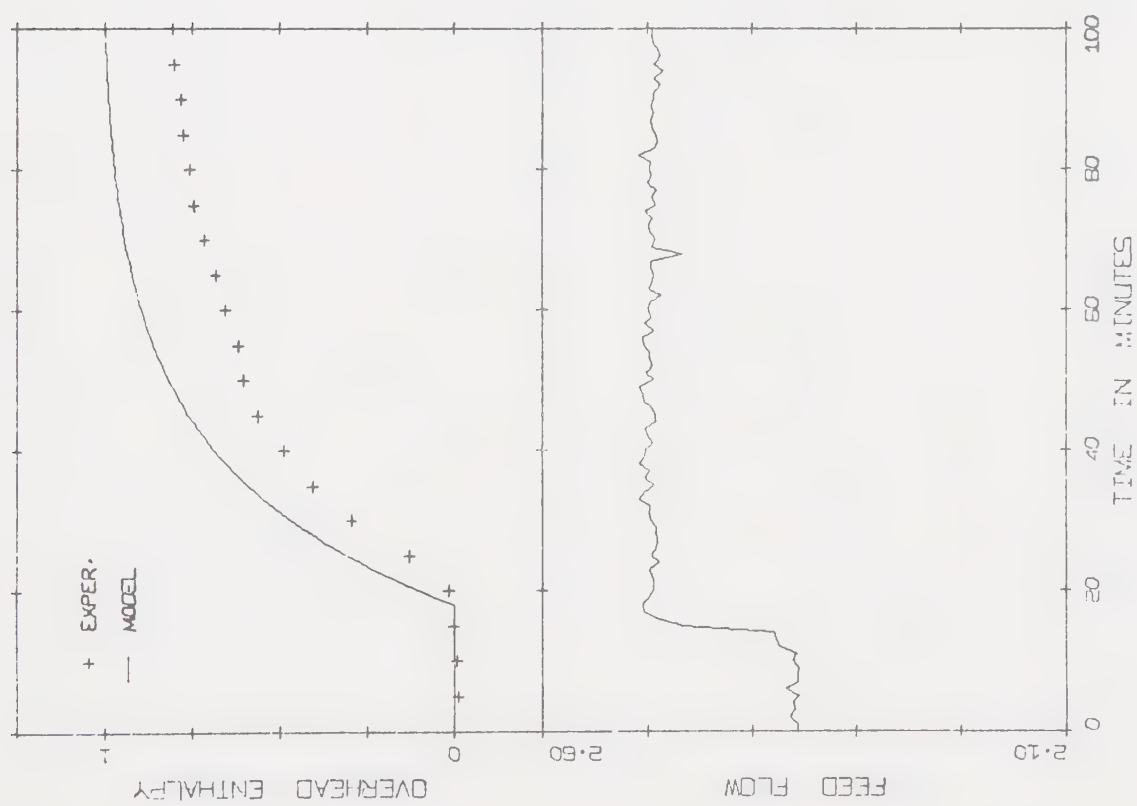
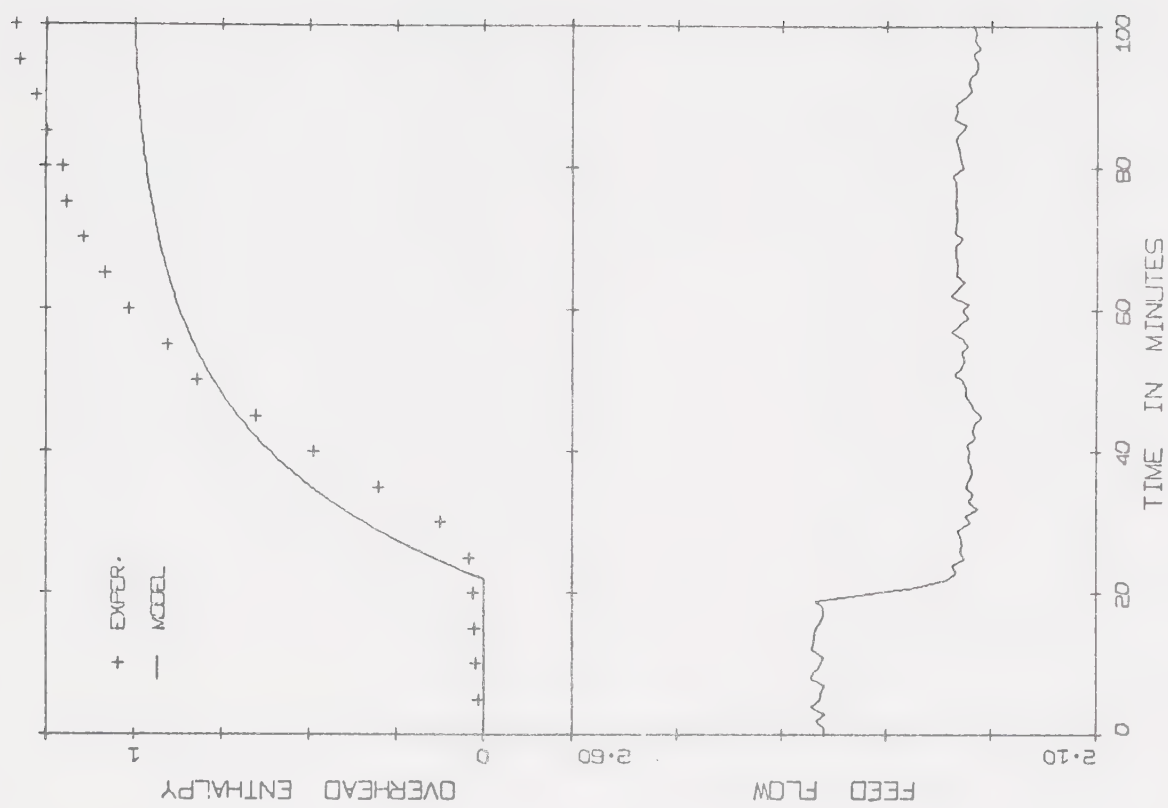


FIGURE 5.4-2: EXPERIMENTAL AND TWO STATE MODEL OVERHEAD ENTHALPY RESPONSES TO FEED FLOW STEP CHANGES

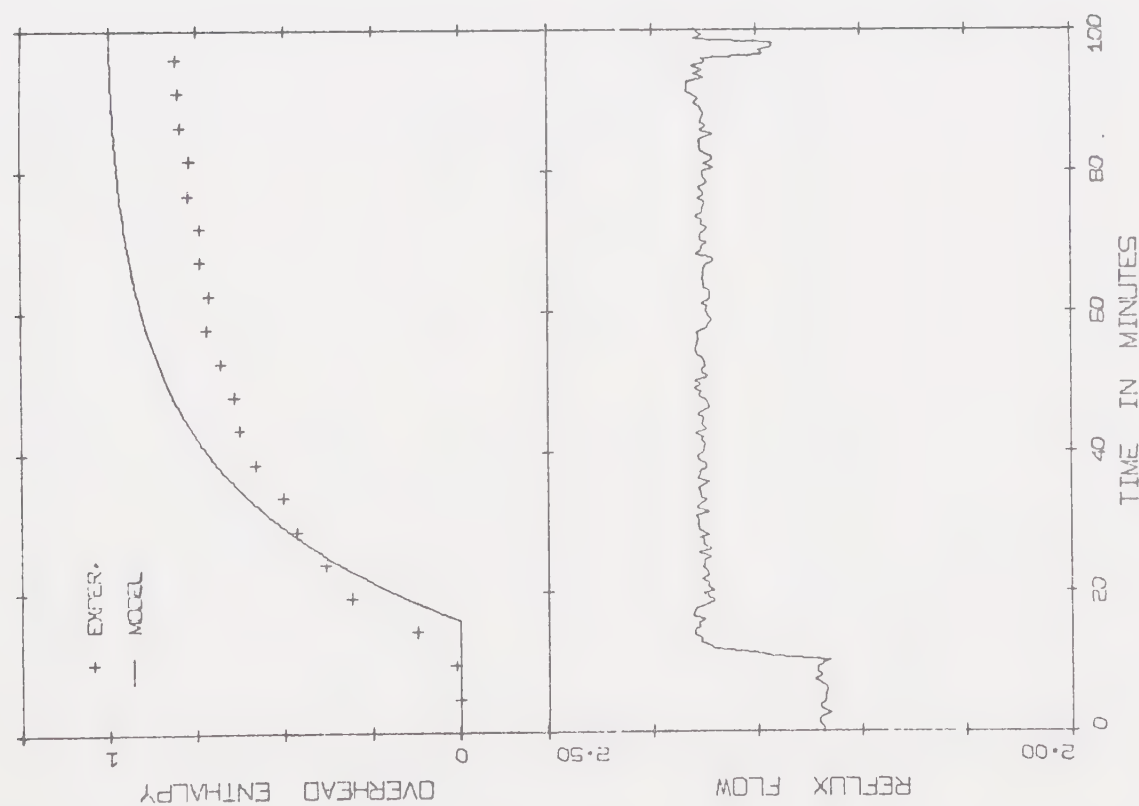
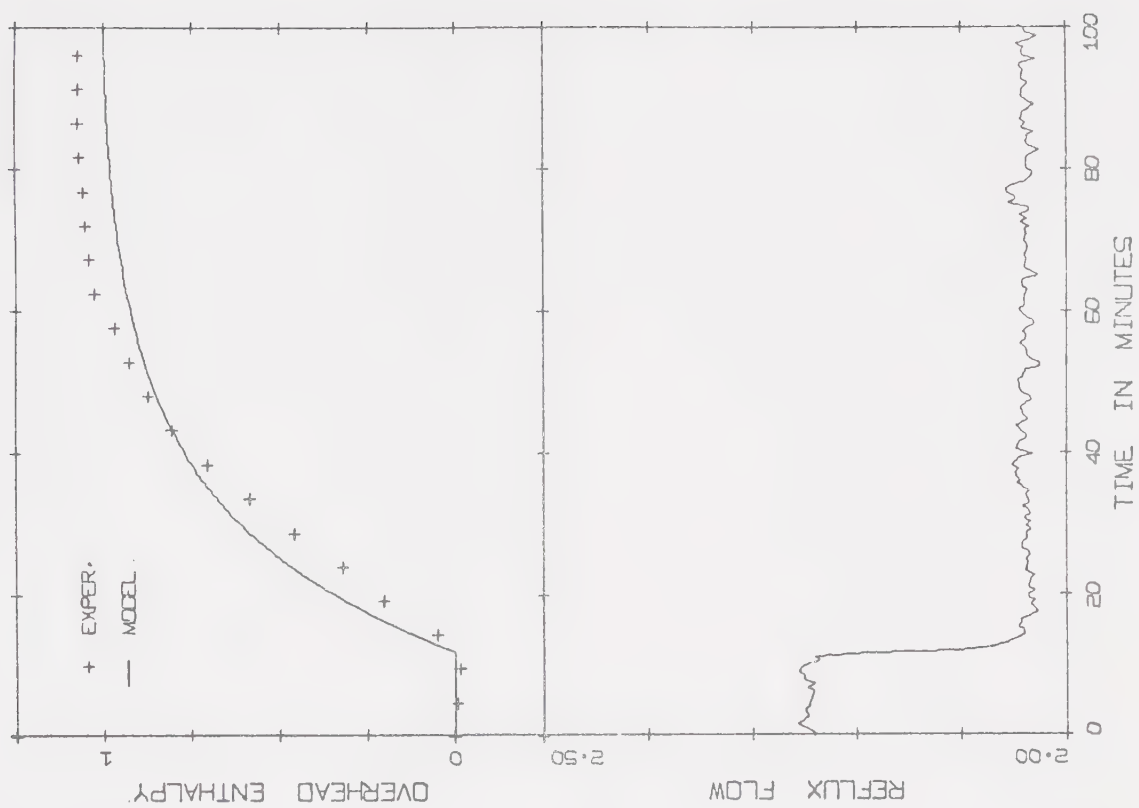


FIGURE 5.4-3: EXPERIMENTAL AND TWO STATE MODEL OVERHEAD ENTHALPY RESPONSES TO REFLUX FLOW STEP CHANGES

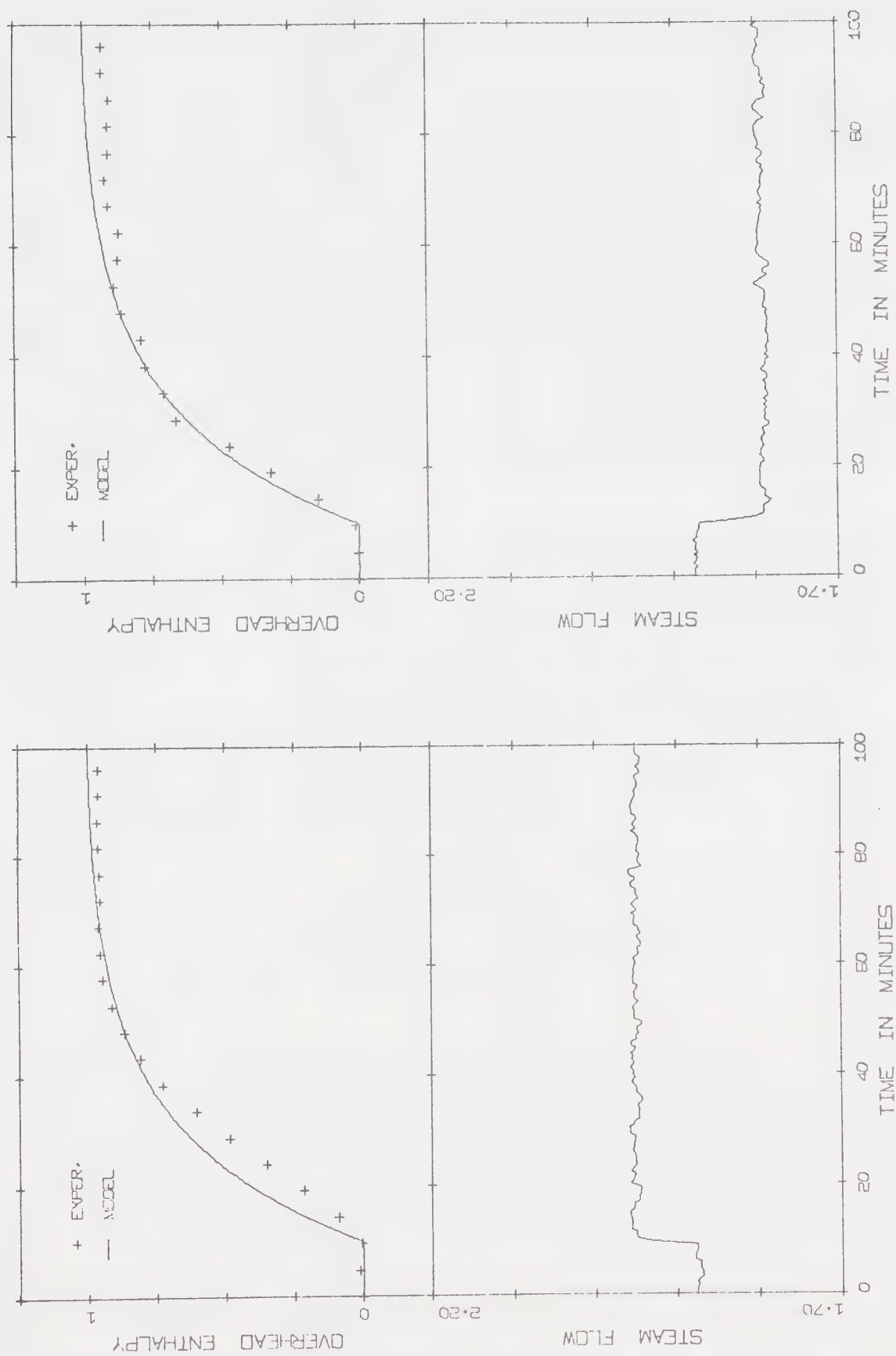


FIGURE 5.4-4: EXPERIMENTAL AND TWO STATE MODEL OVERHEAD ENTHALPY RESPONSES TO STEAM FLOW STEP CHANGES

compare very well to the original model for given disturbances. The four state model compares better than the two state one for reboiler duty changes, but the converse is true for reflux flow changes. The two state model has the obvious advantage that both states can be easily calculated from the measured end product compositions, whereas the four state model has two states, the fourth and sixth stage enthalpies which can only be approximated from noisy temperature measurements. Because of this disadvantage and the comparable response of each model, it was decided to use the two state model for control studies.

Before proceeding to control studies, the two state model was compared to the experimental data used to test the original model. Figures 5.4-1 to 5.4-4 show the comparison of the model and the experimental data. In each case the model response is comparable to the original 20 state model as presented in Chapter IV, and the comparison to experimental data shows moderate agreement.

CHAPTER VI

CONTROL STUDIES

6.1 Introduction

The objective of this study was to attempt to formulate a control strategy whereby both the overhead and bottom product compositions would be simultaneously controlled at preset values. In a single loop configuration the reflux flow is used to control top product composition and heat input to the reboiler, or steam flow is used to control the bottom product composition. However, as described previously, the reflux flow affects the bottoms composition, and the steam flow affects the top product composition. This interaction can give rise to problems when simultaneous control of both product compositions is attempted.

In any attempt to control the end compositions, some indication of their actual values and variations must be available. In this study the compositions themselves were measured and used to adjust the specific control variables. The overhead product composition was continually monitored by an in-line capacitance cell, and the bottom composition by a gas chromatograph operating under digital computer supervision.

In the control studies, the first step involved performing several single loop tests, changing the feedback gains, to establish "suitable" values. This was done for both top and bottom product control loops. The gains found in these tests were then combined in a multiloop configuration to demonstrate the extent of interaction between the loops. The state space model was then used to derive a multivariable control scheme for experimental evaluation.

6.2 Single Loop Control

As previously mentioned the first step in the series of control studies was to perform single loop tests. This served two purposes; to determine actual feedback controller gains, and to test the digital computer control programs. However, prior to the experimental tests, the controllers were studied by digital simulation using the two state model. The following sections describe these tests and their results.

6.2-1 Simulation Studies

The model and general feedback control law can be designated:

$$\underline{x}(k+1) = \underline{\phi} \underline{x}(k) + \underline{\Delta} \underline{d}(k) + \underline{\beta} \underline{u}(k)$$

$$\underline{u}(k) = \underline{K}_{FB} \underline{x}(k)$$

For the single loop tests the feedback matrix \underline{K}_{FB} contained only one element, the one completing a single composition control loop. Figures 6.2-1 to 6.2-3 show the open loop, top composition controlled and bottom composition controlled simulation runs respectively. The top feedback gain used was 22 and the bottom gain was -330. The simulation results show that these values nearly result in unstable operation, so they should be the upper limits of possible values. As the gains are decreased (absolutely), the offsets increase and oscillations decrease. It can be seen from Figure 6.2-2 that the top composition control loop has a large effect on the bottom composition, and actually has a controlling effect since it decreases the offset.

In preliminary experimental tests, it was noted that there was measurement noise in the bottoms composition from the gas

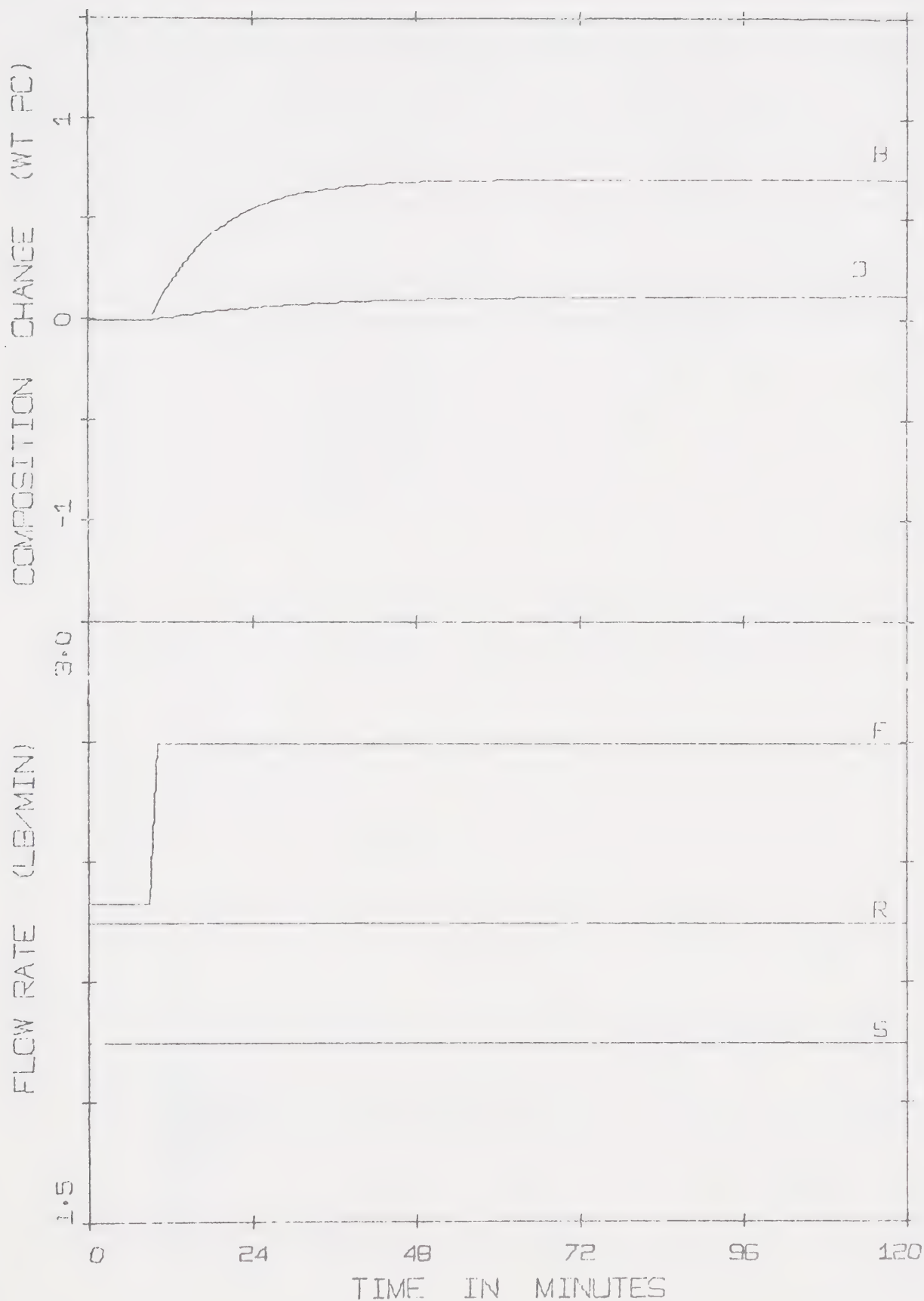


FIGURE 6.2-1: SIMULATED OPEN LOOP BEHAVIOR - POSITIVE FEED FLOW STEP DISTURBANCE

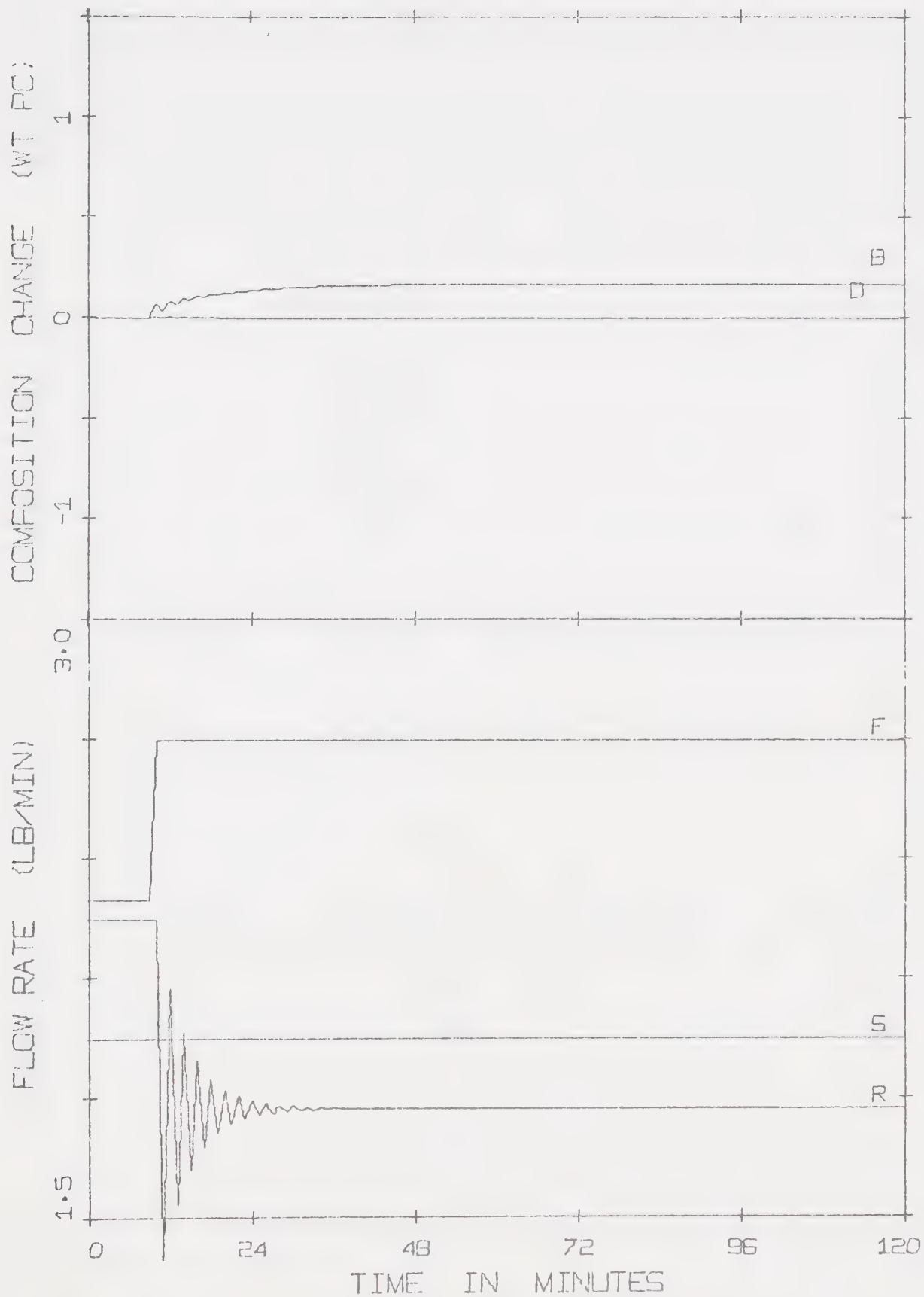


FIGURE 6.2-2 SIMULATED OVERHEAD ENTHALPY CONTROL BEHAVIOR ($K_{PT} = 22$)

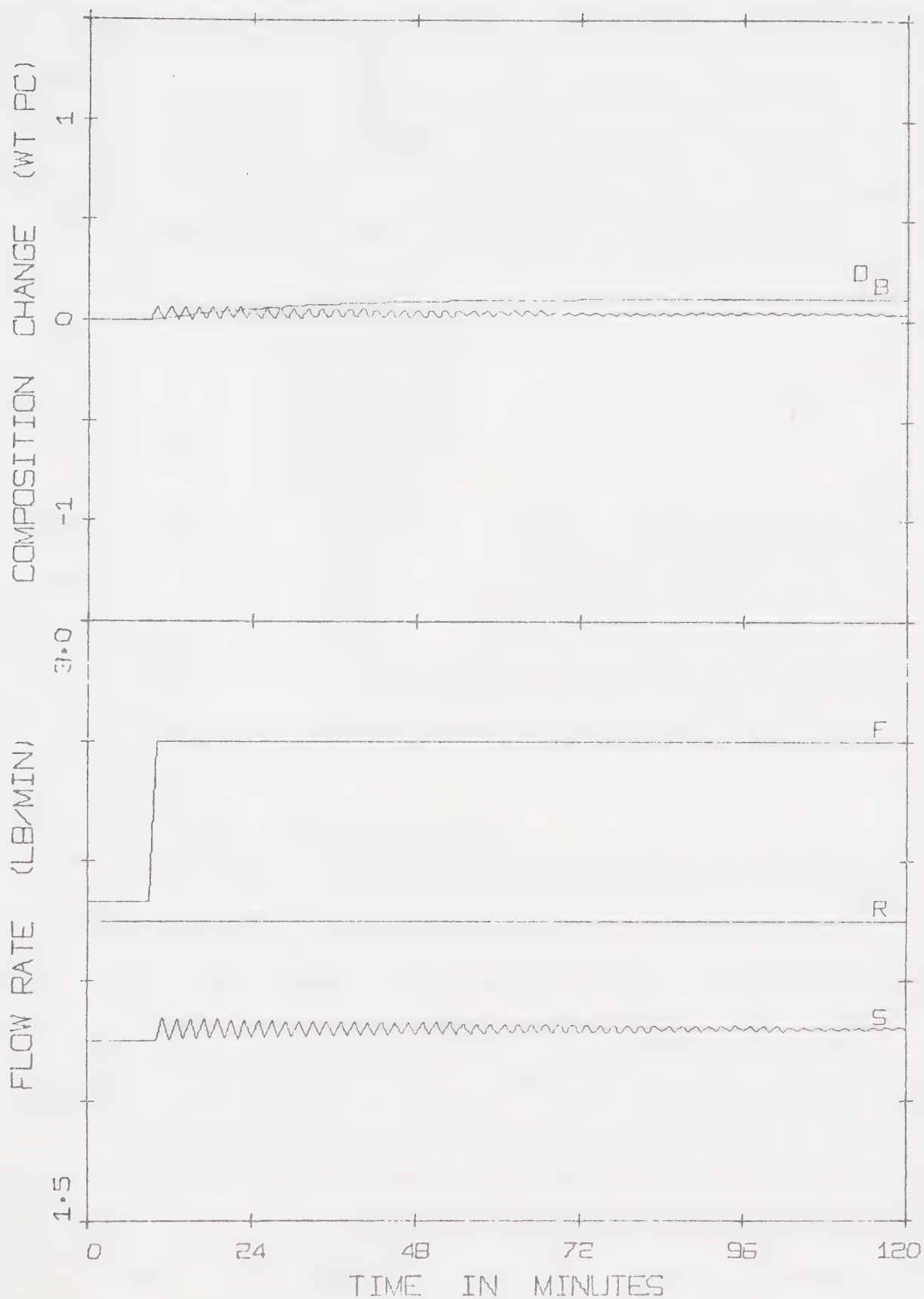


FIGURE 6.2-3: SIMULATED BOTTOM ENTHALPY CONTROL BEHAVIOR ($K_{PB} = -330$)

chromatograph system. It was decided to introduce this noise into the simulation and to add an exponential filter to minimize its effect. The resulting signal was obtained by superimposing an experimentally measured noise signal which had been filtered onto the simulated signal. The filter used was an exponential filter which has the form:

$$x_f(k+1) = \alpha x_f(k) + (1 - \alpha) x_m(k+1)$$

where x_m = actual measurement
 x_f = filtered measurement
 α = filter constant

Figures 6.2-4 to 6.2-6 present the simulation results corresponding to Figures 6.2-1 to 6.2-3 respectively, with the filtered noise added. The filter constant used was 0.8. The open loop gains had to be decreased since the noise tended to yield an oscillatory system. The bottom gain used was -300 and the top gain was 20, and in each case instability was approached.

6.2-2 Top Product Composition Control

The feedback controller gain as found by simulation was then tested experimentally. The disturbance used was a feed flow step. The simulation gain of 20 was found to result in oscillatory operation. This is probably due to process noise. A value of 10 was then tried and found to give a stable result, and moderately good control. The results for both a positive and negative feed flow step are given in Figures 6.2-7 and 6.2-8 respectively. In each case there are only small fluctuations in top product composition. However, there is a very small offset in final steady state values as is expected for feedback control when a step input is used.

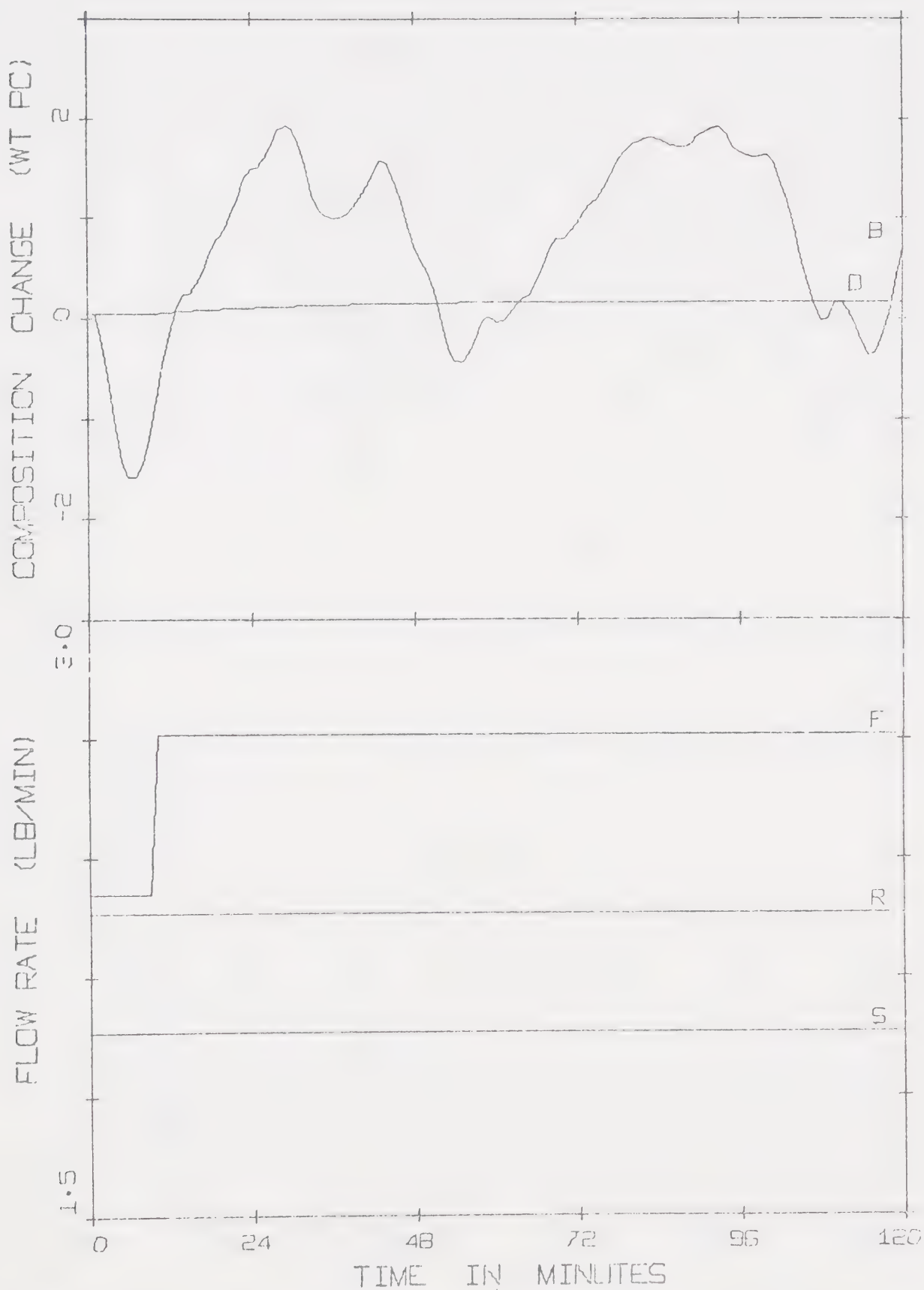


FIGURE 6.2-4: SIMULATED OPEN LOOP BEHAVIOR - FILTERED NOISE INCLUDED IN BOTTOM COMPOSITION MEASUREMENT ($\alpha = 0.8$)

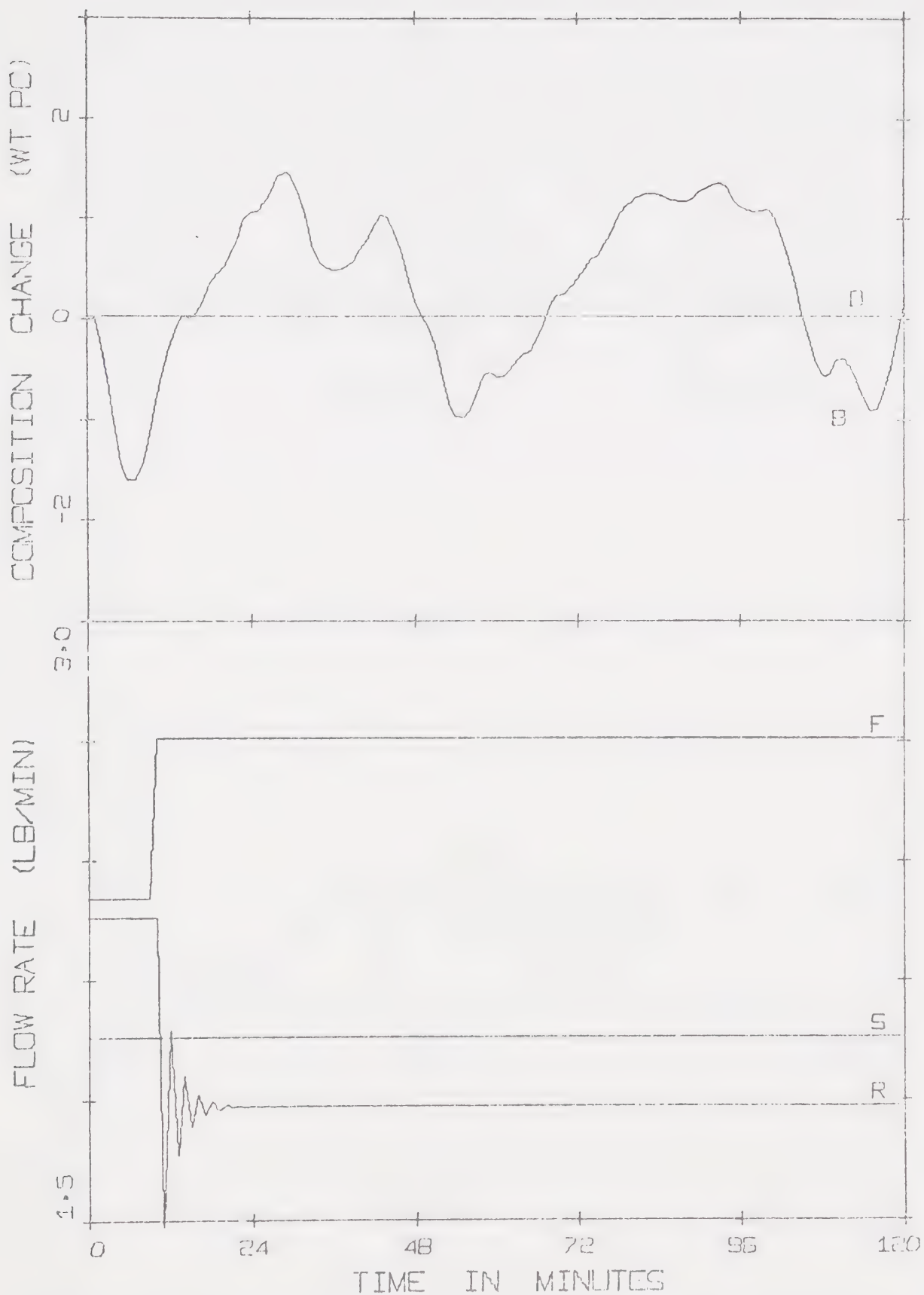


FIGURE 6.2-5: SIMULATED OVERHEAD ENTHALPY CONTROL BEHAVIOR - MEASUREMENT NOISE INCLUDED ($\alpha = 0.8$, $K_{PT} = 20$)

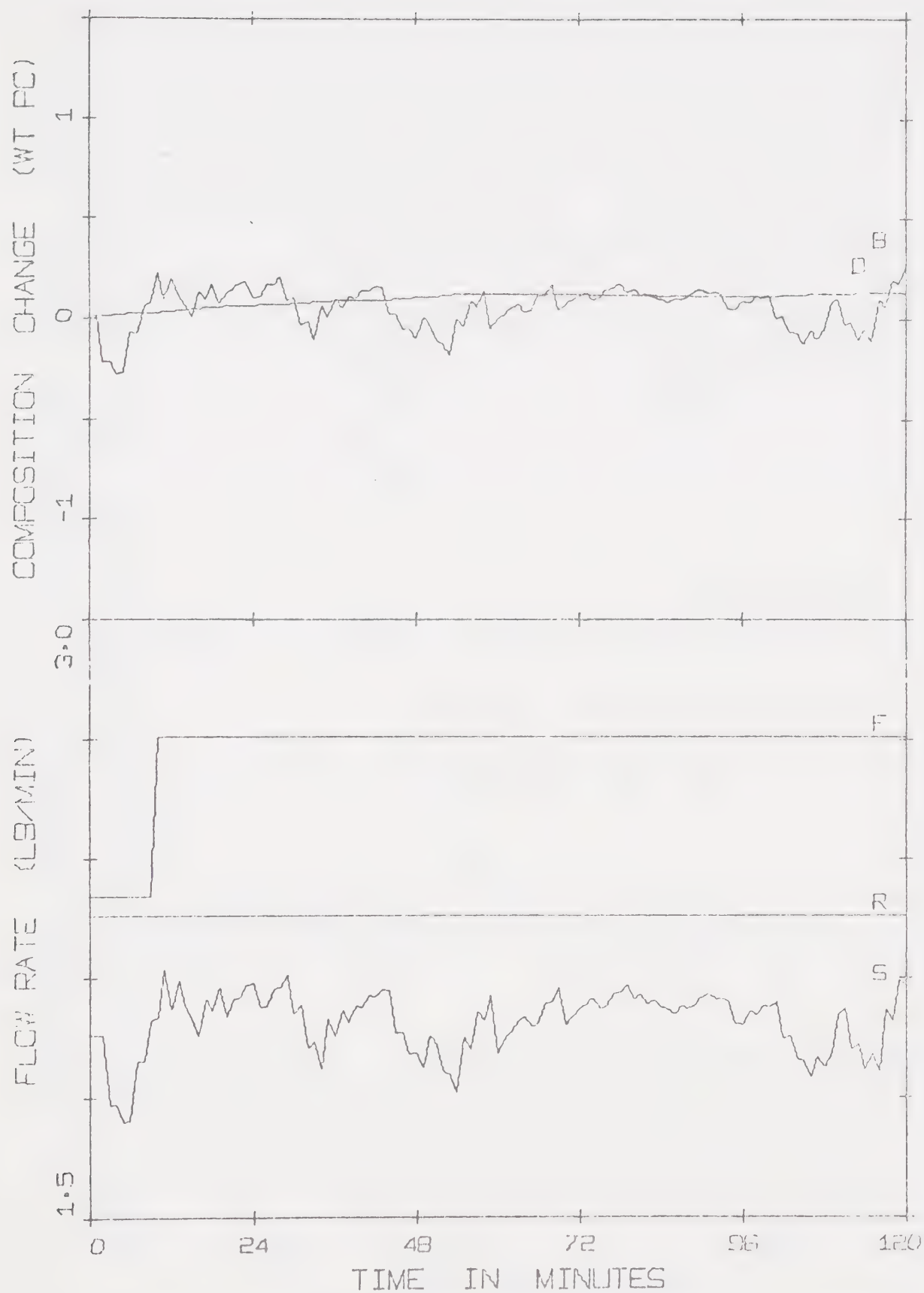


FIGURE 6.2-6: SIMULATED BOTTOM ENTHALPY CONTROL BEHAVIOR - MEASUREMENT NOISE INCLUDED ($\alpha = 0.8$, $K_{PB} = -300$)

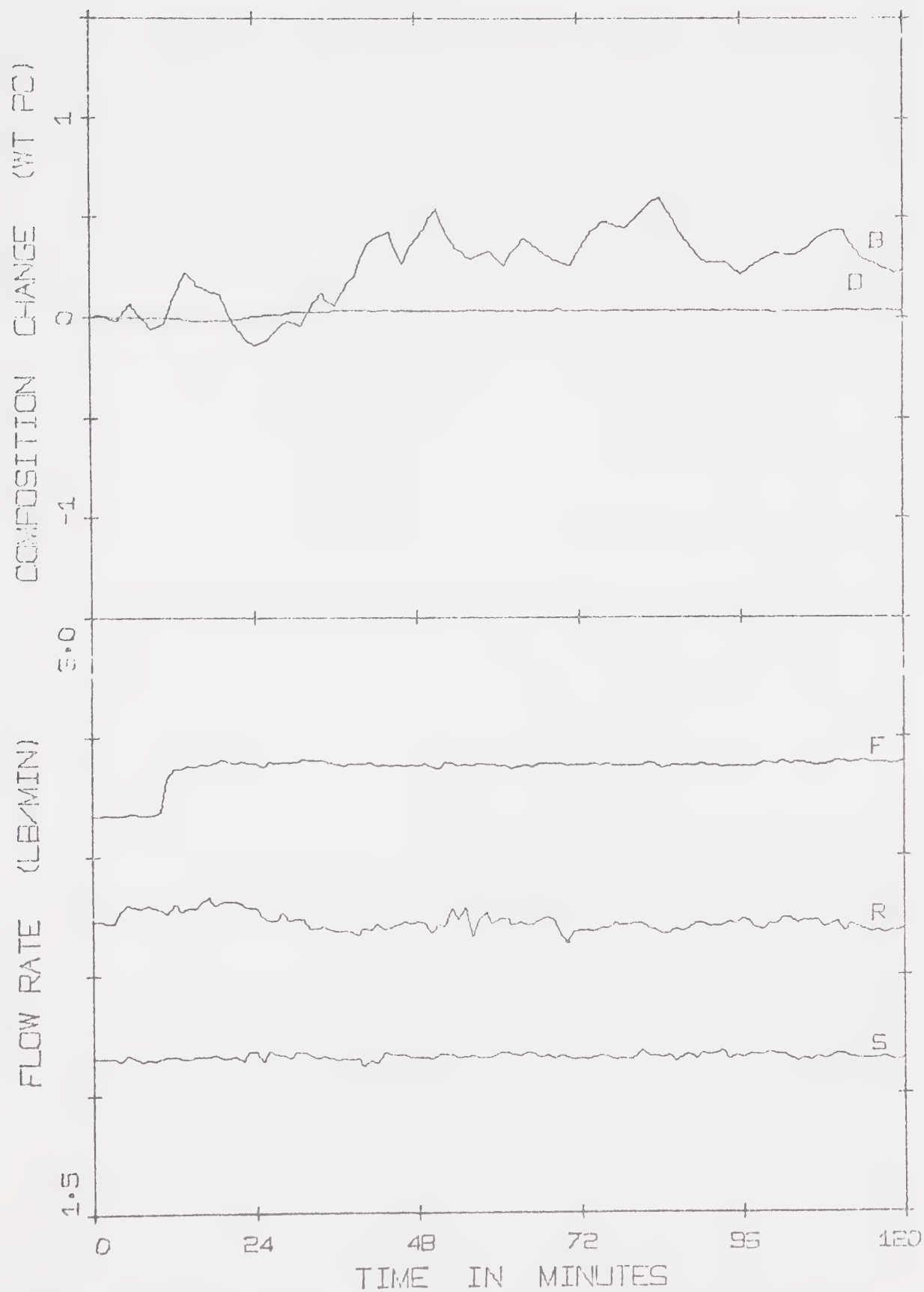


FIGURE 6.2-7: EXPERIMENTAL OVERHEAD ENTHALPY CONTROL BEHAVIOR; +5% FEED FLOW STEP ($\alpha = 0.8$, $K_{PT} = 10$)

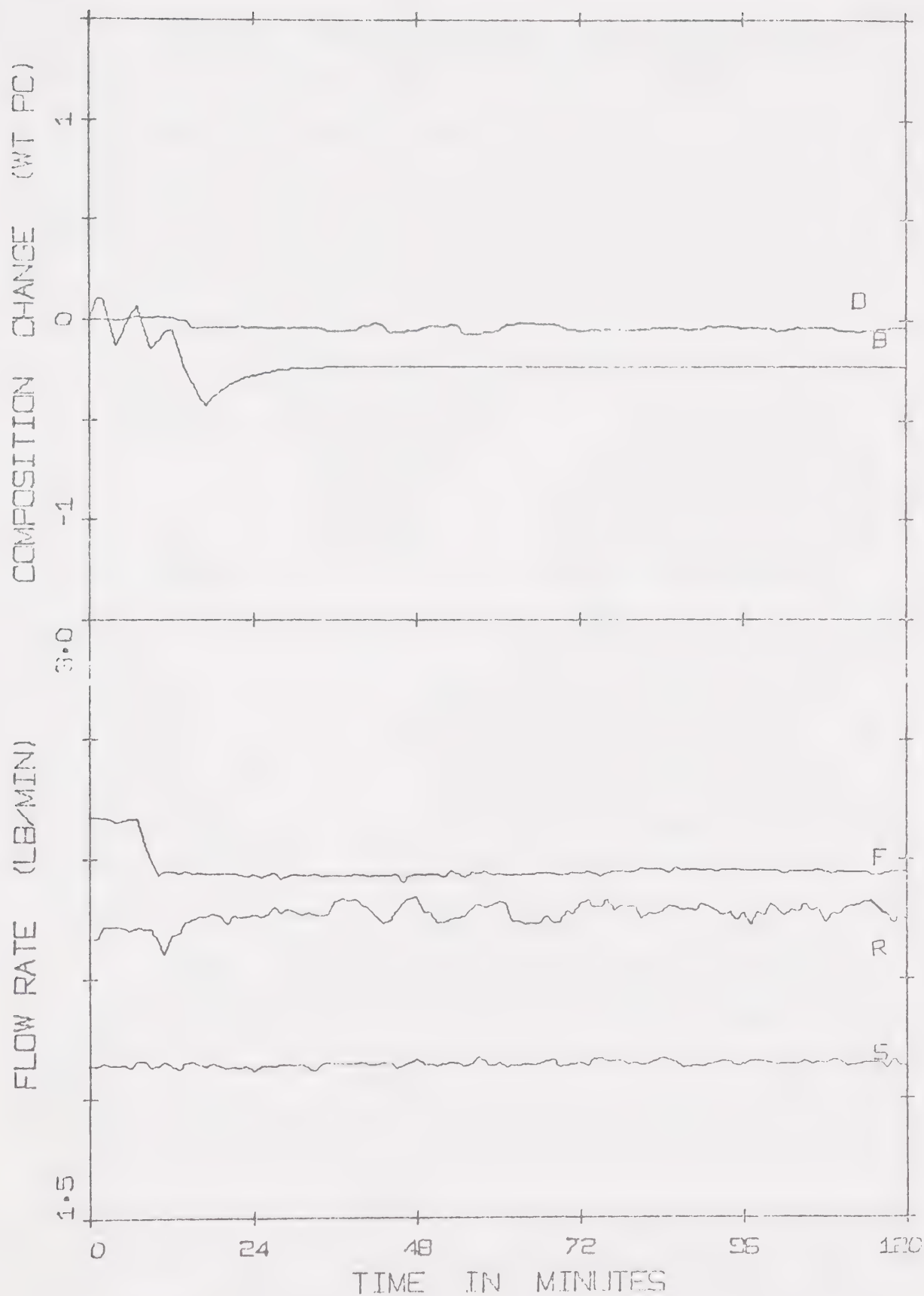


FIGURE 6.2-8: EXPERIMENTAL OVERHEAD ENTHALPY CONTROL BEHAVIOR; -5% FEED FLOW STEP ($\alpha = 0.8$, $K_{PT} = 10$)

The bottom composition response is also shown in these figures. In the case of Figure 6.2-7, the bottom composition reaches a final steady state offset of about 0.4%. This can be contrasted with an expected offset of 0.8 to 1.0% for a corresponding open loop case. This is the same controlling effect as predicted by the simulation results and illustrated in Figure 6.2-2. In the case of Figure 6.2-8 the bottoms composition reaches a composition less than about 0.4% where the bottoms gas chromatograph cannot measure it.

6.2-3 Bottom Product Composition Control

As outlined previously, there was considerable noise in the bottom composition measurement and so an exponential filter was added to the simulation results. A corresponding filter was added to the experimental control system using the same constant as was used in the simulation tests. The control loop gain in the feedback matrix was adjusted to give a stable response, and moderately good control. The simulation value of -300 was found to yield an unstable system, and so smaller values were tried. A gain of -50 was found to yield stable operation, whereas larger values tended to drive the system unstable if a large noise level appeared in the bottoms composition analysis.

Figures 6.2-9 and 6.2-10 present experimental results using this gain, for a positive and a negative feed flow disturbance respectively. It can be seen from Figure 6.2-9 that the bottoms composition exhibits appreciable noise and an offset of about 0.3% compared to the comparable open loop test where an offset of 0.8 to 1.0% is expected. This is a definite improvement, however, the offset must be tolerated due to the necessity of using a low gain value. In the case of Figure 6.2-10, a similar but opposite result is observed with

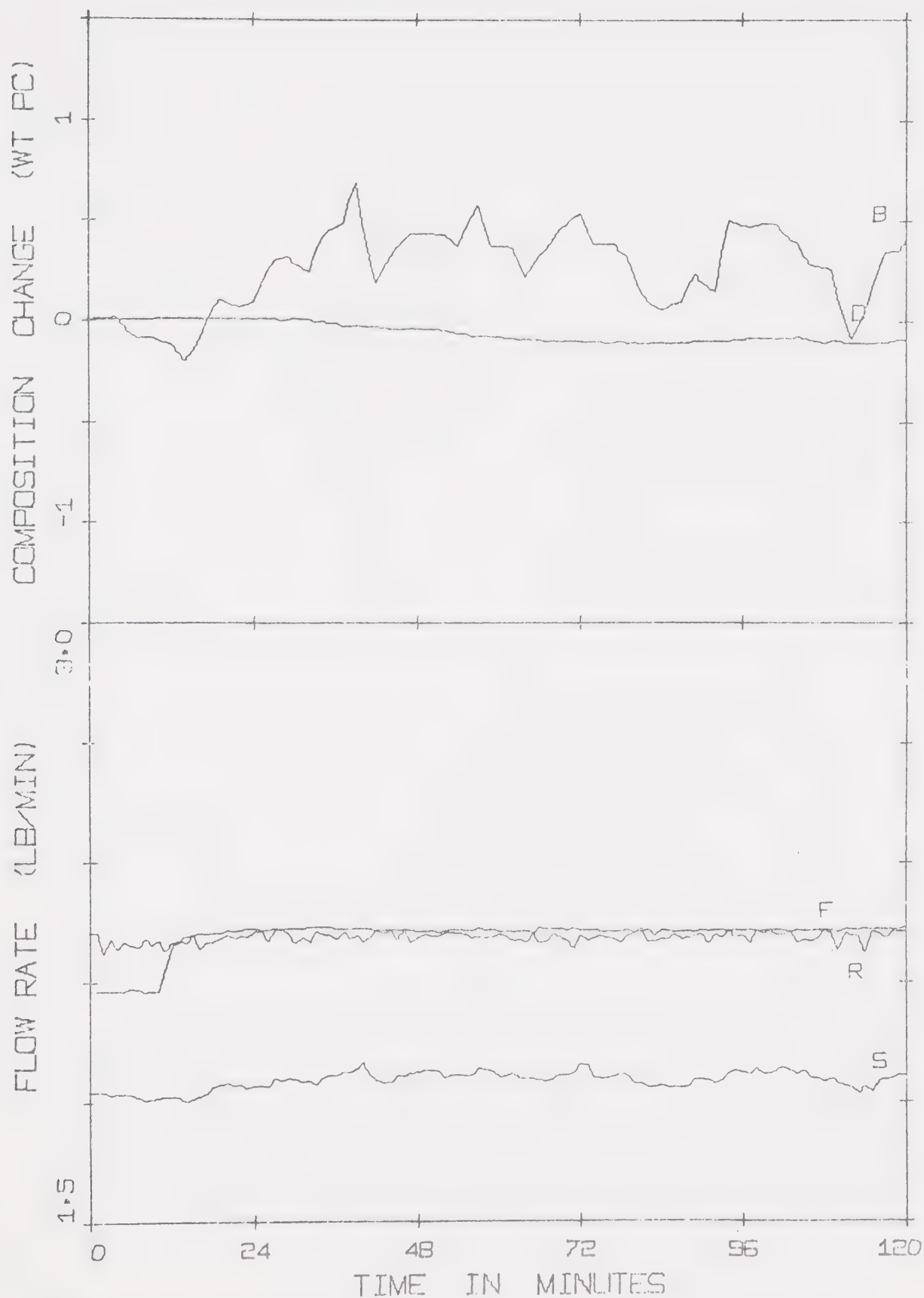


FIGURE 6.2-9: EXPERIMENTAL BOTTOM ENTHALPY CONTROL BEHAVIOR: +5%
FEED FLOW STEP ($\alpha = 0.8$, $K_{PB} = -50$)

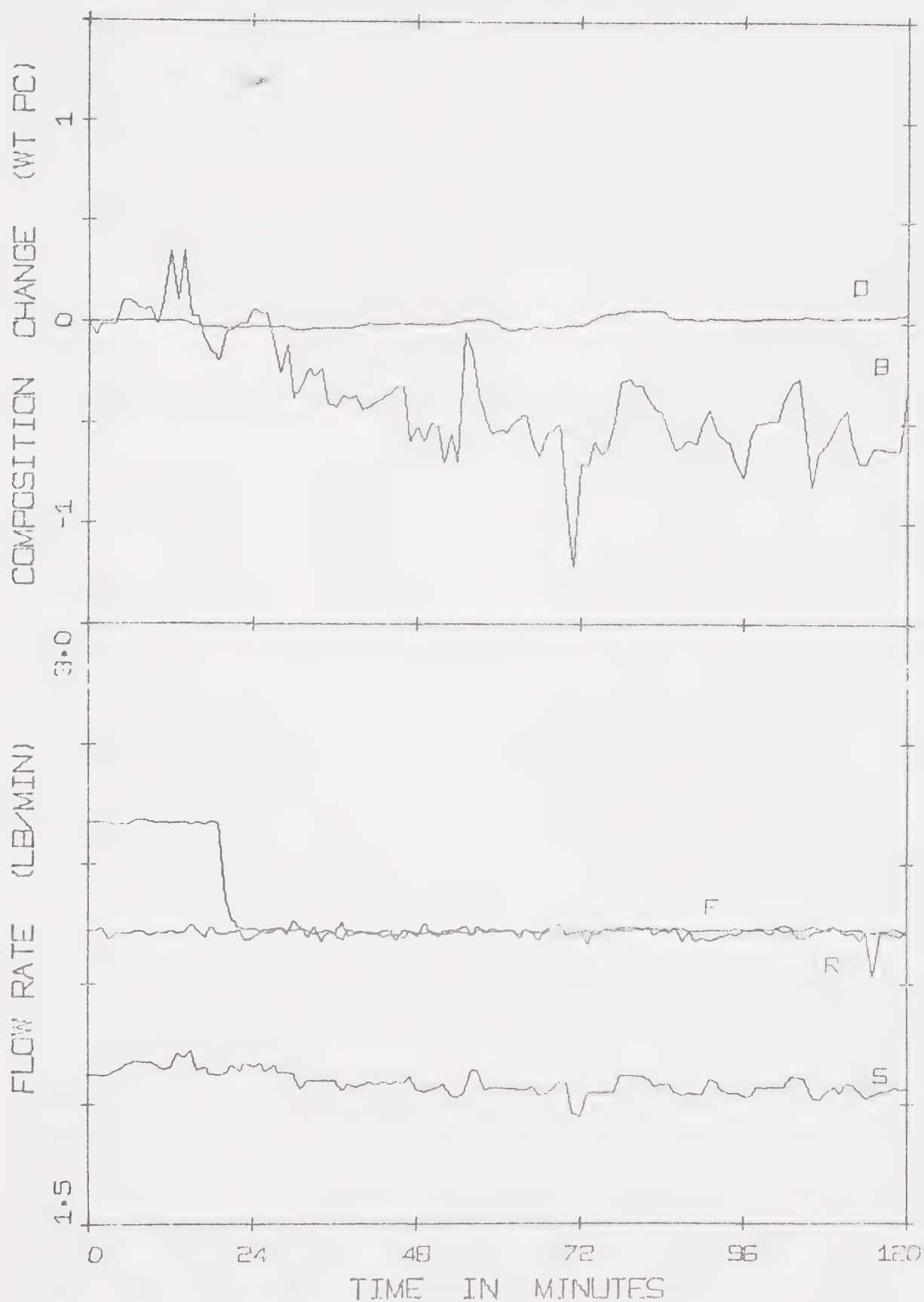


FIGURE 6.2-10: EXPERIMENTAL BOTTOM ENTHALPY CONTROL BEHAVIOR: -5%
FEED FLOW STEP ($\alpha = 0.8$, $K_{PB} = -50$)

a resulting offset in bottom composition of about 0.5%. In both cases the top product composition varies due to changes in steam flow. This effect can be seen most markedly in Figure 6.2-10.

6.3 Multiloop Control

The extension of the previous case, that is two single control loops, is to operate both loops simultaneously. This yields a two point composition control system. This approach was tested by both simulation and experimental testing, and the following sections outline the results of each test.

6.3-1 Simulation Results

The two point control system was simulated using the two state model with measurement noise and filtering added. Initially, the controller gains as found in the single loop simulation studies were applied and were found to result in unstable operation. These gains of $\{-300, +20\}$ were then tuned, and values of $\{-150, +15\}$ were found to give a stable system. Figure 6.3-1 presents the controlled responses for these controller settings. The interaction between the control loops can be seen by the similarity in the shapes of the reflux and steam flow curves.

6.3-2 Experimental Results

The two point control system was then tested experimentally. The composition feedback controller gains from the single loop tests were $\{-50, +10\}$ for the bottom and top composition control loops respectively. These gains were used in the two point system, and feed flow steps were used to disturb the column. Figures 6.3-2 and 6.3-3 present the controlled responses obtained. In Figure 6.3-2, the bottom composition shows large oscillations and is tending to be unstable. The overhead composition, however, shows small changes only, and appears well

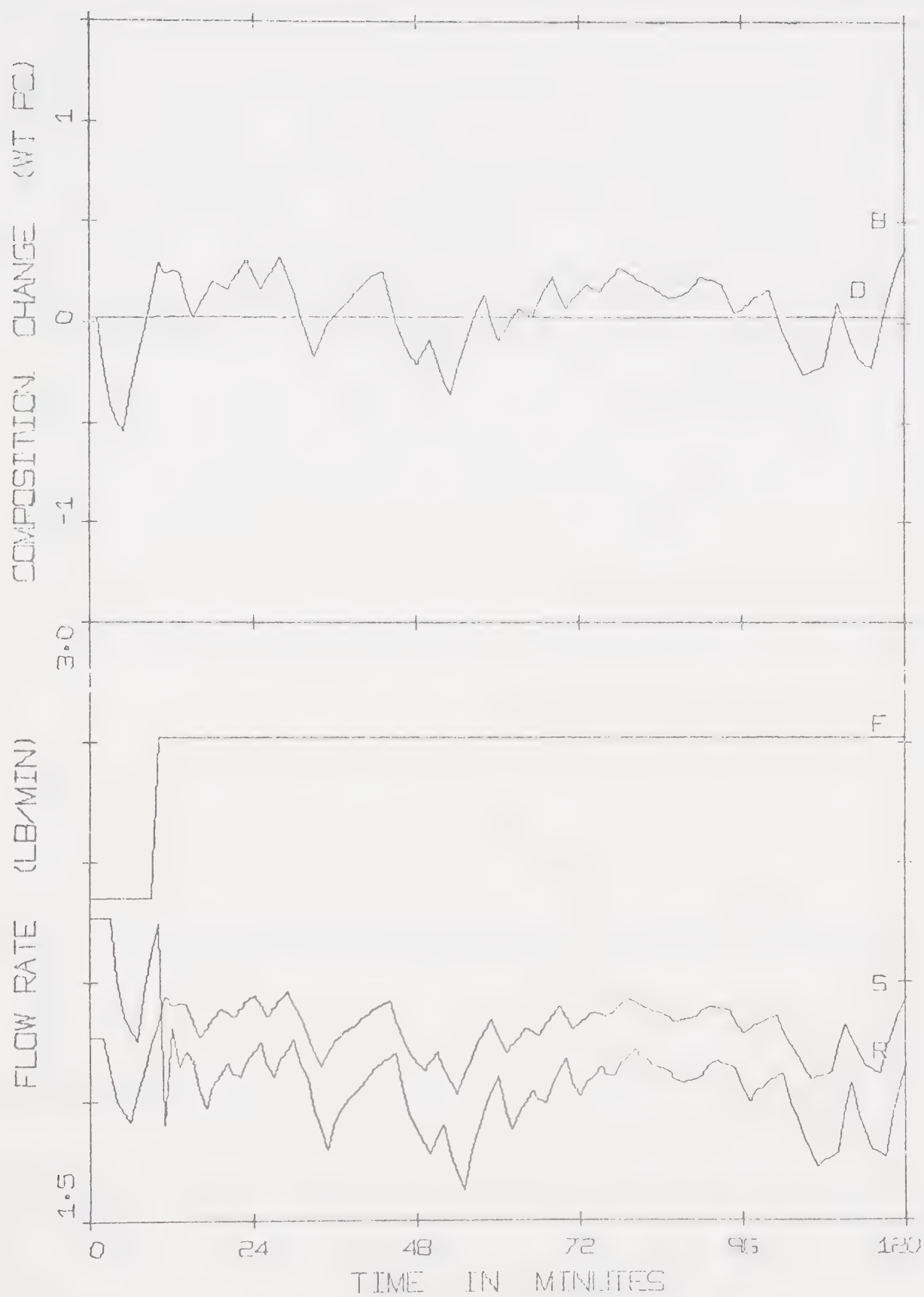


FIGURE 6.3-1: SIMULATED MULTILoop CONTROL BEHAVIOR - MEASUREMENT NOISE INCLUDED ($\alpha = 0.8$, $K_{PT} = 15$, $K_{PB} = -150$)

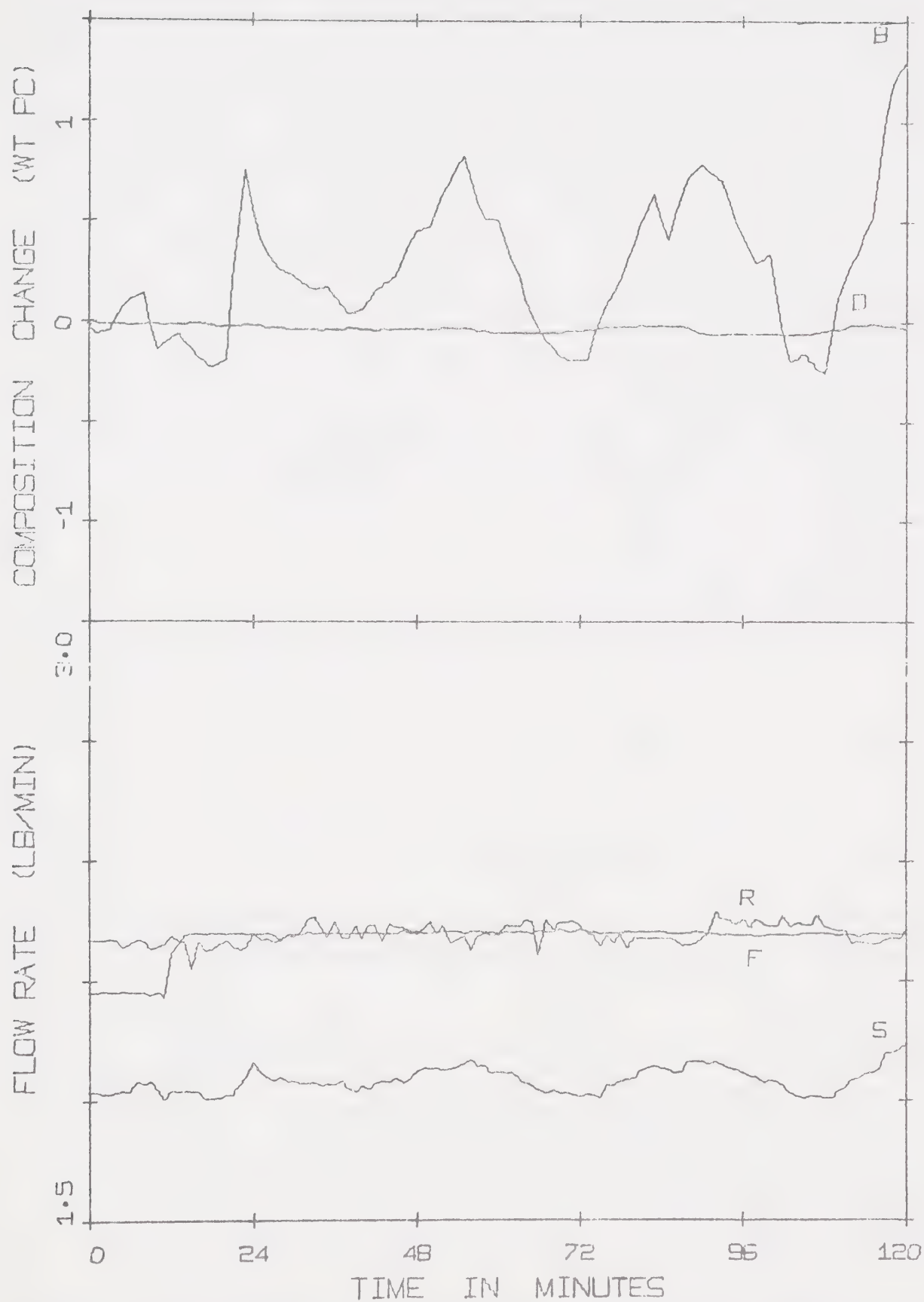


FIGURE 6.3-2: EXPERIMENTAL MULTILoop CONTROL BEHAVIOR: +5% FEED FLOW STEP ($\alpha = 0.8$, $K_{pT} = 10$, $K_{pB} = -50$)

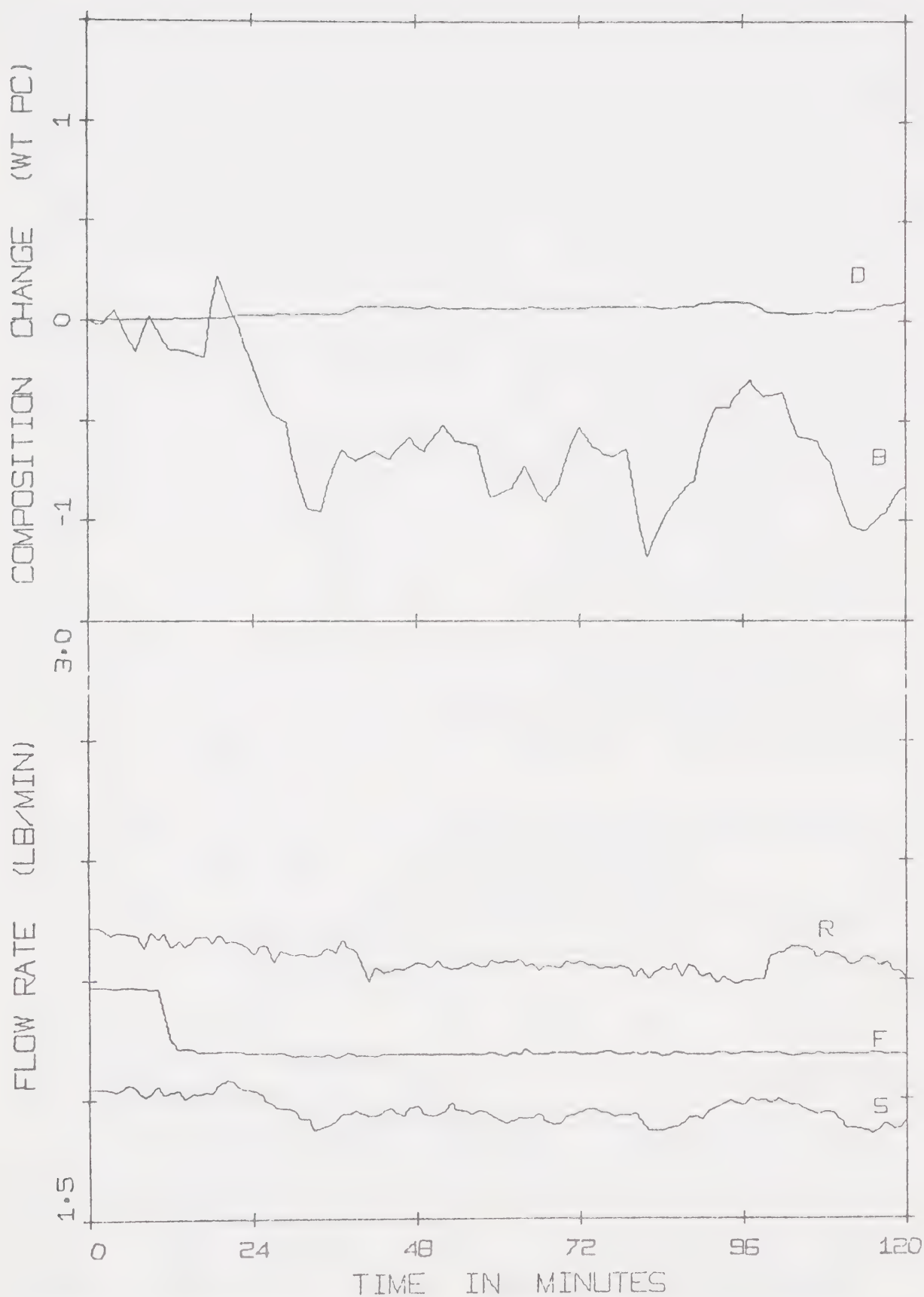


FIGURE 6.3-3: EXPERIMENTAL MULTILoop CONTROL BEHAVIOR: -5% FEED FLOW STEP ($\alpha = 0.8$, $K_{PT} = 10$, $K_{PB} = -50$)

controlled. Figure 6.3-3 shows the response to a negative feed flow step, and it is noted that the bottom composition is stable with large oscillations and an offset of about 0.7%. The overhead composition again shows small fluctuations but also has an offset which is larger than in the comparable single loop case.

The difference in observed stability of these cases may be due to the magnitude of the bottoms composition change expected for the input disturbance. The change for a positive feed step is expected to be larger than that for the negative feed step. The large change in bottoms composition as a result of the positive feed flow step could result in a shortlived period of control yielding instability.

From these multiloop tests the following conclusions can be drawn:

- i) The controller loop gains in a single loop system may yield an unstable control system when applied simultaneously.
- ii) The control loops chosen for this study exhibit interactive effects when applied simultaneously.
- iii) The interaction can be predicted by the two state model of the distillation column.

6.4 Multivariable Control

6.4-1 Multivariable and Multiloop Control

In a multiloop control system there are several control loops operating independently of each other. However, as demonstrated in the previous section, the control actions of these loops can interact and lead to a deterioration in control. The extension to a multivariable control system allows the loops to interact and the control action taken

compensates for this interaction. This approach should therefore lead to better control performance than the simple multiloop case.

6.4-2 Multivariable Control Laws

The application of a multivariable control system requires the availability of a process model. The most widely used form is the stationary state space form:

$$\dot{\underline{x}} = \underline{A} \underline{x} + \underline{D} \underline{d} + \underline{B} \underline{u} \quad (6.4-1)$$

where \underline{x} = an $n \times 1$ state vector

\underline{d} = an $m \times 1$ disturbance vector

\underline{u} = an $\ell \times 1$ control vector

$\underline{A}, \underline{B}, \underline{C}$ = time invariant coefficient matrices of appropriate dimensions

This model can also be expressed in the discrete form:

$$\underline{x}(k+1) = \underline{\phi} \underline{x}(k) + \underline{\Delta} \underline{d}(k) + \underline{\beta} \underline{u}(k) \quad (6.4-2)$$

where k refers to a specific time interval and the matrices and vectors are the discrete forms of those in Equation (6.4-1).

Many types of control laws have been proposed in the literature. The best known are so-called optional laws derived for some specific form of performance criterion. Some of these optional laws have been presented by Newell [32] and by Hu [22], both of whom have applied a dynamic programming approach. In this study it was decided to first employ simple suboptimal control, followed possibly at a later stage in the study by optimal control.

A simple suboptimal law can be derived from the discrete model:

$$\underline{x}(k+1) = \underline{\phi} \underline{x}(k) + \underline{\Delta} \underline{d}(k) + \underline{\beta} \underline{u}(k) \quad (6.4-2)$$

The objective of the control action $\underline{u}(k)$ is to drive the values of the states at the next interval, $\underline{x}(k+1)$, to the state setpoints for any value of $\underline{x}(k)$ and $\underline{d}(k)$. Let the setpoint of the state vector by \underline{x}_s , and assume that the controls are unconstrained, that is, the required changes in controls are physically realizable. Then the control action will make:

$$\underline{x}(k+1) = \underline{x}_s$$

The required control action can then be found by solving for $\underline{u}(k)$ in the expression:

$$\underline{x}_s = \underline{\phi} \underline{x}(k) + \underline{\Delta} \underline{d}(k) + \underline{E} \underline{u}(k)$$

Since, in general, \underline{E} is not square ($n \neq l$), a pseudo-inverse approach [19] must be used. The control law can be expressed as a feedback-forward-setpoint control law:

$$\underline{u}(k) = \underline{K}_{FB} \underline{x}(k) + \underline{K}_{FF} \underline{d}(k) + \underline{K}_{sp} \underline{x}_s$$

where

$$\begin{aligned} \underline{K}_{FB} &= -[\underline{E}^T \underline{E}]^{-1} \underline{E}^T \underline{\phi} \\ \underline{K}_{FF} &= -[\underline{E}^T \underline{E}]^{-1} \underline{E}^T \underline{\Delta} \\ \underline{K}_{sp} &= [\underline{E}^T \underline{E}]^{-1} \underline{E}^T \end{aligned}$$

Figure 6.4-1 presents the two state discrete model of the distillation column, and the resulting control law derived as indicated above.

6.4-3 Simulation of Feedback Control Behavior

The feedback matrix as defined above was used for simulation studies. The setpoint was assumed to be the origin in state space. The effect of neglecting the feedforward term is to cause an offset in

Model

$$\begin{bmatrix} \dot{h}_1(k+1) \\ \dot{h}_{10}(k+1) \end{bmatrix} = \begin{bmatrix} .955 & -.00600 \\ .0130 & .950 \end{bmatrix} \begin{bmatrix} \dot{h}_1(k) \\ \dot{h}_{10}(k) \end{bmatrix} \\
 + \begin{bmatrix} -.0126 & .00257 \\ -.0795 & .00117 \end{bmatrix} \begin{bmatrix} \dot{L}_{10}(k) \\ \dot{Q}_R(k) \end{bmatrix} + \begin{bmatrix} -.0198 & 0.0 & .000177 \\ -.0971 & -.00125 & .00280 \end{bmatrix} \\
 \begin{bmatrix} \dot{F}(k) \\ \dot{Q}_C(k) \\ \dot{h}_f(k) \end{bmatrix}$$

Control Law

$$\begin{bmatrix} \dot{L}_{10}(k) \\ \dot{Q}_R(k) \end{bmatrix} = \begin{bmatrix} -5.72 & +12.9 \\ -400 & 65.7 \end{bmatrix} \begin{bmatrix} \dot{h}_1(k) \\ \dot{h}_{10}(k) \end{bmatrix} + \begin{bmatrix} 6.17 & -13.6 \\ 419 & -66.5 \end{bmatrix} \dot{x}_s \\
 + \begin{bmatrix} -1.19 & -.0169 & .0369 \\ 1.85 & -.0831 & .112 \end{bmatrix} \begin{bmatrix} \dot{F}(k) \\ \dot{Q}_C(k) \\ \dot{h}_f(k) \end{bmatrix}$$

FIGURE 6.4-1: MODEL AND CONTROL LAW

output for a step input. This can be seen in Figure 6.4-2 where the ideal case is considered, i.e. no noise in measurements. Figure 6.4-3 is a similar result with the noise and filter added where it can be seen that controlled responses show small offsets and oscillations.

This feedback matrix was then applied to the experimental system, and was found to yield an unstable system. The reason for the instability was investigated and found to be partially the feedback element which adjusted the reflux flow for bottoms enthalpy changes. The noise in the bottoms composition measurement introduced oscillations in reflux flow, which made the top control loop unstable. Also the large gain in the bottom control loop caused large oscillations in steam flow. It was decided to reduce these two matrix elements. The bottom loop gain was reduced to -50, the value used in the multiloop tests. The other gain term, an interaction term was set to zero. This has the effect of making the reflux flow independent of bottom enthalpy. However, steam flow changes are still dependent on the overhead enthalpy changes. This removes part of the multivariable effect of the control system, however, as demonstrated earlier the reflux flow has an inherent tendency to control the bottom composition. Because of this, it was hoped that the above matrix adjustments would yield a behaviour only slightly different from the ideal controlled response. However, this was not the case as can be seen by the results presented in Figure 6.4-4 which shows the controlled response with the feedback matrix adjusted as described above. By comparing this figure with Figure 6.4-3 it can be seen that these modifications cause larger offsets in both compositions and larger variations in bottoms composition.

As well as the large feedback gains in the original system,

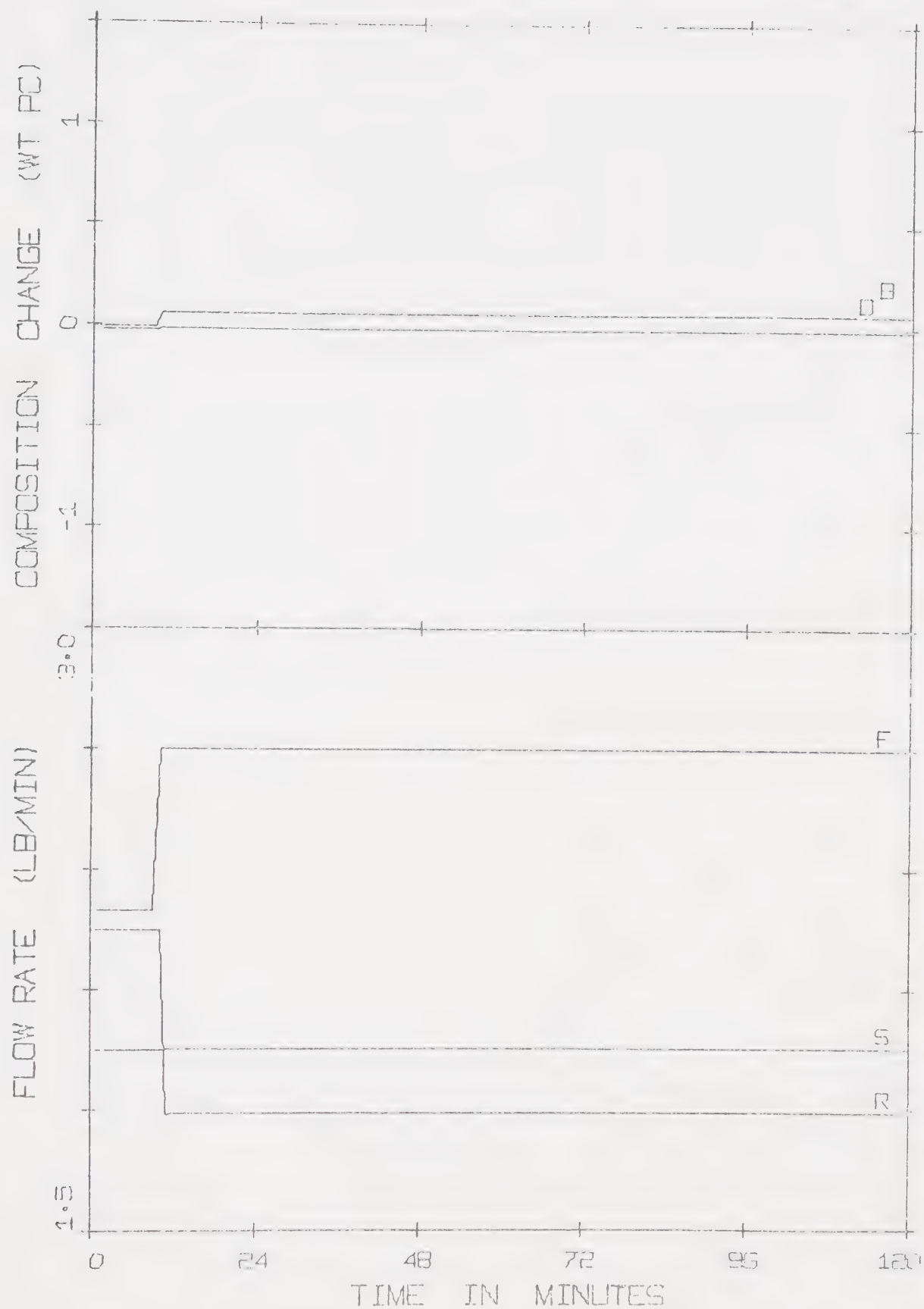


FIGURE 6.4-2: SIMULATED MULTIVARIABLE FEEDBACK CONTROL BEHAVIOR - POSITIVE FEED FLOW STEP DISTURBANCE

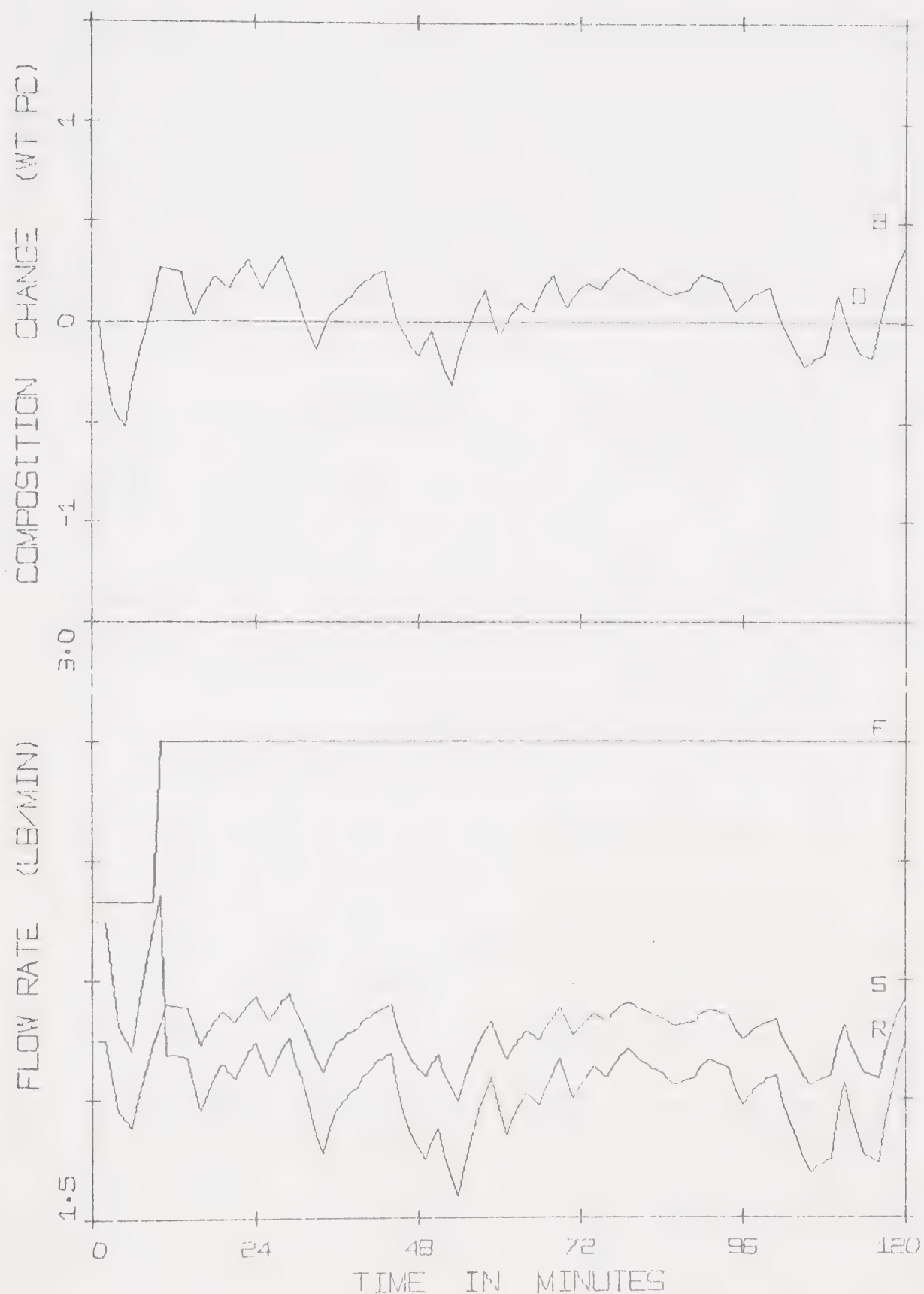


FIGURE 6.4-3: SIMULATED MULTIVARIABLE FEEDBACK CONTROL BEHAVIOR - FILTERED NOISE IN BOTTOM COMPOSITION MEASUREMENT INCLUDED ($\alpha = 0.8$)

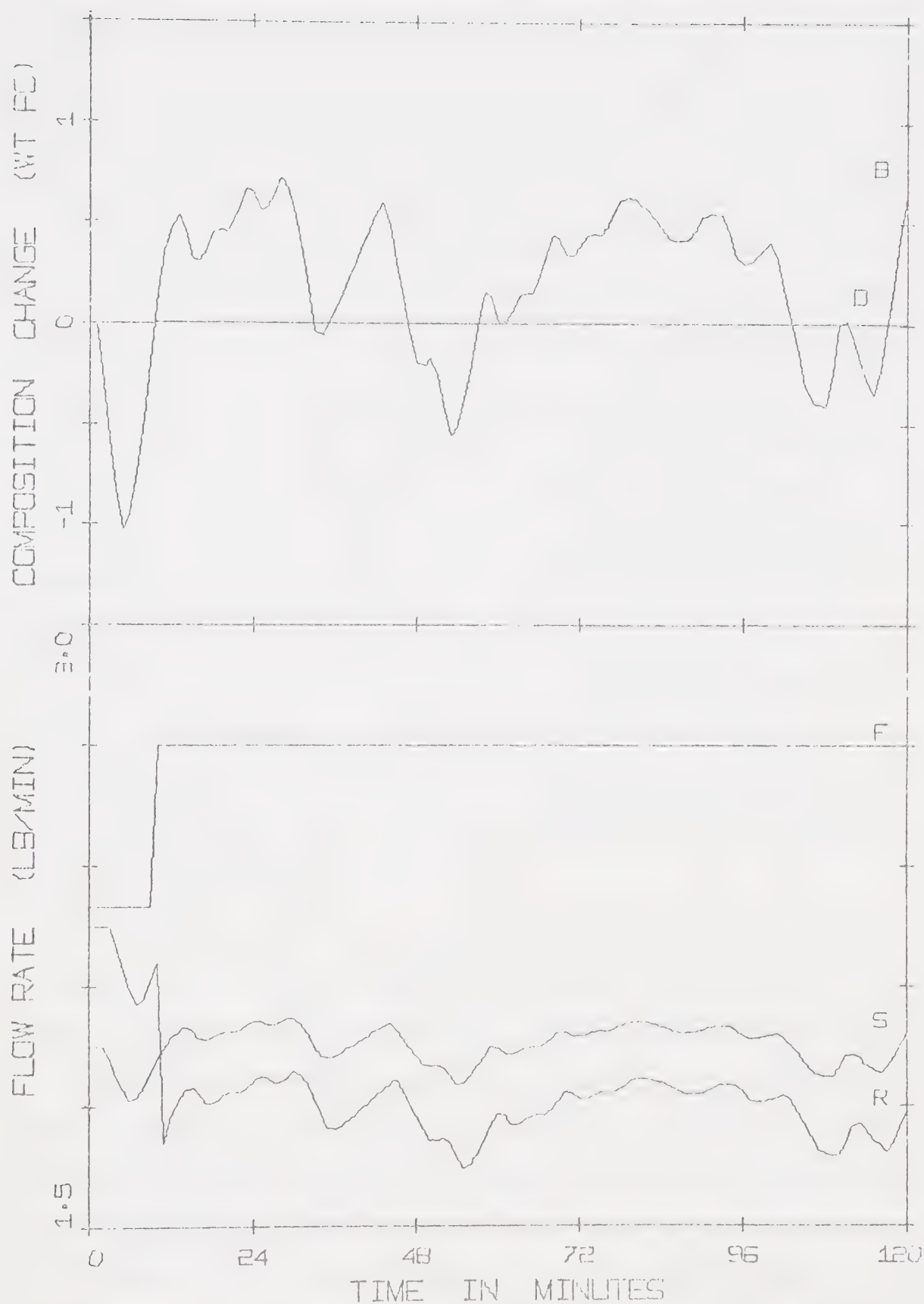


FIGURE 6.4-4: SIMULATED MULTIVARIABLE FEEDBACK CONTROL BEHAVIOR WITH MODIFIED CONTROL MATRIX AND MEASUREMENT NOISE ($\alpha = 0.8$)

another cause of the instability could be the time delays in the control system. The gas chromatograph separation and analysis cycle is an inherent measurement time delay in the system. The filtering of the bottoms composition measurement also introduces a form of time delay. Investigations showed that with the exponential filter used in this study, and a filter constant of 0.8, a maximum delay of about 5 sample intervals could be expected. Also when the filter constant is reduced to 0.5, the time delay is reduced to less than 2 sample intervals. This time delay was added to the simulation work, and some tests done to evaluate the filter constant which should be used experimentally.

Figures 6.4-5 to 6.4-7 present the results of simulation tests showing the manner in which the value of the filter constant that is employed affects the control behavior. The effect of the total time delay has also been shown. Table 6.4-1 presents the filter constant, total time delay, and feedback matrix for these tests, as well as for those presented in Figures 6.4-2 to 6.4-4. The total time delay is less than 4 minutes when the filter constant is 0.5 and is about 6 minutes when the filter constant is 0.8.

Figure 6.4-5 is the simulation result corresponding to the experimental test which was found to be unstable. It can be seen that there are large sustained oscillations in bottoms composition, and that if a measurement was encountered which represented a noise level larger than that used in the simulation, it can be seen that the system would tend to be unstable. Figure 6.4-6 presents the simulation results with no time delay and a filter constant of 0.5. The effect of reducing the filter constant can be seen by comparing the response with that in Figure 6.4-4. This has the effect of increasing the noise level in the

TABLE 6.4-1: Constants for Simulation Tests

Exponential Filter Constant α	Time Delay (τ_D) (minutes)	Feedback Matrix Columnwise	Figure
1.0	0	$\begin{bmatrix} -5.72 & -400 \end{bmatrix}$	6.4-2
0.8	0	$\begin{bmatrix} -5.72 & -400 \end{bmatrix}$	6.4-3
0.8	0	$\begin{bmatrix} 0 & -50.0 \end{bmatrix}$	6.4-4
0.8	6	$\begin{bmatrix} 0 & -50.0 \end{bmatrix}$	6.4-5
0.5	0	$\begin{bmatrix} 0 & -50.0 \end{bmatrix}$	6.4-6
0.5	4	$\begin{bmatrix} 0 & -50.0 \end{bmatrix}$	6.4-7

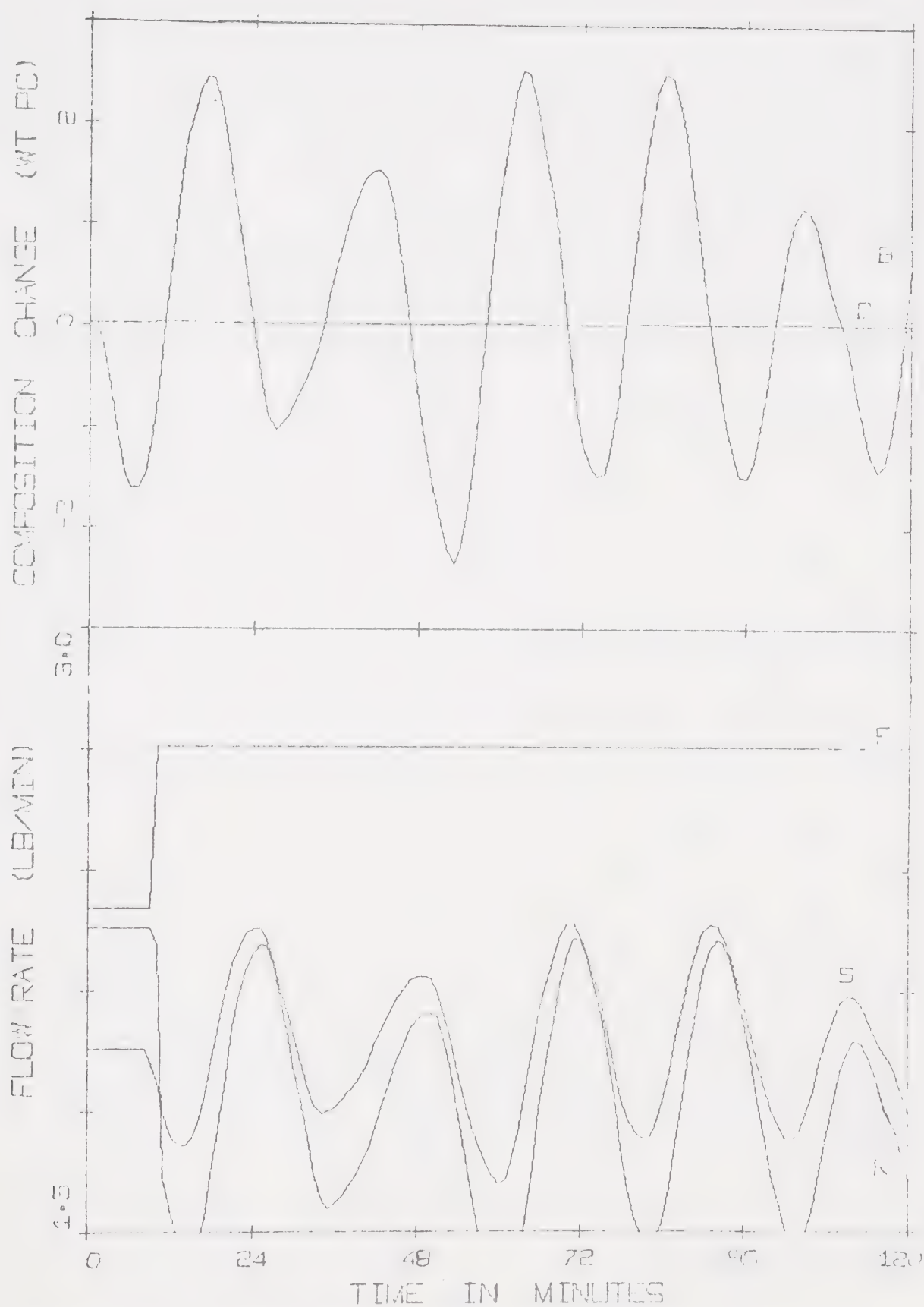


FIGURE 6.4-5: SIMULATED MULTIVARIABLE FEEDBACK CONTROL BEHAVIOR WITH TIME DELAY AND MEASUREMENT NOISE INCLUDED ($\alpha = 0.8$, $\tau_D = 6$)

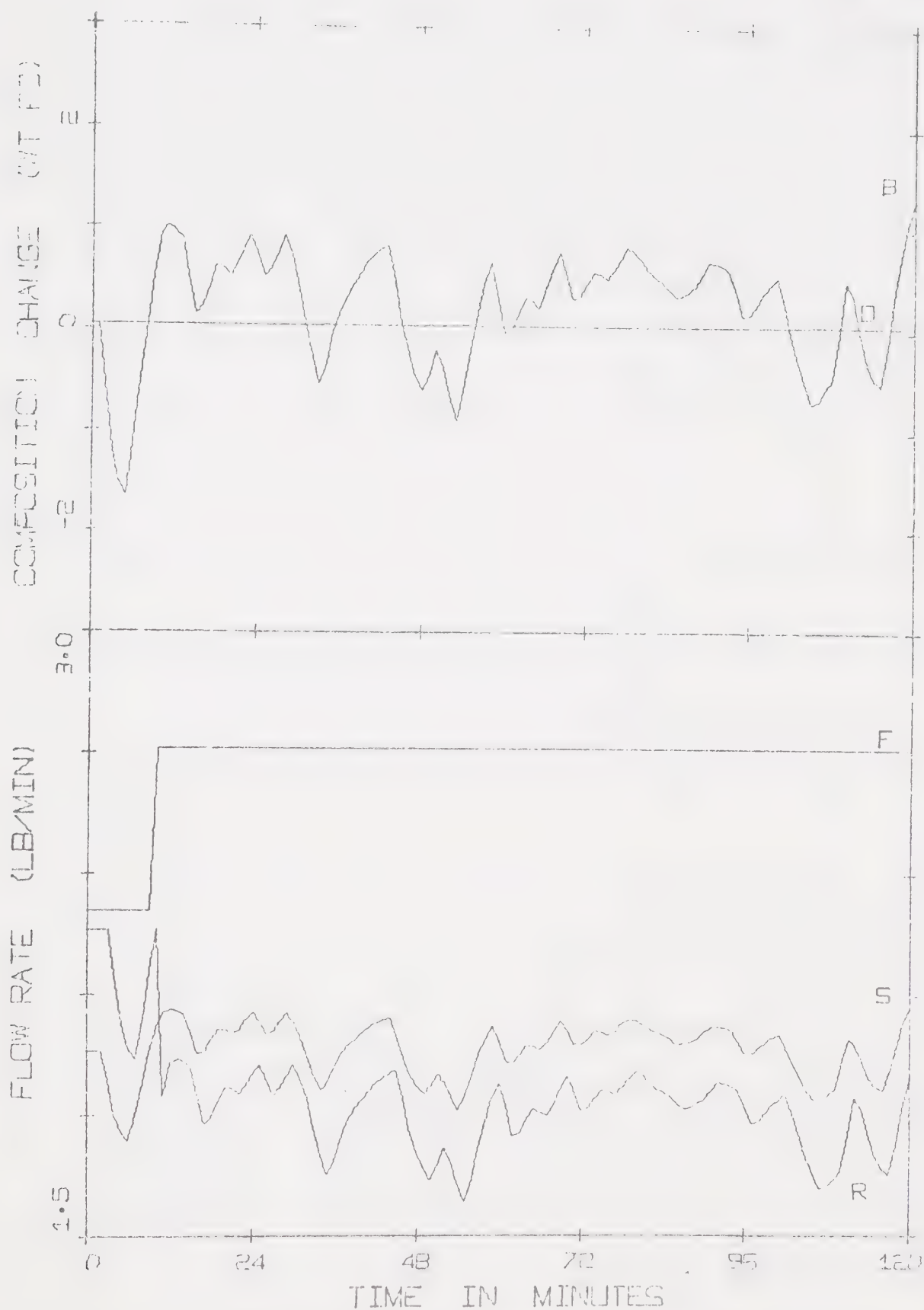


FIGURE 6.4-6: SIMULATED MULTIVARIABLE FEEDBACK CONTROL BEHAVIOR WITH MEASUREMENT NOISE INCLUDED ($\alpha = 0.5$)

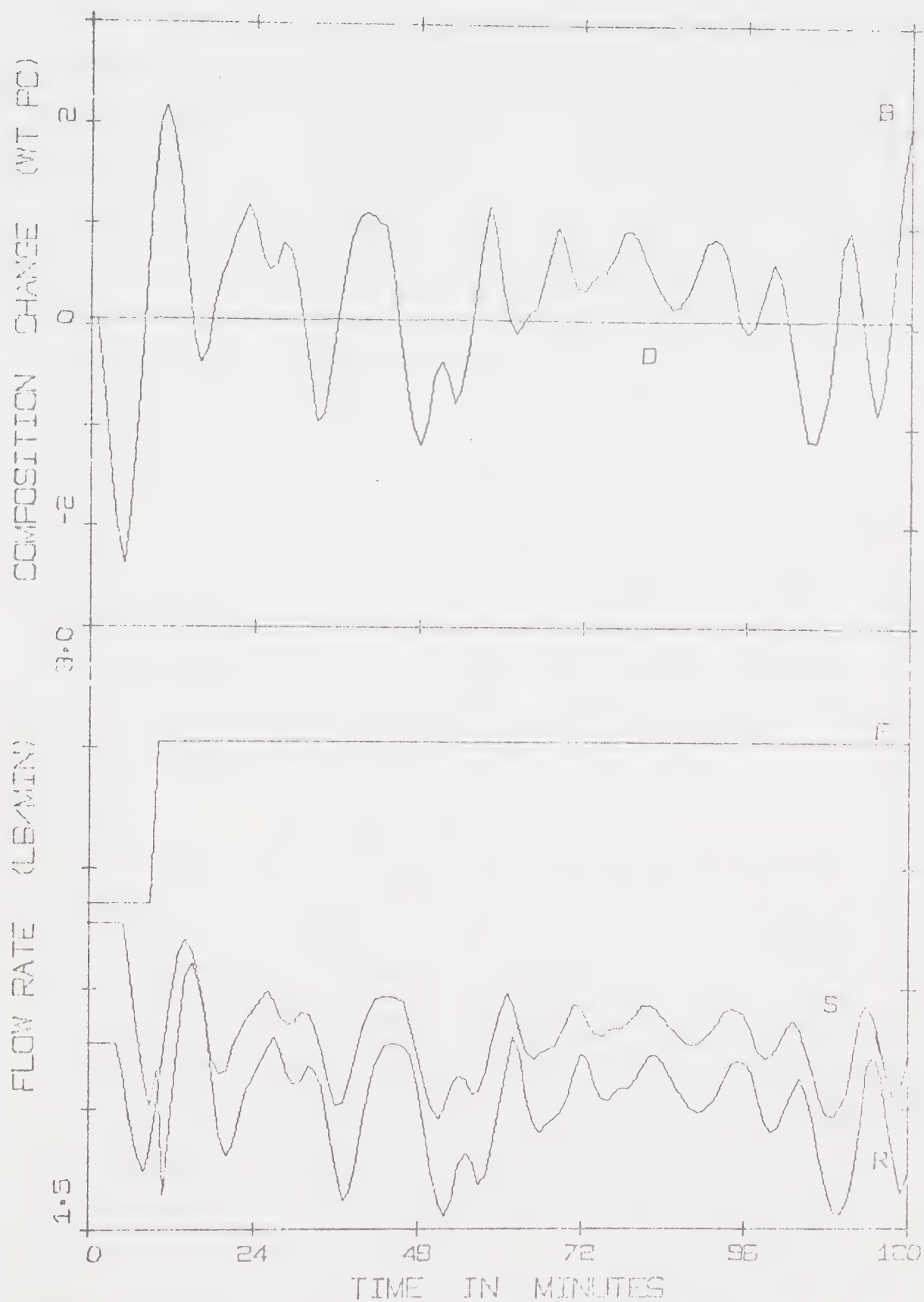


FIGURE 6.4-7: SIMULATED MULTIVARIABLE FEEDBACK CONTROL BEHAVIOR WITH TIME DELAY AND MEASUREMENT NOISE INCLUDED ($\alpha = 0.5$, $\tau_D = 4$)

in the bottoms composition measurement, but also reduces the inherent time delay due to filtering. Figure 6.4-7 shows the simulated control behavior using a filter constant of 0.5 and a time delay of 4 minutes, which is about the maximum that would be expected experimentally.

This transient can be compared with that in Figure 6.4-5 and it can be seen that the magnitude of the oscillations is reduced although the frequency is increased. This test is a good estimate of the conditions which should result experimentally and show a stable system with sustained oscillations.

6.4-4 Experimental Feedback Control Behavior

The simulation results indicated that a filter constant of 0.5 should be used with the adjusted feedback matrix. This test, as indicated in Figure 6.4-7, was attempted experimentally. Figure 6.4-8 presents the results of a test with no input disturbance, which was done to see if the noise level tended to yield instability. As can be seen, the system is stable, with moderate noise in the bottoms composition.

Figures 6.4-9 and 6.4-10 compare the controlled and uncontrolled responses for a positive and a negative feed flow step respectively. As can be seen in Figure 6.4-9, the sustained oscillations as predicted by simulation are present. Also the controlled offset in bottoms composition is only about one-quarter of the uncontrolled offset. The distillate composition shows oscillations in the controlled case, but almost no average offset. In the case of the results using a negative feed step, shown in Figure 6.4-10, the oscillations don't appear to be as drastic as in Figure 6.4-9. The controlled offset in bottoms composition, in this case is only about one-fifth of that in the uncontrolled test.

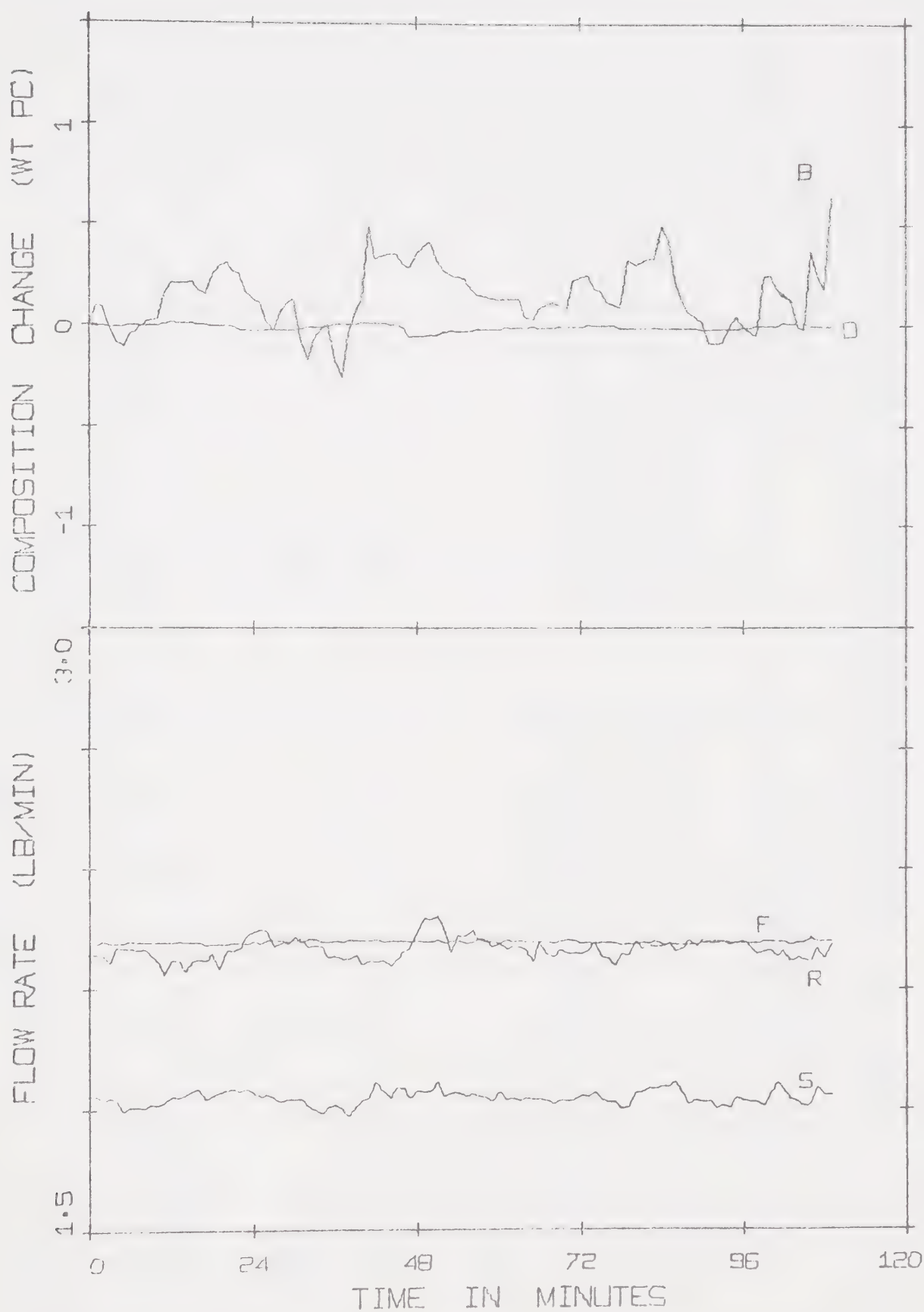


FIGURE 6.4-8: EXPERIMENTAL MULTIVARIABLE FEEDBACK CONTROL BEHAVIOR - NO DISTURBANCE ($\alpha = 0.5$)

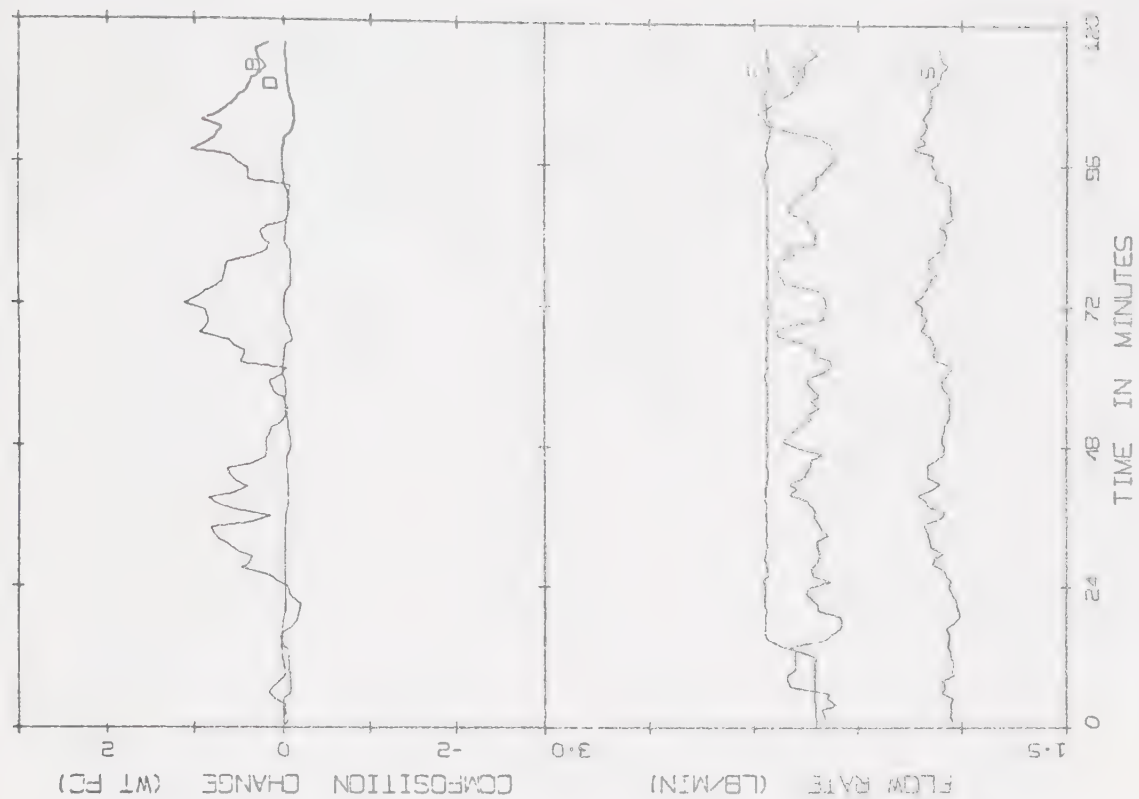
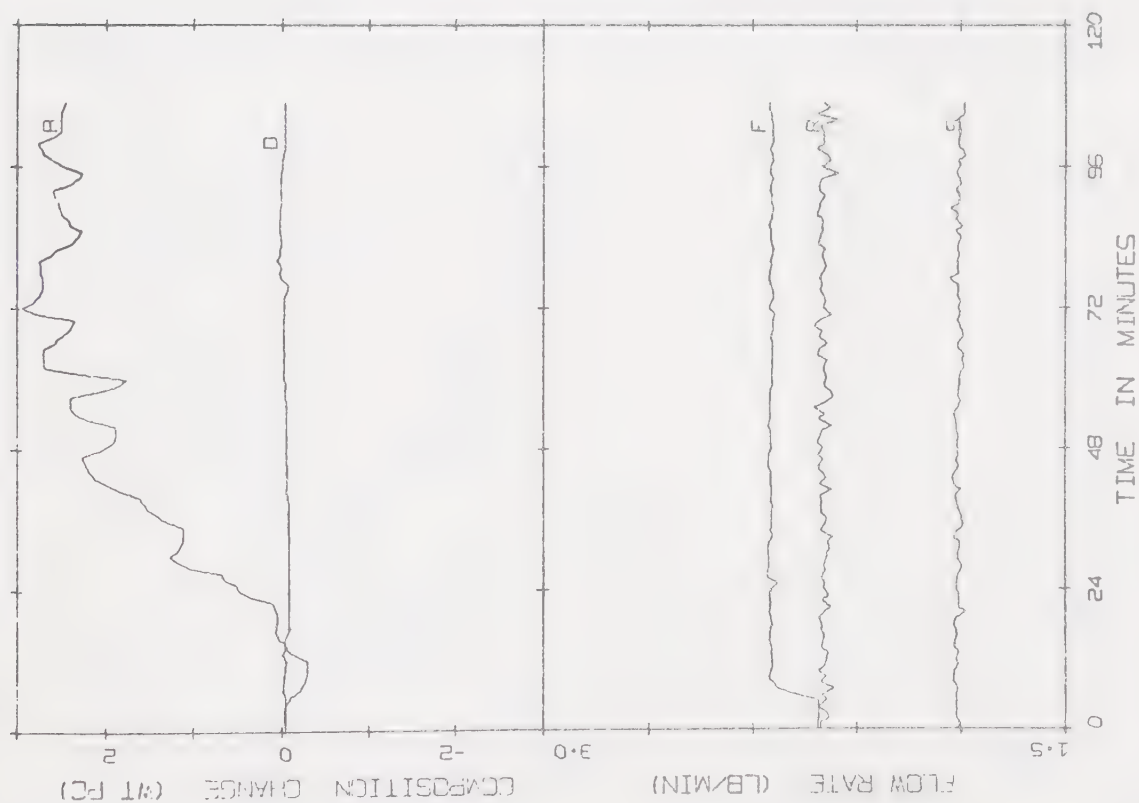


FIGURE 6.4-9: COMPARISON OF EXPERIMENTAL OPEN LOOP AND MULTIVARIABLE FEEDBACK CONTROL BEHAVIOR; +5% FEED FLOW STEP ($\alpha = 0.5$)

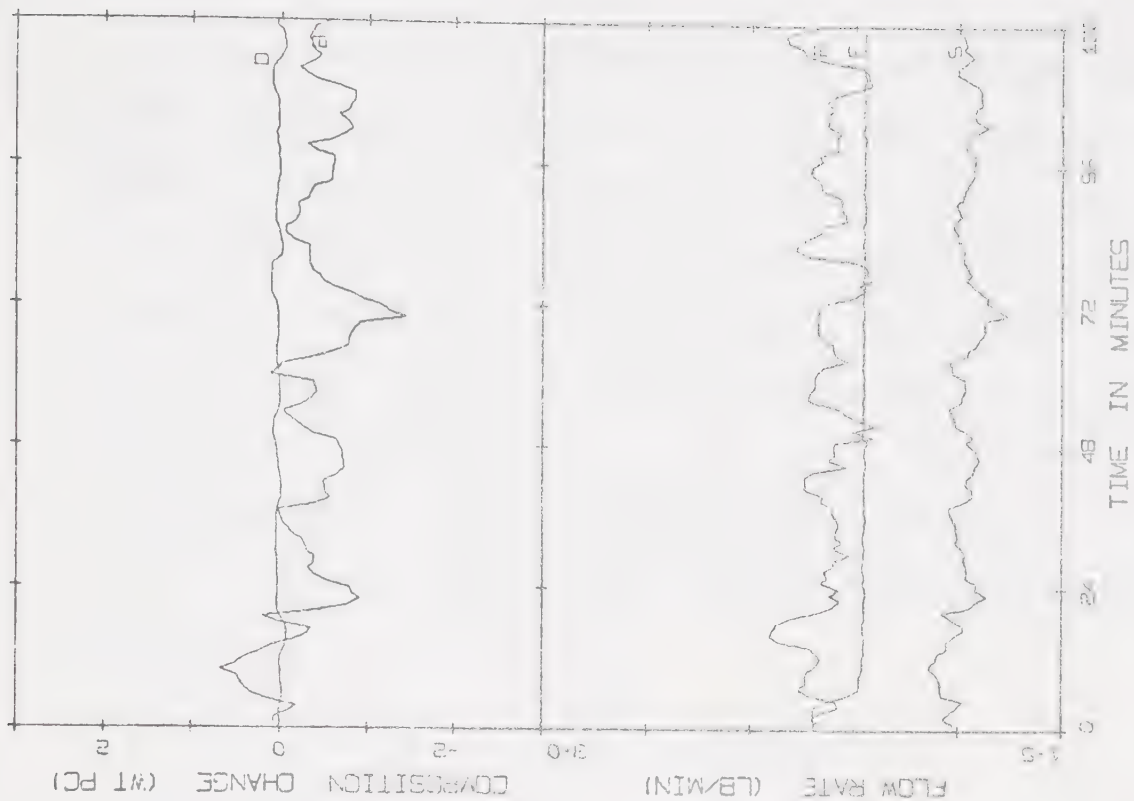
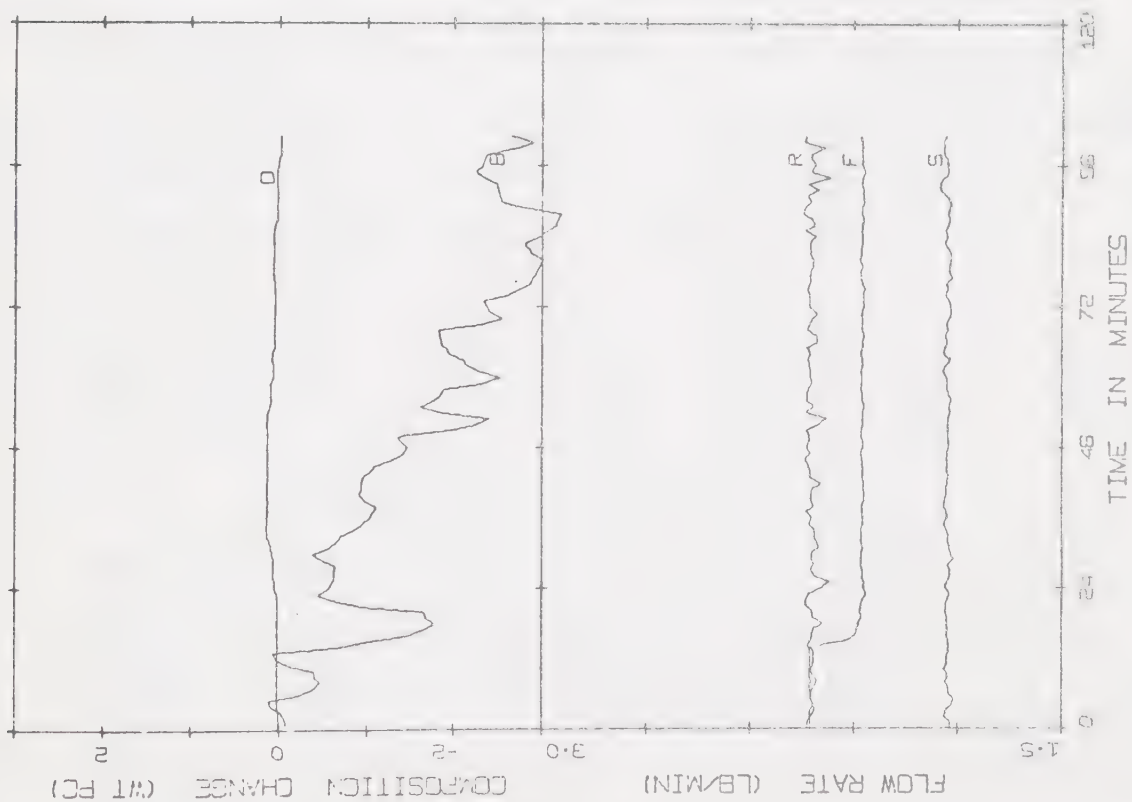


FIGURE 6.4-10. COMPARISON OF EXPERIMENTAL OPEN LOOP AND MULTIVARIABLE FEEDBACK CONTROL BEHAVIOR; -5% FEED FLOW STEP ($\alpha = 0.5$)

These experimental tests support the results predicted by the simulations, that is a reduction in average offset of bottoms composition with sustained oscillations. The overhead composition also shows small oscillations in response to the bottom loop control action, namely, steam flow rate changes. In general, the changes in composition are small, and indicate a satisfactory feedback control law, despite bottoms composition noise.

6.4-5 Simulation of Feedback-Feedforward Control Behavior

The feedback-feedforward control law as defined earlier has the form:

$$\underline{u}(k) = \underline{K}_{FB} \underline{x}(k) + \underline{K}_{FF} \underline{d}(k)$$

When this control law, with the original matrices is applied to the model, with no noise, the result is perfect control, that is, no changes in composition for any disturbance. However, as indicated previously, the experimental system has both a measurement time delay and measurement noise. Also the feedback matrix was modified because of the bottoms composition noise to yield the modified control law where:

$$\underline{K}_{FB} = \begin{bmatrix} 0.00 & 12.9 \\ -50.0 & 65.7 \end{bmatrix} \quad \underline{K}_{FF} = \begin{bmatrix} -1.19 & -.0169 & .0369 \\ 1.85 & -.0831 & .112 \end{bmatrix}$$

This control law was applied to the model with noise and time delay terms added. Figure 6.4-11 shows the simulated controlled responses to a positive step in feed flow. The feedforward action causes an initial change in control action which makes the composition change. There are several large spikes in bottoms composition initially which tend to damp out with time indicating that the feedforward gain may be

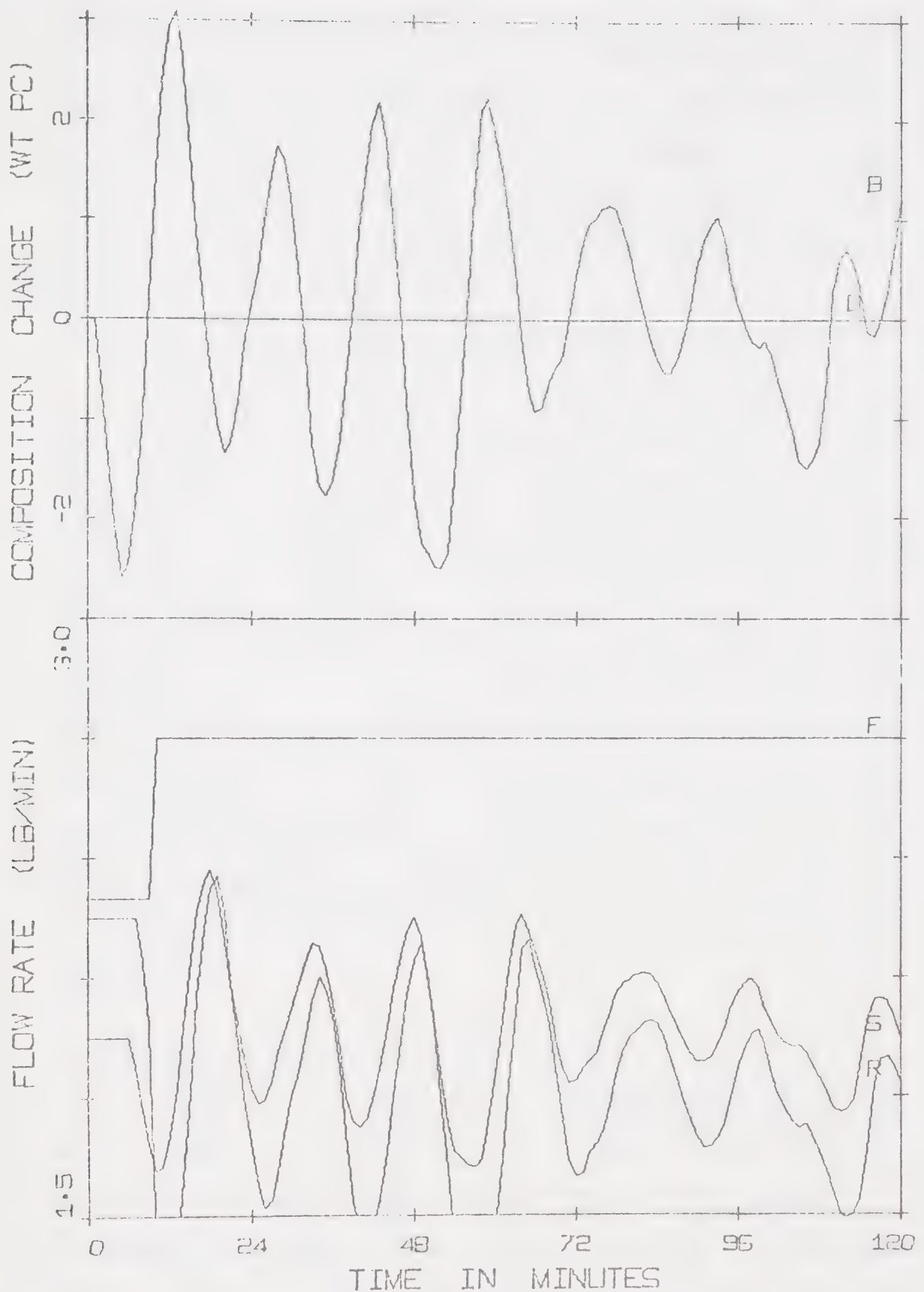


FIGURE 6.4-11: SIMULATED MULTIVARIABLE FEEDBACK-FEEDFORWARD CONTROL BEHAVIOR WITH TIME DELAY AND MEASUREMENT NOISE INCLUDED ($\alpha = 0.5$, $\tau_D = 4$)

too large. This hypothesis is supported by comparing Figures 6.4-11 and 6.4-7 in that an initial deterioration in control appears on inclusion of feedforward compensation. As in the case of feedback control only, there are sustained oscillations in bottoms composition but the system appears to be stable. The bottoms composition change has an average value of about zero, as expected.

6.4-6 Experimental Feedback-Feedforward Control Behavior

The feedback-feedforward control law as presented in the previous section was tested experimentally. Figures 6.4-12 and 6.4-13 show the results obtained for uncontrolled and controlled responses for a positive and negative feed flow step respectively. In both cases the feedforward action can be seen in changes in steam and reflux flow rates. As can be seen the average offsets in bottoms composition are greatly decreased by the presence of the control action. The sustained oscillations evident in the simulation and experimental feedback tests are again evident. The effect of including feedforward control action should be to reduce the average offset in each composition and it can be seen by comparing these responses with those in Figures 6.4-9 and 6.4-10 respectively that this is indeed the case, although the reductions are small.

6.5 Comparison With Previous Control Studies

Berry [6] has carried out an experimental evaluation of two control systems on the column used in this study. One system involved the design of decoupler elements using a transfer function model derived from pulse data. The other system was a ratio controller which tended to remove the interactive effects by physical means. This ratio controller was a two point controller in that steam rate was used to

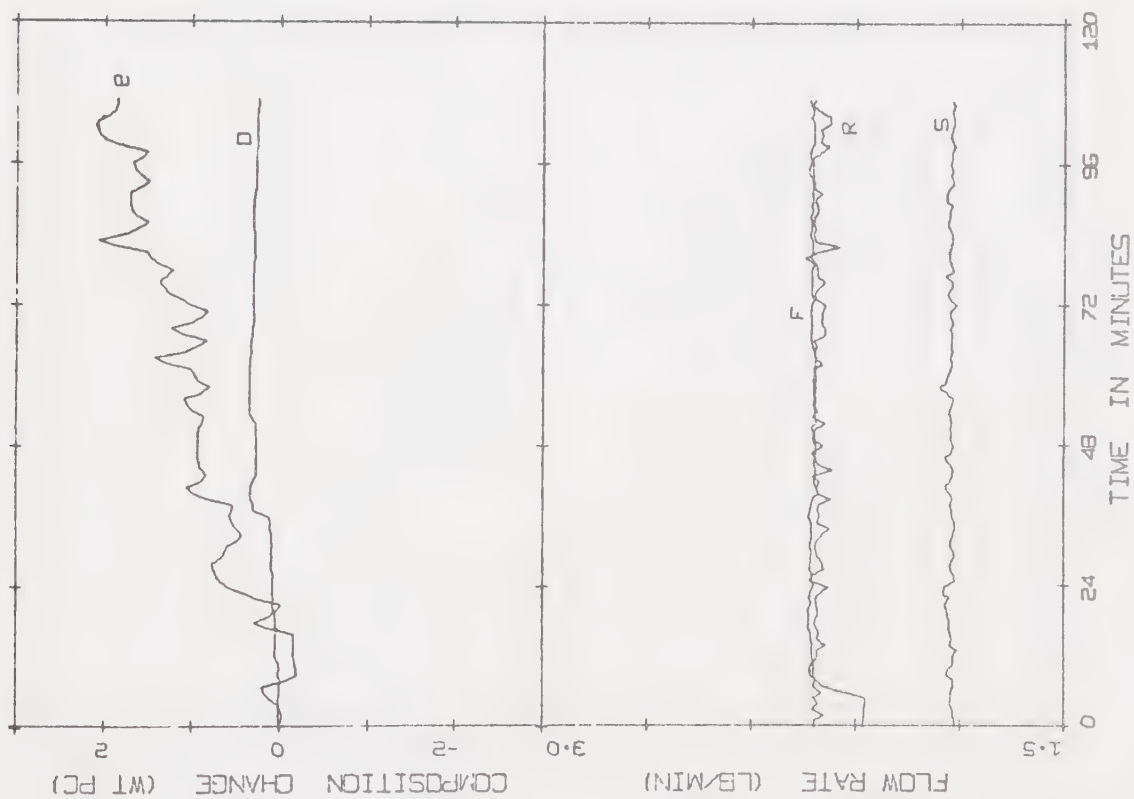
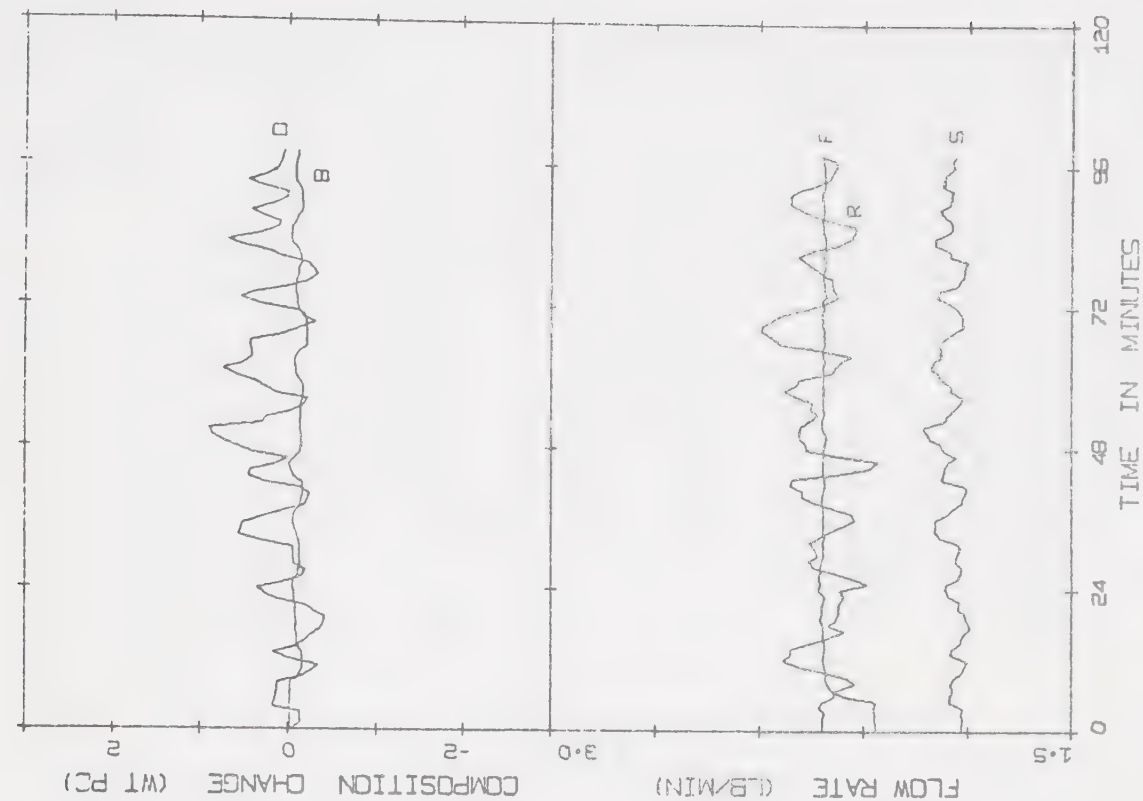


FIGURE 6.4-12: COMPARISON OF EXPERIMENTAL OPEN LOOP AND MULTIVARIABLE FEEDBACK-
FEEDFORWARD CONTROL BEHAVIOR; +5% FEED FLOW STEP ($\alpha = 0.5$)

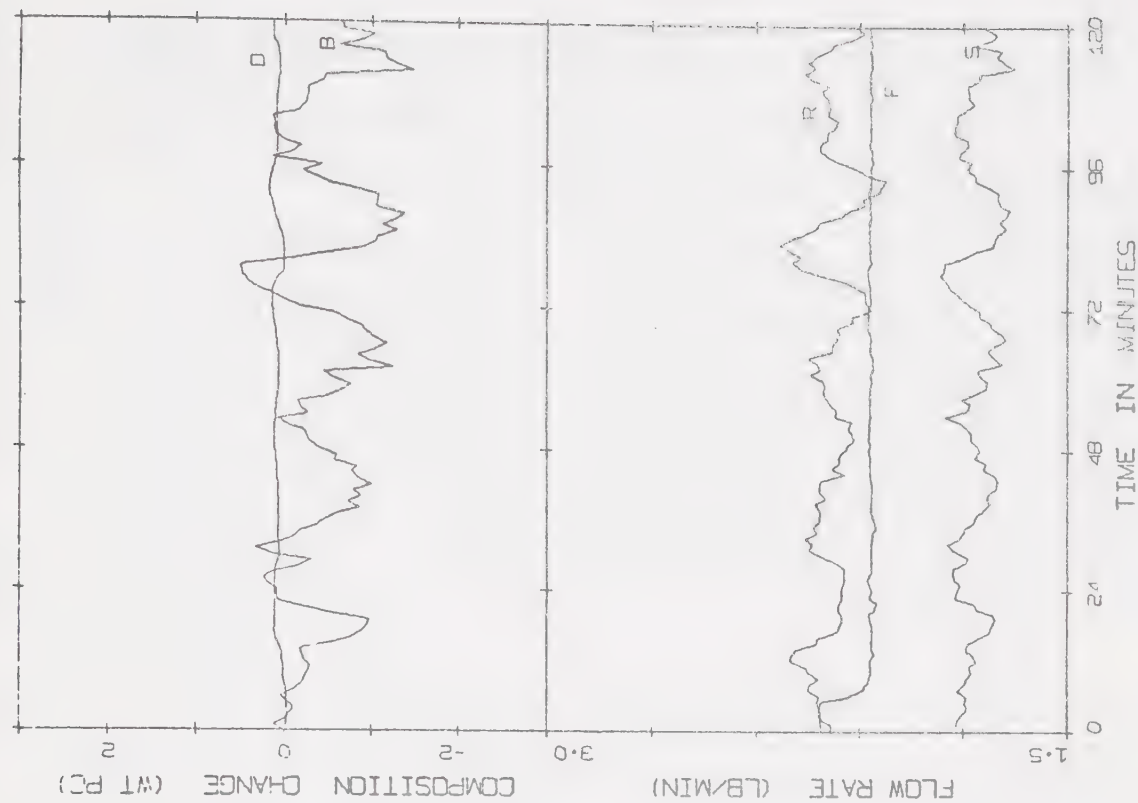
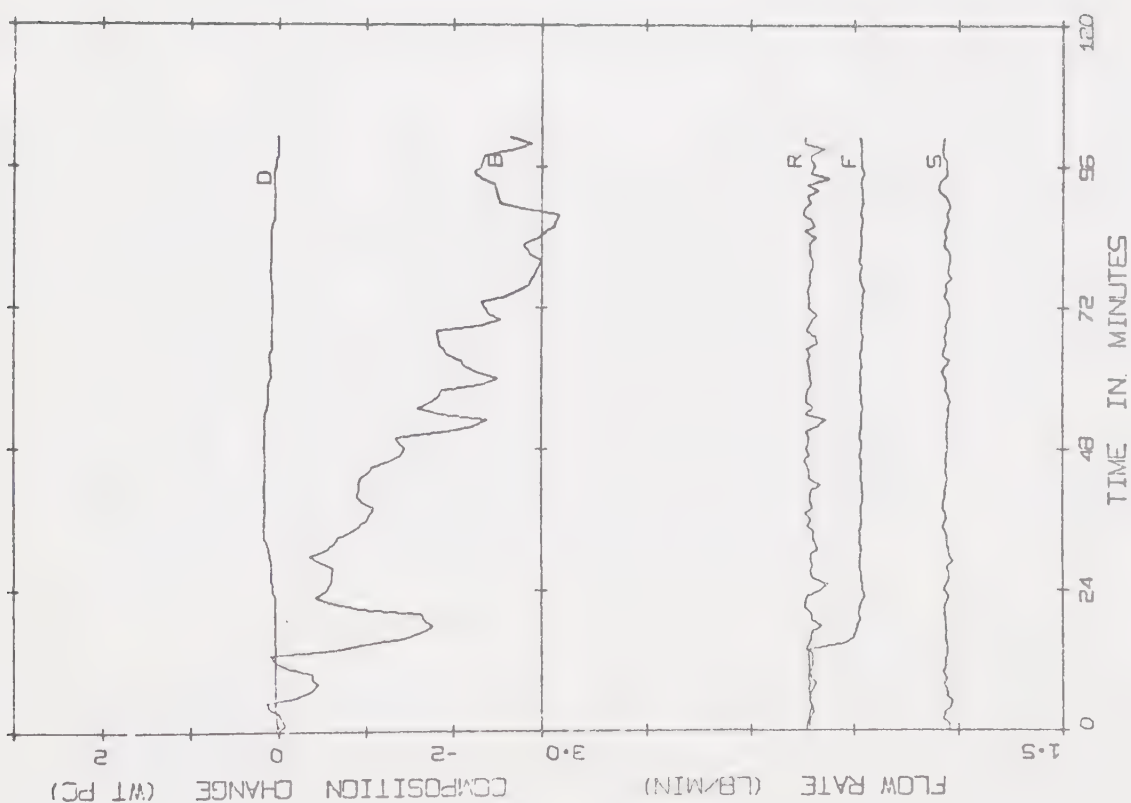
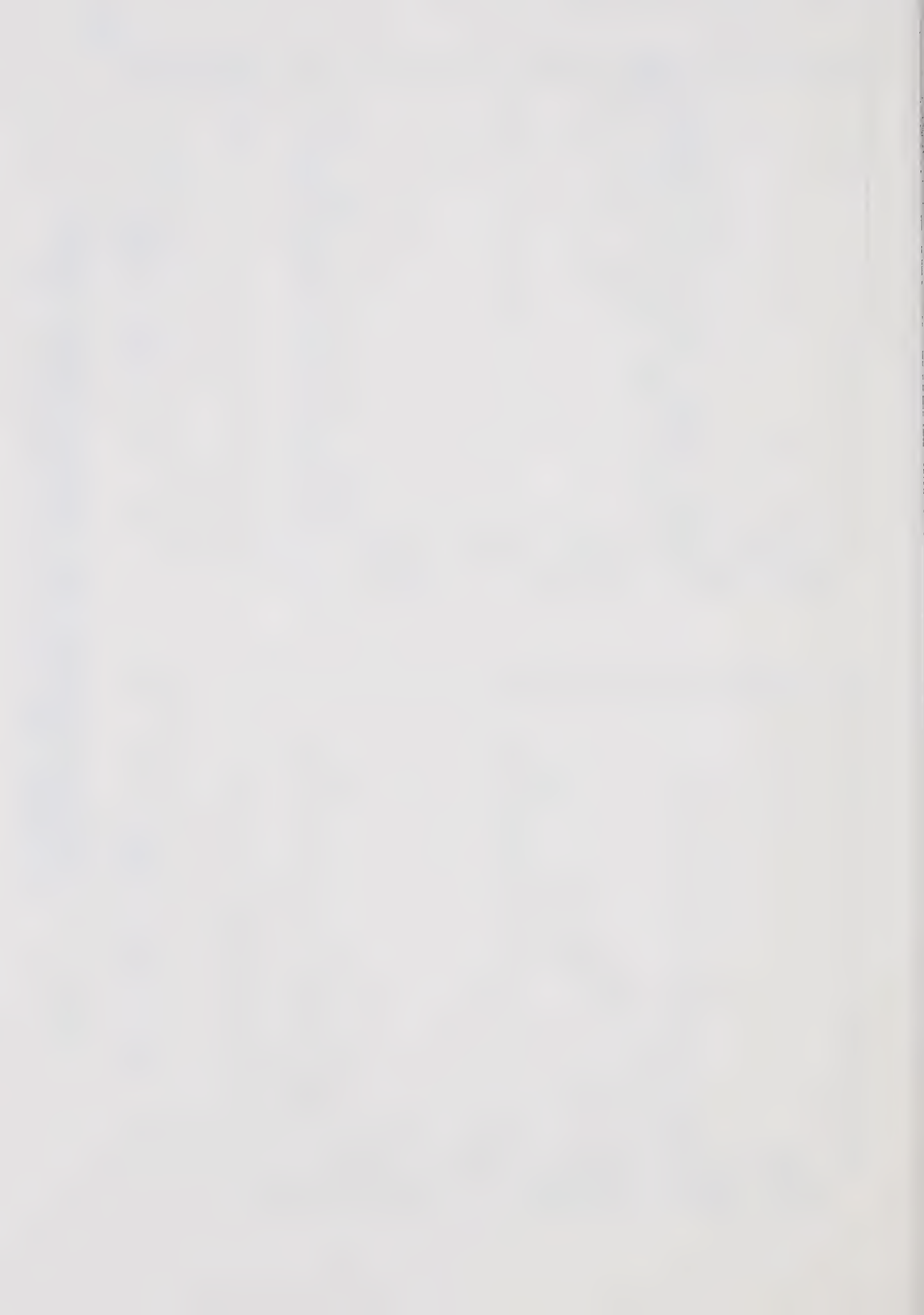


FIGURE 6 4-13: COMPARISON OF EXPERIMENTAL OPEN LOOP AND MULTIVARIABLE FEEDBACK FEEDFORWARD CONTROL BEHAVIOR; -5% FEED FLOW STEP ($\alpha = 0.7$)

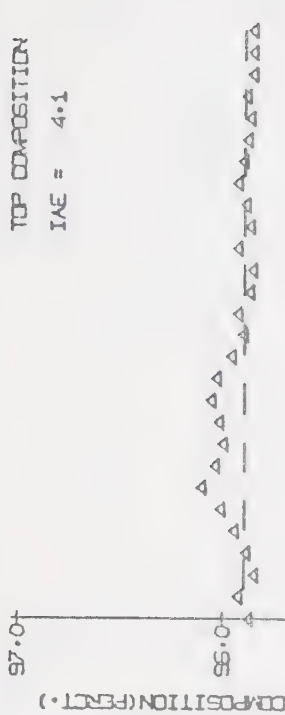
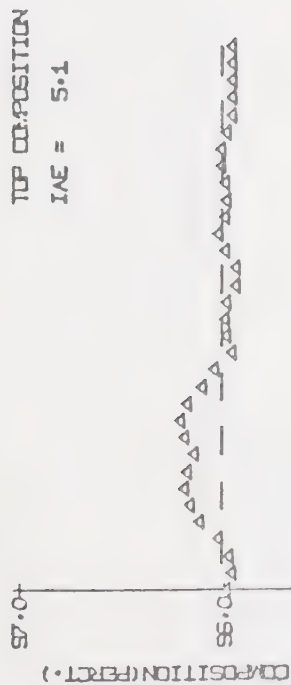


control bottoms composition and the ratio of reflux rate to overhead vapour rate was used to control overhead composition.

Figures 6.5-1 and 6.5-2 (from thesis by Berry) compare these control systems for similar feed flow step disturbances. The feed flow step magnitude was 15%. The controlled responses indicate similar behavior of these systems and both appear to be superior to the multi-variable control system investigated in this study, since both end compositions appear to be well controlled. This can be seen by comparing the results in these figures with those presented in Figures 6.4-9, 10, 12, 13.

The reason for the superiority of the noninteracting control system is the inclusion of time delays in its design. The experimental open loop transients presented in Chapter IV indicate that there is a time delay between the initiation of a disturbance and the beginning of the composition response. These time delay terms were included in Berry's transfer function model and appeared in the decouplers derived from this model. The original 20 state model exhibited these delays to some extent, since they appeared because of the series of first order terms. However, the reduced two state model does not have the number of terms required to introduce the delay to the same extent. This means that the control system designed from the two state model tended to over-compensate and yield oscillations, especially in the bottoms composition control loop where the delay is largest.

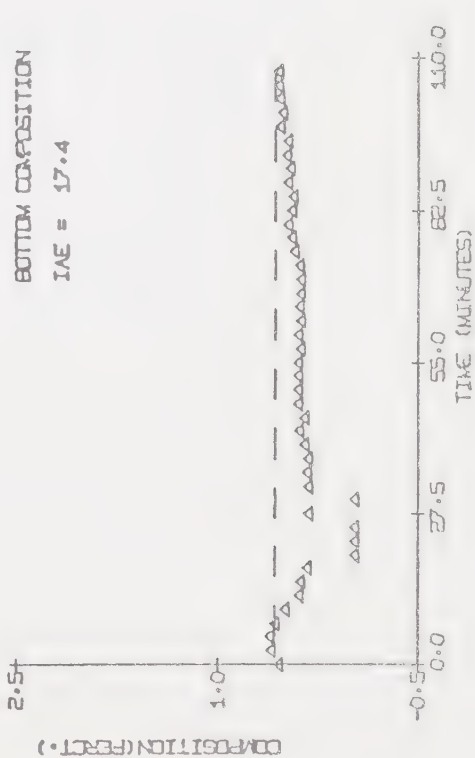
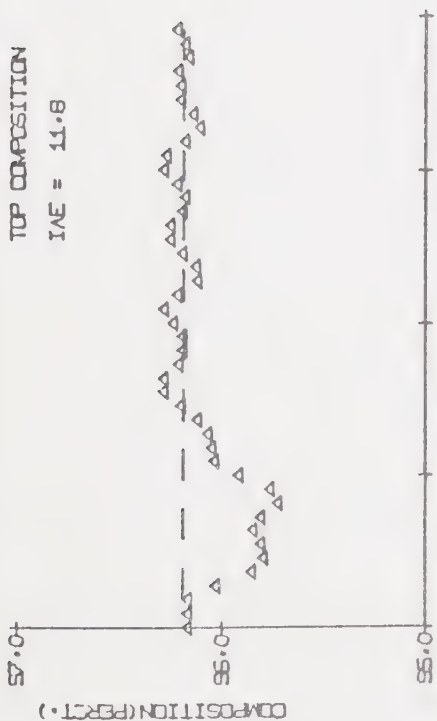
The ratio control system also gave better results than the multivariable control system. This is due to the inherent physical decoupling of this system. It tends to remove the effect of steam flow on overhead composition, which tends to upset the overhead control loop.



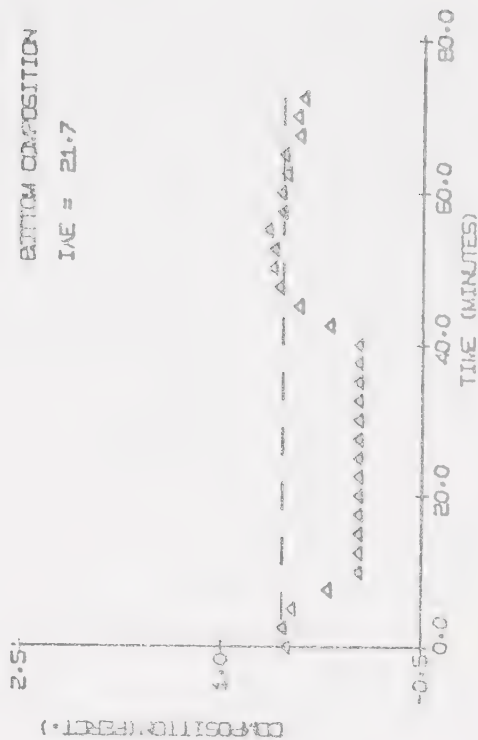
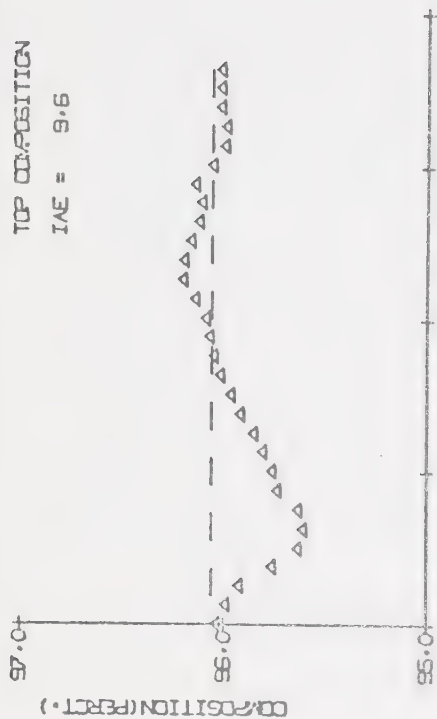
RATIO CONTROL OF THE TOP COMPOSITION [1ST INCREASE
OF FLOW, RUN R-1]

RATIO CONTROL OF THE TOP COMPOSITION [1ST INCREASE
OF FLOW, RUN C-1]

COMPARISON OF RATIO AND NONINTERACTING CONTROL SYSTEMS AS
IMPLEMENTED BY BERRY [67: 41% FEED FLOW STEP]



RATIO CONTROL OF THE TOP COMPOSITION [15% DECREASE
IN FEED FLOW, RUN R-2]



RATIO CONTROL OF THE BOTTOM COMPOSITION [15% INCREASE IN FEED
FLOW, RUN C-3]

This allowed the loops to function almost independently as was the case for the noninteracting control system. The multivariable control system should also account for the interaction but with the interaction time delays absent, the problem of over-compensation and oscillations results.

CHAPTER VII

DISCUSSION AND CONCLUSIONS

The objective of this study was to obtain a process model based on transient balance equations and to apply this model to the design of a multivariable two-point control system. The 20 state model derived in Chapter III and tested in Chapter IV satisfies the requirement for a valid process model. It was found necessary to reduce the order of the model as outlined in Chapter V. The control strategy as outlined in Chapter VI was formulated using the reduced model and was used in subsequent experimental evaluation.

The progression of study allows the following sequence of conclusions to be drawn:

- 1) The distillation column is a linear system with respect to product compositions only over a small operating region, that is for small input disturbances, so linearized perturbation techniques can be used in this region.
- 2) It is not necessary to have detailed information regarding tray efficiencies as in perturbation form the slopes of the equilibrium data curves represent good approximation to the slopes of the actual operating curves.
- 3) In the binary system used (methanol/water) the internal liquid flow dynamics cannot be neglected, and can be adequately represented by a first order expression.
- 4) The distillation column used in this study can be adequately represented by a twenty state model, with stage enthalpies and liquid flows as the states.

- 5) The two model reduction techniques tried in this study both yield acceptable reduced models. However, the two state model obtained by using Anderson's method was more attractive for the design of a control system as used in this study.
- 6) The bottom composition measurement exhibited an appreciable amount of noise, due to the small composition of methanol and the approximate peak area calculation.
- 7) The combination of top product enthalpy (composition) control by reflux flow manipulation, and bottom product enthalpy (composition) control by steam flows manipulation yields a two point control system which exhibits interactive effects.
- 8) The gas chromatograph separation and analysis cycle represents a measurement time delay. The application of an exponential filter to the noisy bottoms composition measurement has the effect of introducing another time delay. The combination of these time delays causes a deterioration in the controlled behavior.
- 9) It was necessary to modify the feedback control laws due to the bottoms composition noise. This feedback control system yields an oscillatory controlled response with a small offset in each composition. This behavior has been predicted by simulation tests and has been subsequently verified experimentally.
- 10) The inclusion of feedforward compensation with the feedback control system decreases the average offsets in compositions. The simulation and experimental tests verify this result, and indicate that sustained oscillations are present, as in the case of feedback control only.

A comparison of this multivariable control scheme with those

investigated by Berry [6] indicates that the latter schemes are superior. This would imply that the method of model derivation, testing and reduction and control law calculation yields a control system which does not warrant the effort necessary. This multivariable approach is, however, the logical sequel to the simpler control schemes. This suggests that some method of process identification should be used to eliminate the initial steps of model derivation and verification.

The major problems encountered in this study were time delays and measurement noise, both of which are due to the use of the gas chromatograph to analyze the bottoms. However, the properties of the dilute solution product are not conducive to other on-line analysis techniques such as capacitance probe or refractometer.

CHAPTER VIII

RECOMMENDATIONS

As indicated in the previous chapter the process of model derivation and testing appears to be superfluous when the model is then reduced for control application. A more reasonable path is to derive a lower order model by the use of experimental data. Pulse testing has been applied to the column used in this study and a good transfer function model obtained [6]. It is also expected that in the near future, pseudo-random binary sequence testing will be applied, and the model obtained will be compared to that derived from the pulse test data. However, if a model of the state space form is desired, it would probably be much simpler to apply some form of learning or model-reference adaptive identification procedure. However, all these methods give only approximate models, when applied to a non-linear system such as a distillation column, and the one chosen must depend on the operating range and application.

The overhead product control configuration used in this study was to control the reflux flow and use the overhead product flow to control the condenser level. Recently some indication has been given that the reverse scheme, i.e. controlling overhead product flow and using reflux flow to control condenser level, yields a more stable control system. It also has the effect of partially accounting for changes in overhead vapour flow, and so may produce a physical decoupling. This configuration should be tested and compared to the scheme used in this study to see if this improvement actually appears.

The major problem encountered in this study was the noise and time delay in the bottom composition measurement. It may prove

advantageous to employ a Kalman filter or an observer to counter the effect of the noise. It may also be advantageous to use a predictor such as a Smith predictor which accounts for the time delays in the control system. However, both of these alternatives require the use of a good process model and so the model would need to be carefully evaluated before being applied.

The non-linearity of the distillation system, coupled with the problems of process modelling, suggest the application of a learning or adaptive control system. This approach removes the need for a process model, and any control law derivation. Such a method could be applied providing some form of filter were used on the bottoms composition.

Each of the alternatives to modelling and control presented above has been suggested as a possible improvement to the method used in this study. It is felt that each of these warrants some consideration and possible subsequent experimental study.

REFERENCES

1. Anderson, J.E., "Dynamic Behaviour and Feedforward Control of a Binary Distillation Column", Ph.D. Thesis, Department of Chemical Engineering, University of Delaware, 1964.
2. Anderson, J.H., "Geometrical Approach to Reduction of Dynamical Systems", PROC. IEE, Vol. 114, No. 7, 1014, (1967).
3. Archer, D.H., Rothfus, R.R., "The Dynamics and Control of Distillation Units and Other Mass Transfer Equipment", Chem. Eng. Prog. Symp. Ser., 57, No. 36, 2, (1961).
4. Baber, M.F., Edwards, L.L., Harper, W.T., Witte, M.D., Gerster, J.A., "Experimental Transient Response of a Pilot Plant Distillation Column", Chem. Eng. Prog. Symp. Ser., 57, No. 36, 148, (1961).
5. Baber, M.F., Gerster, J.A., "Experimental Transient Response of a Pilot Plant Distillation Column: Part II. Response to Liquid and Vapour Rate Perturbations", AIChE Journal, 8, No. 3, 407, (1962).
6. Berry, M.W., M.Sc. Thesis, Department of Chemical and Petroleum Engineering, University of Alberta, Edmonton, Alberta (to be published).
7. Boyd, D.M., "Fractionation Instrumentation and Control - Part I", Petrol. Ref., 27, No. 10, 533, (1948).
8. Boyd, D.M., "Fractionation Instrumentation and Control - Part II", Petrol. Ref., 27, No. 11, 594, (1948).
9. Brosilow, C.B., Handley, K.R., "Optimal Control of a Distillation Column", AIChE Journal, 14, No. 3, 467, (1968).
10. Chanh, B.M., M.Sc. Thesis, Department of Chemical and Petroleum Engineering, University of Alberta, Edmonton, Alberta, 1971.
11. Davison, E.J., "An Automatic Way of Finding 'Optimal' Control Systems for Large Multivariable Plants", Proc. IFAC Tokyo Symposium, 376, (1965).
12. Davison, E.J., "Control of a Distillation Column with Pressure Variation", Trans. Instr. Chem. Engrs., 45, T 229, (1967).
13. Davison, E.J., "The Interaction of Control Systems in a Binary Distillation Column", Automatica, 6, 447 (1970).
14. Davison, E.J., Chadha, K.J., "On the Control of a Large Chemical Plant", Paper presented at the 20th Canadian Chemical Engineering Conference, Sarnia, Ontario, (1970).

15. Distefano, G.P., "Transient Response of a Continuous Distillation Tower to a Sequence of UPSets", Ph.D. Thesis, Department of Chemical Engineering, University of Florida, Gainesville, Florida, (1964).
16. Distefano, G.P., May, F.P., Huckaba, C.E., "Transient Response and Feed-forward Control of a Distillation Tower Subject to a Sequence of Upsets", *AIChE Journal*, 13, No. 1, 125, (1967).
17. Gerster, J.A., Shoneman, K.F., "Feedback Control of an Enriching Column", *AIChE Journal*, 16, No. 6, 1080, (1970).
18. Gilliland, E.R., Mohr, C.M., "Transient Behaviour in Plate-Tower Distillation of a Binary Mixture", *Chem. Eng. Prog. Symp. Ser.* 59, No. 46, 32, (1963).
19. Greville, T.N.E., "The Pseudoinverse of a Rectangular or Singular Matrix and Its Application to the Solution of Systems of Linear Equations", *SIAM Review*, 1, No. 1, 38, (1958).
20. Hammond, P.H., Williams, B.J., "On Determining a Dynamic Model of a Distillation Column Using a Computer Program", 2nd U.K. Conference on Computer Control, University of Bristol, April, (1967).
21. Hightower, J.R., "A Practical Implementation of Feedforward Control", Ph.D. Thesis, Department of Chemical Engineering, Tulane University, New Orleans, Louisiana, (1964).
22. Hu, Y., "Application of Modern Control Theory to Distillation Columns", Ph.D. Thesis, Department of Chemical Engineering, University of Colorado, Boulder, Colorado, (1970).
23. Huckaba, C.E., May, F.P., Franke, F.R., "An Analysis of Transient Conditions in Continuous Distillation Operations", *Chem. Eng. Prog. Symp. Ser.*, 59, No. 46, 38, (1963).
24. Janis, R.F., "Feedforward Control of Binary Distillation", Ph.D. Thesis, Department of Chemical Engineering, Virginia Polytechnic Institute, Blacksburg, Virginia, (1967).
25. Lamb, D.E., Pigford, R.L., Rippin, D.W.T., "Dynamic Characteristics and Analogue Simulation of Distillation Columns", *Chem. Eng. Prog. Symp. Ser.*, 57, No. 36, 132, (1961).
26. Luyben, W.L., Verneuil, V.S., Gerster, J.A., "Experimental Transient Response of a Pilot-Plant Distillation Column: Part IV. Response of a Ten-Tray Column", *AIChE Journal*, 10, No. 3, 357, (1964).
27. Luyben, W.L., "Feed Plate Manipulation in Distillation Column Feedforward Control", *IEC Fund.*, 7, 502, (1968).

28. Luyben, W.L., "Distillation Decoupling", *AIChE Journal*, 16, No. 2, 198, (1970).
29. Luyben, W.L., "Control of Distillation Columns with Sharp Temperature Profiles", *AIChE Journal*, 17, No. 3, 713, (1971).
30. Mah, R.S.H., Michaelson, S., Sargent, R.W.H., "Dynamic Behaviour of Multi-component Multi-stage Systems. Numerical Methods for the Solution", *Chem. Eng. Sci.*, 17, 619, (1962).
31. Marshall, S.A., "An Approximate Method for Reducing the Order of a Linear System", *Control*, 10, 642, (1966).
32. Newell, R.B., "Multivariable Computer Control of an Evaporator", Ph.D. Thesis, Department of Chemical and Petroleum Engineering, University of Alberta, Edmonton, Alberta, (1971).
33. Niederlinski, A., "Two-Variable Distillation Control: Decouple or Not Decouple", *AIChE Journal*, 17, No. 5, 1261, (1971).
34. Pyle, C., "Control Systems for Distillation Towers", *The Oil and Gas Journal*, 19, Oct. 13, (1949).
35. Rees, N.W., "Dynamic Identification and Optimum Control Studies on a Pilot Distillation Column", *Automatic and Remote Control*, Proc. IFAC Moscow, Paper 32-C, (1960).
36. Rijnsdorp, J.E., "Interaction in Two-Variable Control Systems for Distillation Columns - I", *Automatica*, 3, 15, (1965).
37. Rijnsdorp, J.E., "Interaction in Two-Variable Control Systems for Distillation Columns - II", *Automatica*, 3, 29, (1965).
38. Rijnsdorp, J.E., van Kampen, J.A., "Automatic Feedback Control of Two Product Qualities of a Distillation Column", 3rd IFAC Congress, Paper 32B, London, (1966).
39. Rosenbrock, H.H., "Calculation of the Transient Behaviour of Distillation Columns - Part I", *Brit. Chem. Eng.*, 3, 364, (1958).
40. Rosenbrock, H.H., "Calculation of the Transient Behaviour of Distillation Columns - Part II", *Brit. Chem. Eng.*, 3, 432, (1958).
41. Rosenbrock, H.H., "Calculation of the Transient Behaviour of Distillation Columns - Part III", *Brit. Chem. Eng.*, 3, 491, (1958).
42. Rosenbrock, H.H., "Control of Columns: Report by the Rapporteur", *I. Chem. E. Symp. Ser.*, No. 32, Session 6, (1969).
43. Sargent, R.W.H., "The Dynamic Behaviour of Multi-Stage Systems: Further Improvements in the Numerical Solution", *Trans. Instr. Chem. Engrs.*, 41, 51, (1963).

44. Speicher, E.J., Luyben, W.L., "Experimental Studies of Feed Plate Manipulation for Distillation Column Feedforward Control", IEC Fund., 10, No. 1, 147, (1971).
45. Sproul, J.S., Gerster, J.A., "Experimental Transient Response of a Pilot-Plant Distillation Column: Part III. Condensing and Reboiling Systems", Chem. Eng. Prog. Symp. Ser., 46, No. 59, 21, (1965).
46. Svrcek, W.Y., "Binary Distillation Column Dynamics", Ph.D. Thesis, Department of Chemical and Petroleum Engineering, University of Alberta, Edmonton, Alberta, (1967).
47. Tivy, V.V. St. L., "Automatic Control of Fractionating Columns", Petrol. Ref., 27, No. 11, 603, (1948).
48. Wahl, E.F., "The Practical Prediction of Binary Distillation Column Transfer Functions and an Analysis of the Single Point Control System", Ph.D. Thesis, Department of Chemical Engineering, Cornell University, (1967).
49. Williams, T.J., "The Status of Studies of the Dynamics of Mass-Transfer Operations - A Review and Commentary", Chem. Eng. Prog. Symp. Ser., 59, No. 46, 1, (1963).
50. Williams, B.J., "The Estimation by Computer of Composition from Temperature and Pressure Measurements in a Binary Distillation System", National Physical Laboratory, Autonomics Division, Auto 27, Teddington, United Kingdom, (Jan. 1967).
51. Williams, B.J., "Optimal Control of a Distillation Column", National Physical Laboratory, Autonomics Division, Auto 21, Teddington, United Kingdom, (July 1966).
52. Williams, B.J., "The Computer Control of a Distillation Column", National Physical Laboratory, Division of Computer Science, Com. Sci. 37, Teddington, United Kingdom, (July 1968).
53. Wilson, R.G., Fisher, D.G., Seborg, D.E., "Model Reduction for Discrete-Time Dynamic Systems", Int. Journal of Cont., (to be published).
54. Wilson, R.G., "Computer Control of Processes with Inaccessible State Variables", current Ph.D. project, Department of Chemical and Petroleum Engineering, University of Alberta, Edmonton, Alberta.
55. Wood, C.E., "Tray Selection for Column Temperature Control", Chem. Eng. Prog., 64, No. 1, 85, (1968).
56. Wood, R.K., Pacey, W.C., "Experimental Evaluation of Feedback, Feedforward and Combined Feedforward-Feedback Binary Distillation Column Control", Paper presented at the 20th Canadian Chemical Engineering Conference, Sarnia, Ontario, (Oct. 1970).

57. Wood, R.K., Berry, M.W., "Terminal Composition Control of a Binary Distillation Column", Paper presented at the 21st Canadian Chemical Engineering Conference, Montreal, Quebec, (Oct. 1971).
58. Zahradnik, R.L., Archer, D.H., Rothfus, R.R., "Dynamic Optimization of a Distillation Column", Chem. Eng. Prog. Symp. Ser., 59, No. 46, 132, (1963).
59. Zalkind, C.S., "Practical Approach to Non-Interacting Control - Part I", Instrum. Contr. Syst., 40, No. 3, 89, (1967).
60. Zalkind, C.S., "Practical Approach to Non-Interacting Control - Part II", Instrum. Contr. Syst., 40, No. 4, 111, (1967).

APPENDIX A

NOMENCLATURE

Chapter III: Model Derivation

Scalars

b_1, b_2	- liquid/vapour enthalpy linearization factors
D	- distillate flow rate (lb/min)
F	- feed flow rate (lb/min)
h	- liquid phase enthalpy (BTU/lb)
H	- vapour phase enthalpy (BTU/lb)
K	- liquid dynamics flow variation constant
L	- liquid flow rate from a stage (lb/min)
Q	- heat loss from a stage (BTU/min)
Q_C	- condenser heat duty (BTU/min)
Q_R	- reboiler heat duty (BTU/min)
t	- time
T	- temperature
τ	- liquid flow dynamics time constant
v	- vapour flow rate from a stage (lb/min)
W	- stage mass holdup
x	- liquid phase composition (wt % MeOH)
y	- vapour phase composition (wt % MeOH)

Vectors

\underline{D}	- disturbance/control vector
\underline{h}	- vector of liquid phase enthalpy perturbations
\underline{H}	- vector of vapour phase enthalpy perturbations
\underline{L}	- vector of liquid flows from each stage
\underline{M}_L	- vector of liquid mass holdups

- \underline{M}_G - vector of vapour mass holdups
 \underline{V} - vector of vapour flows from each stage

Matrices

- $\underline{A}, \underline{\hat{A}}, \underline{B}, \underline{\hat{B}}, \underline{C}_1, \underline{C}_2, \underline{\hat{C}}, \underline{G}, \underline{H}, \underline{M},$
 \underline{N} - model coefficient matrices (as defined)
 \underline{B}_1 - diagonal matrix of enthalpy linearization factors
 $\underline{\bar{h}}$ - diagonal matrix of steady state liquid enthalpies
 $\underline{\bar{H}}$ - diagonal matrix of steady state vapour enthalpies
 $\underline{\bar{L}}$ - diagonal matrix of steady state liquid flows
 $\underline{\bar{V}}$ - diagonal matrix of steady state vapour flows
 \underline{W}_G - diagonal matrix of steady state vapour mass holdups
 \underline{W}_L - diagonal matrix of steady state liquid mass holdups

Subscripts

- 1-10 - individual stage designation
 f - feed stream
 G - gaseous or vapour phase
 i - general ith stage
 L - liquid phase

Superscripts

- - initial steady state value
 ' - perturbation from steady state
 · - time derivative

Chapter IV: Model Evaluation

Scalars

a	- scalar example coefficient
α	- constant
b	- scalar example coefficient
β	- constant
d	- scalar example input disturbance
g	- scalar example state coefficient
h	- scalar example input coefficient
k	- number of incremental time intervals in model time base
λ	- eigenvalue of matrix \underline{G}
t	- time
T	- model time base
x	- scalar example state

Vectors

\underline{x}	- state vector
\underline{D}	- disturbance/control vector
\underline{z}	- canonical state vector

Matrices

\underline{G}	- continuous model state transition matrix
\underline{H}	- continuous model input weighting matrix
\underline{M}	- similarity transformation matrix
$\underline{\Delta}$	- discrete model state transition matrix
$\underline{\theta}$	- Jordan canonical form input weighting matrix
$\underline{\phi}$	- discrete model input weighting matrix
$\underline{\Lambda}$	- Jordan canonical form state transition matrix

Chapter V: Model Reduction

Vectors

- \underline{x} - state vector
- \underline{z} - canonical state vector
- \underline{b}_q - vector of time domain solution of q th state
- \underline{c}_q - vector of q th row of elements of $\underline{\phi}_R$ and $\underline{\Delta}_R$
- \underline{u} - vector of model inputs

Matrices

- \underline{A} - original model state transition matrix
- \underline{A}_R - reduced model state transition matrix
- $\underline{\alpha}$ - Jordan canonical form state transition matrix
(diagonal elements are eigenvalues of \underline{A})
- \underline{B} - original model input weighting matrix
- \underline{B}_R - reduced model input weighting matrix
- $\hat{\underline{B}}$ - matrix with \underline{b}_q vectors as columns
- $\hat{\underline{\beta}}$ - Jordan canonical form input weighting matrix
- $\hat{\underline{C}}$ - matrix with \underline{c}_q vectors as columns
- \underline{M} - similarity transformation matrix
- $\hat{\underline{M}}$ - coefficient matrix for Anderson's method
- $\underline{\phi}$ - original model discrete form transition matrix
- $\underline{\phi}_R$ - reduced model discrete form transition matrix
- $\underline{\Delta}$ - original model discrete form input weighting matrix
- $\underline{\Delta}_R$ - reduced model discrete form input weighting matrix

Chapter VI: Control Studies

Scalars

- α - exponential filter constant
- k - designation of general time interval

Vectors

- \underline{d} - vector of input disturbances
- \underline{v} - vector of control variables
- \underline{x} - state vector
- \underline{x}_f - filtered state vector
- \underline{x}_m - measured state vector
- \underline{x}_s - vector of state setpoints

Matrices

- \underline{A} - continuous model state transition matrix
- \underline{B} - continuous model controls weighting matrix
- \underline{b} - discrete model controls weighting matrix
- \underline{D} - continuous model disturbance weighting matrix
- $\underline{\Delta}$ - discrete model disturbance weighting matrix
- \underline{K}_{FB} - feedback control matrix
- \underline{K}_{FF} - feedforward control matrix
- \underline{K}_{sp} - setpoint control matrix
- $\underline{\Phi}$ - discrete model state transition matrix

APPENDIX B

MATRIX REPRESENTATION OF BALANCE EQUATIONS

The dynamic equations outlined in Chapter III represent two sets of ten coupled differential equations. These can be written as two matrix-vector equations as outlined in the following sections.

B-1 Overall Balances

The total mass balance relations represent ten differential equations relating the changes in mass holdup in each stage to the stream flows to and from that stage. The following is a summary of these equations:

a) Reboiler (Stage 1)

$$\dot{W}'_{G1} + \dot{W}'_{L1} = L'_2 - V'_1 - L'_1$$

b) General Tray (Stage I)

$$\dot{W}'_{Gi} + \dot{W}'_{Li} = V'_{i-1} + L'_{i+1} - V'_i - L'_i$$

$$i = 2, 3, 4, 6, 7, 8, 9$$

c) Feed Tray (Stage 5)

$$\dot{W}'_{G5} + \dot{W}'_{L5} = V'_4 + L'_6 - V'_5 - L'_5 + F'$$

d) Condenser (Stage 10)

$$\dot{W}'_{G10} + \dot{W}'_{L10} = V'_9 - L'_{10} - D'$$

These equations can be written as a matrix-vector equation of order 10 of the form:

$$\begin{aligned}
 & \begin{bmatrix} W'_{L1} \\ W'_{L2} \\ W'_{L3} \\ W'_{L4} \\ W'_{L5} \\ W'_{L6} \\ W'_{L7} \\ W'_{L8} \\ W'_{L9} \\ W'_{L10} \end{bmatrix} + \begin{bmatrix} W'_{G1} \\ W'_{G2} \\ W'_{G3} \\ W'_{G4} \\ W'_{G5} \\ W'_{G6} \\ W'_{G7} \\ W'_{G8} \\ W'_{G9} \\ W'_{G10} \end{bmatrix} = \begin{bmatrix} -1 & 1 & 0 & 0 & 0 & 0 & 0 & 0 & 0 & 0 \\ 0 & -1 & 1 & 0 & 0 & 0 & 0 & 0 & 0 & 0 \\ 0 & 0 & -1 & 1 & 0 & 0 & 0 & 0 & 0 & 0 \\ 0 & 0 & 0 & -1 & 1 & 0 & 0 & 0 & 0 & 0 \\ 0 & 0 & 0 & 0 & -1 & 1 & 0 & 0 & 0 & 0 \\ 0 & 0 & 0 & 0 & 0 & -1 & 1 & 0 & 0 & 0 \\ 0 & 0 & 0 & 0 & 0 & 0 & -1 & 1 & 0 & 0 \\ 0 & 0 & 0 & 0 & 0 & 0 & 0 & -1 & 1 & 0 \\ 0 & 0 & 0 & 0 & 0 & 0 & 0 & 0 & -1 & 0 \\ 0 & 0 & 0 & 0 & 0 & 0 & 0 & 0 & 0 & -\frac{1}{2} \end{bmatrix} \times \begin{bmatrix} L'_1 \\ L'_2 \\ L'_3 \\ L'_4 \\ L'_5 \\ L'_6 \\ L'_7 \\ L'_8 \\ L'_9 \\ D'_1 \end{bmatrix} \\
 & + \begin{bmatrix} -1 & 0 & 0 & 0 & 0 & 0 & 0 & 0 & 0 & 0 \\ 1 & -1 & 0 & 0 & 0 & 0 & 0 & 0 & 0 & 0 \\ 0 & 1 & -1 & 0 & 0 & 0 & 0 & 0 & 0 & 0 \\ 0 & 0 & 1 & -1 & 0 & 0 & 0 & 0 & 0 & 0 \\ 0 & 0 & 0 & 1 & -1 & 0 & 0 & 0 & 0 & 0 \\ 0 & 0 & 0 & 0 & 1 & -1 & 0 & 0 & 0 & 0 \\ 0 & 0 & 0 & 0 & 0 & 1 & -1 & 0 & 0 & 0 \\ 0 & 0 & 0 & 0 & 0 & 0 & 1 & -1 & 0 & 0 \\ 0 & 0 & 0 & 0 & 0 & 0 & 0 & 1 & -1 & 0 \\ 0 & 0 & 0 & 0 & 0 & 0 & 0 & 0 & 1 & -\frac{1}{2} \end{bmatrix} \times \begin{bmatrix} V'_1 \\ V'_2 \\ V'_3 \\ V'_4 \\ V'_5 \\ V'_6 \\ V'_7 \\ V'_8 \\ V'_9 \\ D'_1 \end{bmatrix} \\
 & + \begin{bmatrix} F'_1 \\ L'_{10} \\ Q'_R \\ Q'_C \\ h'_f \\ h'_{10} \end{bmatrix}
 \end{aligned}$$

FIGURE B-1.1: TOTAL MASS BALANCE: $\dot{M}'_L + \dot{M}'_G = A' \underline{L}' + B' \underline{V}' + C' \underline{D}'$

$$\dot{\underline{M}}_L + \dot{\underline{M}}_G = \underline{A} \underline{L} + \underline{B} \underline{V} + \underline{C}_1 \underline{D} \quad (\text{B-1.1})$$

This equation is shown in its expanded form in Figure B-1.1 where \underline{A} , \underline{B} and \underline{C}_1 are defined. The vector \underline{D} includes terms not appearing in the total mass balances but which appear in the enthalpy balances and are either controls or input disturbances.

B-2 Enthalpy Balances

The ten enthalpy balance equations represent a set of ten equations, similar to those for the total mass balances. They give the rate of change of enthalpy content in each stage as a function of the stream enthalpies. The following is a summary of these equations:

a) Reboiler (Stage 1)

$$\begin{aligned} \bar{W}_{G1} \dot{H}_1' + \bar{H}_1 \dot{W}_{G1}' + \bar{W}_{L1} \dot{h}_1' + \bar{h}_1 \dot{W}_{L1}' \\ = \bar{L}_2 h_2' + \bar{h}_2 L_2' - \bar{V}_1 H_1' - \bar{H}_1 V_1' - \bar{L}_1 h_1' - \bar{h}_1 L_1' + Q_R' \end{aligned}$$

b) General Tray (Stage I)

$$\begin{aligned} \bar{W}_{Gi} \dot{H}_i' + \bar{H}_i \dot{W}_{Gi}' + \bar{W}_{Li} \dot{h}_i' + \bar{h}_i \dot{W}_{Li}' \\ = \bar{L}_{i+1} h_{i+1}' + \bar{h}_{i+1} L_{i+1}' + \bar{V}_{i-1} H_{i-1}' + \bar{H}_{i-1} V_{i-1}' \\ - \bar{L}_i h_i' - \bar{h}_i L_i' - \bar{V}_i H_i' - \bar{H}_i V_i' \end{aligned}$$

c) Feed Tray (Stage 5)

$$\begin{aligned} \bar{W}_{G5} \dot{H}_5' + \bar{H}_5 \dot{W}_{G5}' + \bar{W}_{L5} \dot{h}_5' + \bar{h}_5 \dot{W}_{L5}' \\ = \bar{L}_6 h_6' + \bar{h}_6 L_6' + \bar{V}_4 H_4' + \bar{H}_4 V_4' - \bar{L}_5 h_5' \\ - \bar{h}_5 L_5' - \bar{V}_5 H_5' - \bar{H}_5 V_5' + \bar{F} h_f' + \bar{h}_f F' \end{aligned}$$

d) Condenser (Stage 10)

$$\begin{aligned} \bar{W}_{G10} \dot{H}'_{10} + \bar{H}_{10} \dot{W}'_{G10} + \bar{W}_{L10} \dot{h}'_{10} + \bar{h}_{10} \dot{W}'_{L10} \\ = \bar{V}_9 H'_9 + \bar{H}_9 V'_9 - (\bar{L}_{10} + \bar{D}) h'_{10} - \bar{h}_{10} (L'_{10} + D) - Q'_C \end{aligned}$$

These equations can be expressed as a matrix-vector equation of order 10.

The equation is as follows:

$$\begin{aligned} \underline{\underline{W}}_G \underline{\underline{\dot{H}}} + \underline{\underline{H}} \underline{\underline{\dot{W}}}_G + \underline{\underline{W}}_L \underline{\underline{\dot{h}}} + \underline{\underline{h}} \underline{\underline{\dot{W}}}_L \\ = \underline{\underline{A}} [\underline{\underline{\bar{L}}} \underline{\underline{h}} + \underline{\underline{\bar{h}}} \underline{\underline{L}}] + \underline{\underline{B}} [\underline{\underline{\bar{V}}} \underline{\underline{H}} + \underline{\underline{\bar{H}}} \underline{\underline{V}}] + \underline{\underline{C}}_2 \underline{\underline{D}} \end{aligned} \quad (\text{B-2.1})$$

The matrices and vectors in this equation are defined in Figure (B-2.1) and the nomenclature appears in Appendix A. The term h'_{10} which appears in the vector $\underline{\underline{D}}$, allows equation (B-2.1) to be written in the same form as equation (B-1.1).

$$\underline{\underline{C}}_2 = \begin{bmatrix} 0 & 0 & 1 & 0 & 0 & 0 \\ 0 & 0 & 0 & 0 & 0 & 0 \\ 0 & 0 & 0 & 0 & 0 & 0 \\ 0 & 0 & 0 & 0 & 0 & 0 \\ \bar{h}_f & 0 & 0 & 0 & \bar{F} & 0 \\ 0 & 0 & 0 & 0 & 0 & 0 \\ 0 & 0 & 0 & 0 & 0 & 0 \\ 0 & 0 & 0 & 0 & 0 & 0 \\ 0 & \bar{h}_{10} & 0 & 0 & 0 & \bar{L}_{10} \\ 0 & -\bar{h}_{10} & 0 & -1 & 0 & 0 \end{bmatrix}$$

$$\underline{\underline{W}}_G = \text{diag } (\bar{W}_{Gi}; i=1,10)$$

$$\underline{\underline{W}}_L = \text{diag } (\bar{W}_{Li}; i=1,10)$$

$$\underline{\underline{H}} = \text{diag } (\bar{H}_i; i=1,10)$$

$$\underline{\underline{h}} = \text{diag } (\bar{h}_i; i=1,10)$$

$$\underline{\underline{L}} = \text{diag } (\bar{L}_i; i=1,9: 2\bar{V}(9))$$

$$\underline{\underline{V}} = \text{diag } (\bar{V}_i; i=1,9: 0)$$

$$\underline{H} = \text{vect } (H_i^1; i=1,10)$$

$$\underline{h} = \text{vect } (h_i^1; i=1,10)$$

$$\underline{M}_L, \underline{M}_G, \underline{L}, \underline{V}, \underline{D}, \underline{A}, \underline{B} \quad - \quad \text{as in Figure (B.1-1)}$$

FIGURE B-2.1: ENTHALPY BALANCE MATRICES AND VECTORS

C-1 Experimental Control Configuration

The distillation column used in this study is completely instrumented with local analog controllers and data display recorders. It is also interfaced to an IBM 1800 Data Acquisition and Control computer which can be used in an analog supervisory mode for control and data gathering purposes. A schematic diagram of the distillation column showing the complete instrumentation is presented in Figures A, B and C with an accompanying legend. From these figures it can be seen that numerous different control configurations are possible. The local analog controllers were all operated in the proportional-integral mode. The controller settings used are presented in Table C-1.1, and were found by on-line controller tuning.

C-2 Sample Experimental Data

C-2.1 Steady State Data

As indicated previously, the distillation column used in this study is interfaced to an IBM 1800 Data Acquisition and Control computer, to enable continuous data gathering. A computer program has been written by previous workers to sample all measurable variables at a given interval and do a steady state analysis of the data. A mass and energy balance is performed and closure errors and heat losses calculated. A sample of the output from this program is given in Table C-2.1.

C-2.2 Steady State Parameters

In addition to the data collected, several additional parameters of the column operation are necessary for the model. Utilizing all the data collected coupled with a knowledge of the physical properties of the system, it is possible to calculate the values of

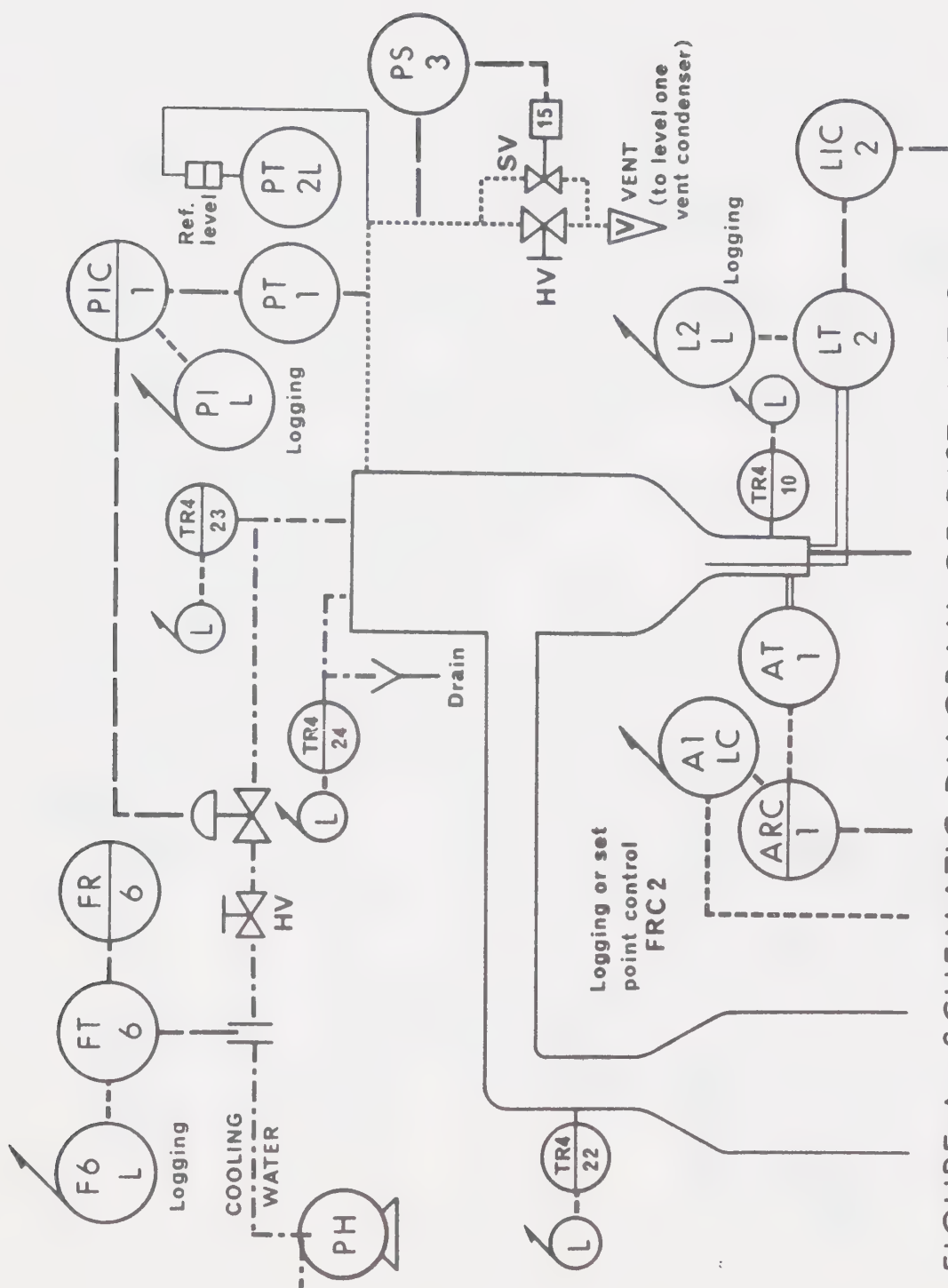


FIGURE A. SCHEMATIC DIAGRAM OF DISTILLATION COLUMN - OVERHEAD SECTION

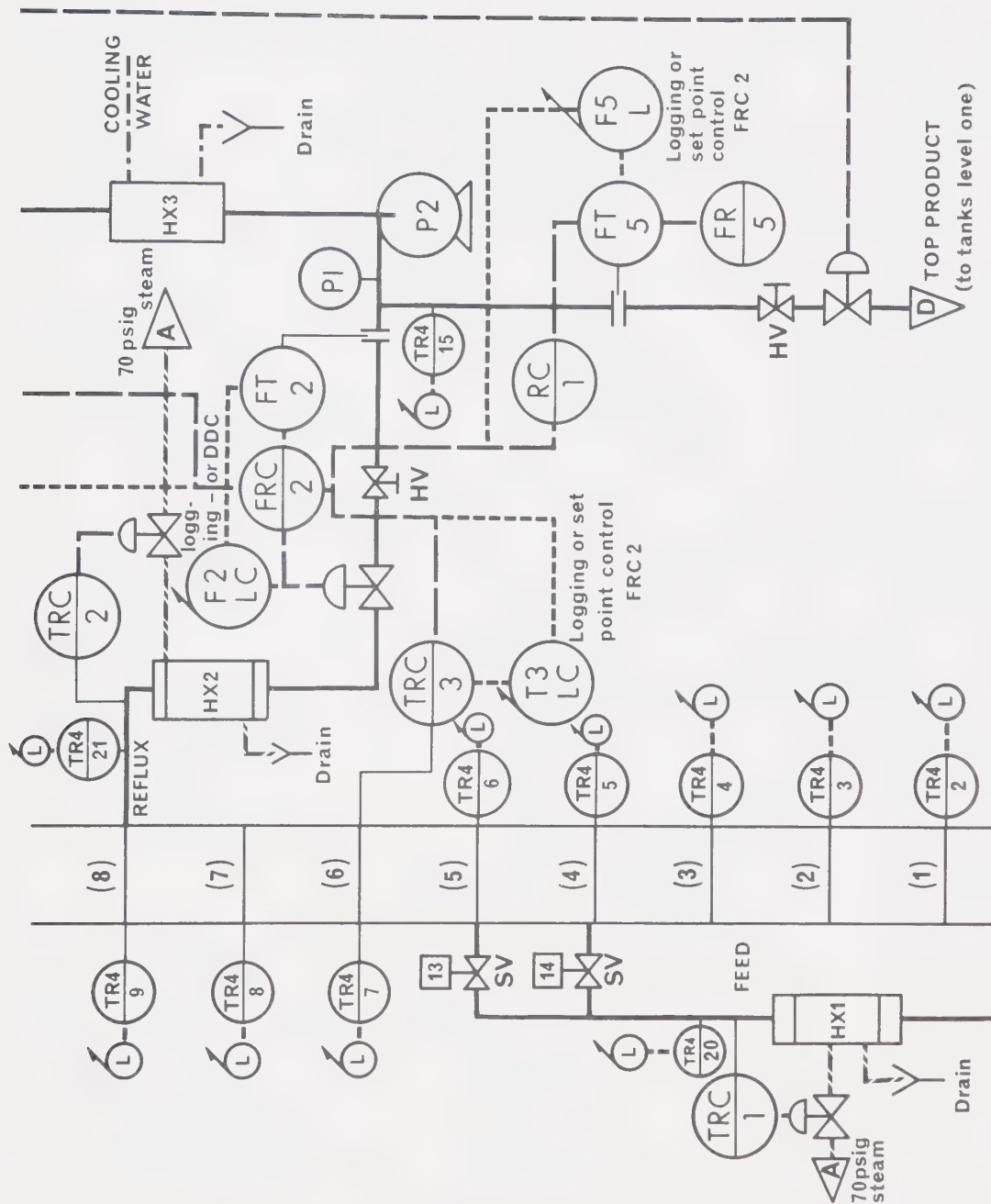


FIGURE B. SCHEMATIC DIAGRAM OF DISTILLATION COLUMN - MID - SECTION

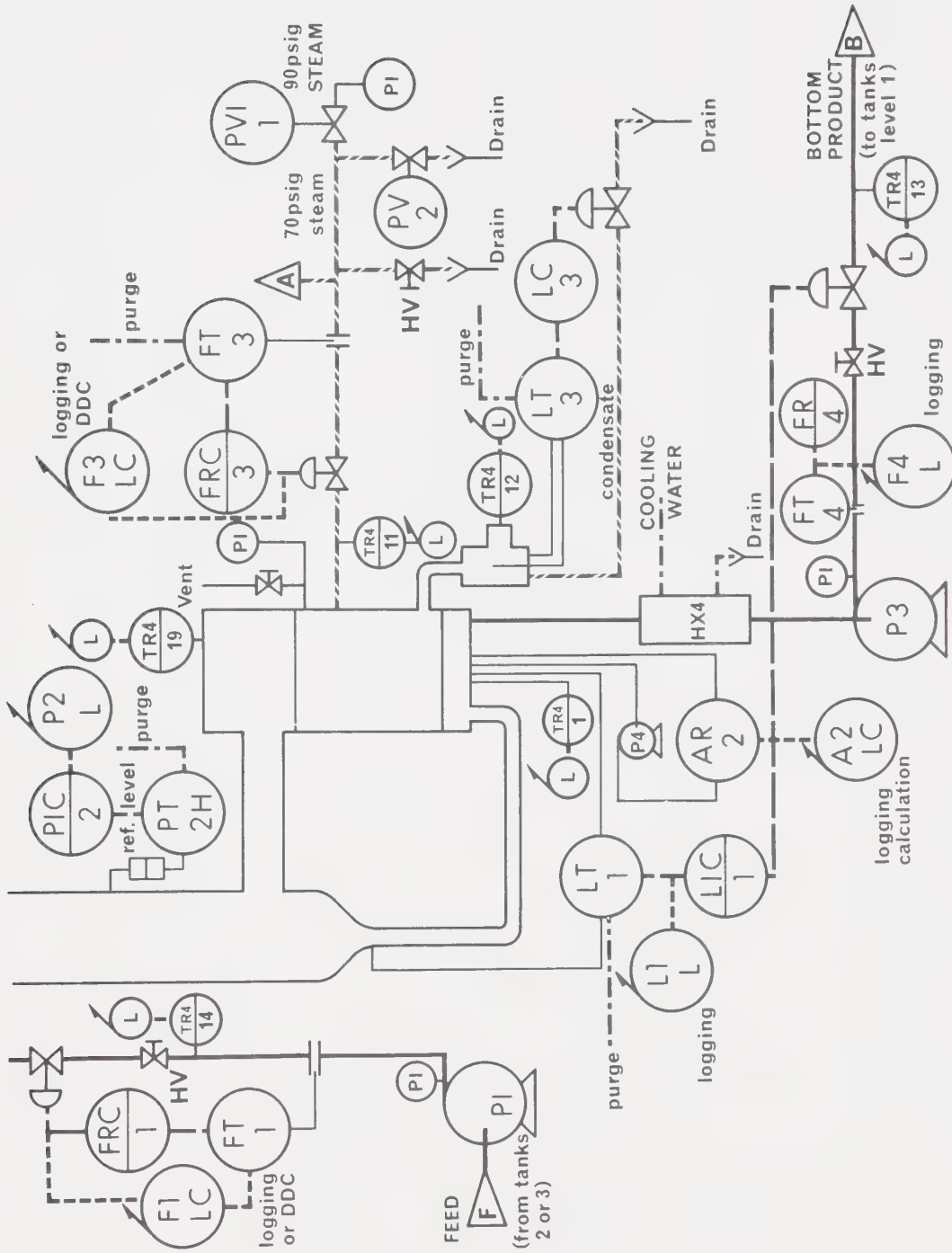


FIGURE C. SCHEMATIC DIAGRAM OF DISTILLATION
COLUMN - BOTTOM SECTION

LEGEND :

$\frac{AR}{n}$	COMPOSITION RECORDER (Chromatograph)	$\frac{PIC}{n}$	PRESSURE INDICATOR/CONTROLLER
$\frac{ARC}{n}$	COMPOSITION RECORDER/CONTROLLER (capacitance)	PRV	PRESSURE REGULATING VALVE
$\frac{AT}{n}$	COMPOSITION TRANSDUCER (Capacitance probe)	Ps	PRESSURE SWITCH
$\frac{FR}{n}$	FLOW RECORDER	$\frac{PT}{n}$	PRESSURE TRANSDUCER
$\frac{FRC}{n}$	FLOW RECORDER CONTROLLER	$\frac{PT}{nH}$ $\frac{PT}{nL}$	PRESSURE TRANSDUCER High Low
$\frac{FT}{n}$	FLOW TRANSDUCER (d/p cell)	$\frac{TRn}{m}$	MULTIPOINT TEMPERATURE RECORDER
HV	HAND VALVE	$\frac{TRC}{n}$	TEMPERATURE RECORDER/CONTROLLER
$\frac{LIC}{n}$	LEVEL INDICATOR/CONTROLLER	SV	SOLENOID VALVE
$\frac{LT}{n}$	LEVEL TRANSDUCER	$\frac{nn}{nL}$	LOGGING (VARIABLE nn-n) BY COMPUTER
P-n	PUMP	$\frac{nn}{nLC}$	LOGGING AND CONTROL (VARIABLE nn-n) BY COMPUTER

PROCESS LINES

	PNEUMATIC INSTRUMENT LINES		METHANOL/WATER PROCESS LINES
	PROCESS INSTRUMENT LINES		VENT
	COOLING WATER PROCESS LINES		70 PSIG STREAM
			DATA TRANSMISSION LINES TO COMPUTER

TABLE C-1.1: TYPICAL CONTROLLER SETTINGS

Controller	Prop. Action Kp	Int. Action (reset time) (min)
Feed Flow	175	0.8
Reflux Flow	100	0.4
Steam Flow	125	0.1
Column Pressure	50	8.
Reboiler Level	50	10.
Condenser Level	50	10.
Feed Temp.	-150	1.8
Reflux Temp.	- 30	7.0
Overhead Comp.	-200	7.0

variables which cannot be measured such as internal column flowrates and compositions. However, difficulties can arise in estimation of tray efficiencies and equilibrium factors. In this study the stage liquids were sampled and the samples analyzed by use of a gas chromatograph. This composition data, with the assumption of saturated phase enthalpy relations, allowed simple calculation of values for all variables.

The steady state material and energy balance equations for a general stage are:

$$L_i + V_i = L_{i+1} + V_{i-1} + S_i \quad (C-1)$$

$$L_i x_i + V_i y_i = L_{i+1} x_{i+1} + V_{i-1} y_{i-1} + S_i x_{si} \quad (C-2)$$

$$L_i h_i + V_i H_i + Q_{Li} = L_{i+1} h_{i+1} + V_{i-1} H_{i-1} + S_i h_{si} \quad (C-3)$$

where S_i is a sidestream input to stage i and Q_{Li} is the heat loss from stage i . The heat losses were obtained from an overall heat balance and were distributed as indicated by Svrcek [46].

With the measured liquid compositions and heat losses, and the enthalpy relations, there are five unknowns in equations (C-1,2,3). However, if values of L_{i+1} and V_i (from the stage above the i^{th} stage) were available, the equations could be solved. Since a steady state balance on the condenser yields values for V_9 and L_{10} , the equations that apply to the top tray can be solved, and subsequently each tray can be solved, working from the top of the column. A computer program was written to employ the available data to calculate the internal flows and compositions. A sample of the output from this program using the steady state data given in Table C-2.1 is presented in Table C-2.2.

TABLE C-2.1: SAMPLE STEADY STATE DATA

STEADY STATE DATA
 RUN NO SAMPLE
 30/3/72

FEED FLOW	2.135 LB/MIN	BOTTOM PROD	1.262 LB/MIN
REFLUX FLOW	1.956 LB/MIN	TOP PROD	1.002 LB/MIN
STEAM FLOW	1.827 LB/MIN	COOL WATER	68.988 LB/MIN
FEED PLATE	4	FEED COMP	45.49 WT P C
TOP PROD	96.88 WT P C	BOTTOMS COMP	1.35 WT P C
FEED INLET	163.4 DEG F	REFLUX INLET	137.2 DEG F
STEAM TEMP	228.9 DEG F	PRESSURE	0.7 IN H2O

M A T E R I A L B A L A N C E

	FLOW (LB/MIN)	COMP (WT PCT)	METHANOL (LB/MIN)	WATER (LB/MIN)
FEED	2.135	45.499	0.971	1.163
BOTTOM PRODUCT	1.262	1.350	0.017	1.245
TOP PRODUCT	1.002	96.889	0.971	0.031
CLOSURE ERROR-PC	6.0		1.6	9.7

E N E R G Y B A L A N C E

	ENTHALPY IN (BTU/MIN)	ENTHALPY OUT (BTU/MIN)
COOLING WATER	3733.3	5058.7
REFLUX	189.8	203.2
TOP PRODUCT		104.1
FEED	308.3	
STEAM	2184.6	418.2
BOTTOM PRODUCT		264.3
TOTAL	6416.1	6048.7
HEAT LOSS		367.4

TABLE C-2.1 Continued

STEADY STATE CONDITIONS BASED ON 20 POINTS
 RUN NO SAMPLE 30/3/72

FEED FLOW	=	2.231	LB/MIN	DEV=	0.0041
REFLUX FLOW	=	2.233	LB/MIN	DEV=	0.0093
STEAM FLOW	=	1.827	LB/MIN	DEV=	0.0082
BOTTOM PROD	=	1.264	LB/MIN	DEV=	0.0823
TOP PROD	=	1.144	LB/MIN	DEV=	0.0117
COOL WATER	=	68.919	LB/MIN	DEV=	0.0641
TOP PROD	=	96.889	WT P C	DEV=	0.0811
BOTTOMS COMP	=	1.350	WT P C	DEV=	0.0000
FEED COMP	=	45.499	WT P C	DEV=	0.0000
PRESSURE	=	0.758	IN H2O	DEV=	0.0968
COND LEVEL	=	5.055	PSIG	DEV=	0.0246
REB'R LEVEL	=	9.759	PSIG	DEV=	0.1780
DIFF PRESS	=	10.458	PSIG	DEV=	0.1520
REBOILER TEM	=	208.3	DEG F	DEV=	0.3700
PLATE 1 TEMP	=	193.1	DEG F	DEV=	0.4771
PLATE 2 TEMP	=	178.9	DEG F	DEV=	0.3384
PLATE 3 TEMP	=	163.6	DEG F	DEV=	0.2786
PLATE 4 TEMP	=	166.3	DEG F	DEV=	0.3099
PLATE 5 TEMP	=	158.0	DEG F	DEV=	0.2833
PLATE 6 TEMP	=	152.8	DEG F	DEV=	0.2603
PLATE 7 TEMP	=	150.0	DEG F	DEV=	0.2653
PLATE 8 TEMP	=	147.5	DEG F	DEV=	0.2690
COND TEMP	=	144.5	DEG F	DEV=	0.3314
STEAM TEMP	=	228.9	DEG F	DEV=	0.4987
COND'T TEMP	=	226.6	DEG F	DEV=	0.3244
REFLUX FLOW	=	121.7	DEG F	DEV=	0.2714
FEED FLOW	=	89.6	DEG F	DEV=	0.2161
BOTTOM FLOW	=	99.0	DEG F	DEV=	0.1767
REB O'HEAD	=	206.6	DEG F	DEV=	0.3682
FEED INLET	=	163.4	DEG F	DEV=	0.2947
REFLUX INLET	=	137.2	DEG F	DEV=	0.4435
COL O'HEAD	=	148.2	DEG F	DEV=	0.2935
WATER INLET	=	54.1	DEG F	DEV=	0.2801
WATER OUTLET	=	73.4	DEG F	DEV=	0.3059

TABLE C-2.2: SAMPLE STEADY STATE PARAMETERS

DISTILLATION COLUMN
STEADY STATE DATA

	FLOW (LB/MIN)	COMP WT FR)
FEED	2.135	0.4550
DISTILLATE	1.002	0.9662
BOTTOMS	1.133	0.0135

STAGE	LIQUID		VAPOUR	
	FLOW	COMP	FLOW	COMP
1	1.133	0.0135	2.152	0.0579
2	3.285	0.0390	2.207	0.1452
3	3.340	0.0970	2.346	0.3619
4	3.479	0.2450	2.429	0.4957
5	3.562	0.3390	2.652	0.6975
6	1.650	0.5345	2.838	0.8052
7	1.836	0.7175	2.960	0.8833
8	1.958	0.8410	2.984	0.9321
9	1.982	0.9150	2.958	0.9662
10	1.956	0.9662	0.000	0.0000

C-3 Sample Model Parameters

C-3.1 Liquid and Vapour Volumes

The model as derived earlier has as parameters the steady state liquid mass holdups. Values were calculated from a knowledge of the liquid volume in each stage employing a composition dependent density relation. The condenser and reboiler volumes were found by filling each with liquid to the controlled setpoint and measuring the volume of liquid by draining each vessel. The tray volumes were more difficult to obtain as observation indicated that there was more liquid (and foam) on the trays adjacent to, and including the feed tray than on the others. A weighting factor for each tray was estimated by observing the holdups and was used to compensate for variations in liquid loading throughout the column. The procedure followed in determining the tray holdups was to operate the column at steady state and then abruptly (and simultaneously) stop all inputs and outputs. The column was then drained and the total tray volume determined by subtracting the previously measured reboiler and condenser volumes. The individual tray volumes were then arrived at by applying the weighting factors. Table C-3.1 presents the weighting factors used and the volumes allocated to each stage.

The vapour volumes were also required, to estimate the vapour enthalpy contribution to the transient heat balance. These volumes were found by calculating the total volume between stages from a knowledge of the column dimensions and then subtracting the liquid volume holdup. Table C-3.1 also contains the calculated vapour volumes of each stage.

C-3.2 Enthalpy Linearization Factors

As outlined previously, in Section 3.5, the vapour enthalpy

TABLE C-3.1: LIQUID AND VAPOUR STAGE VOLUMES

Stage	Liquid Volume Weighting Factor	Liquid Volume (ft ³)	Vapour Volume (ft ³)
1	-	.2474	1.258
2	1.00	.0259	.4151
3	1.05	.0271	.4139
4	1.10	.0285	.4125
5	1.15	.0298	.4112
6	1.20	.0311	.4099
7	1.20	.0311	.4099
8	1.15	.0298	.4112
9	1.10	.0285	1.090
10	-	.0557	1.302

perturbations can be expressed in terms of the liquid perturbations by an expression of the form:

$$H' = b_1 h'$$

where b_1 is the slope of some pseudo-equilibrium/enthalpy relation for each stage at the initial steady state values.

In general

$$H = f_1(y, T)$$

$$h = f_2(x, T)$$

and more specifically for constant pressure and stage efficiency

$$y = f_3(T)$$

$$x = f_4(T)$$

so that:

$$H = f_5(y)$$

$$h = f_6(x)$$

So the factor b_1 can be expressed as:

$$b_1 = \left. \frac{dH}{dh} \right|_{s.s.} = \frac{df_5}{dy} \cdot \frac{dy}{dx} / \left. \frac{df_6}{dx} \right|_{s.s.}$$

The physical property data for the methanol-water system have been presented by Svrcek. Although the phases in each stage are not in thermodynamic equilibrium, if a constant efficiency is assumed, the slope of the actual operating curves will be the same as the equilibrium

curves. So the equilibrium data can be used, and the assumption of constant efficiency should introduce only a small error.

Suppose that stage 9 is considered. Table C-2.2 gives the compositions to be:

$$y = 96.62 \text{ wt\%}$$

$$x = 91.50 \text{ wt\%}$$

so from the data presented by Svrcek;

$$\frac{dH}{dy} = -613.8 \text{ (linear over entire range)}$$

$$\frac{dh}{dx} = -10.0 \text{ (linear between nearest tabulated values)}$$

$$\frac{dy}{dx} = .342 \text{ (linear between nearest tabulated values)}$$

therefore

$$\begin{aligned} b_1 &= \frac{dH}{dy} \cdot \frac{dy}{dx} / \frac{dh}{dx} \\ &= \frac{(-613.8)(.342)}{(-10.0)} = 20.95 \end{aligned}$$

This value and the values for the other stages are given in Table C-3.2. All values were calculated using the compositions presented in Table C-2.2. It can be seen from Table C-3.2 that there is a large variation in the parameter b_1 from stage to stage. This is due to the S-shaped y - x and h - x curves.

C-3.3 Liquid Dynamic Constants

The model outlined in Chapter III of this work accounts for

TABLE C-3.2: ENTHALPY LINEARIZATION FACTORS

Stage	b_1
1	23.35
2	19.40
3	9.30
4	3.12
5	2.05
6	8.04
7	8.38
8	18.62
9	20.95
10	20.95

liquid dynamics by the use of first order expressions of the form:

$$\dot{L}_i' = \frac{1}{\tau_i} [L_{i+1}' K_i - L_i']$$

where τ_i is a flow change time constant and K_i is a final steady state flow correction factor. The K_i term is necessary since, in general, the liquid flow from a stage will not change by the same amount as the flow onto the stage for input changes. The estimation of these parameters τ_i and K_i requires data for the internal liquid flows as a function of time. This type of data, for the column used in this study has been given by Svrcek, and so was used in the estimation of the required values. Table C-3.3 presents the calculated values which are averages of values determined for several sets of data. The large value at the feed stage is due to slight subcooling of the feed.

The feed tray liquid dynamic equation has one extra term for the feed input and is of the form:

$$\dot{L}_5' = \frac{1}{\tau_5} [L_6' K_5 + F' K_{F5} - L_5']$$

Also the distillate flow is dependent on the feed and reflux flows and the expression is:

$$\dot{D}' = \frac{1}{\tau_D} [F' K_{FD} + L_{1D}' K_{RD} - D' L_{1D}']$$

The values of the parameters in these expressions were also estimated from Svrcek's data and are also given in Table C-3.3.

TABLE C-3.3: LIQUID DYNAMIC CONSTANTS

Stage	K_i	τ_i (min)
1	0.35	1.0
2	0.60	2.5
3	0.78	2.5
4	0.78	2.5
5	1.35	2.5
6	0.75	2.5
7	0.80	2.5
8	1.00	2.5
9	1.30	2.5
10	1.00	10.0 [τ_D]

$K_{F5} = 1.1$

$K_{FD} = 0.34$

$K_{RD} = 0.66$

C-4 Reproducibility

Some investigation was done to establish the reproducibility of steady state conditions, and of transient data. The steady state reproducibility entailed the definition of an initial steady state and subsequent introduction of a pulse disturbance of about 10 minutes duration. The column was then allowed to come to steady state. The overhead composition was used to indicate the steady state reproducibility. Table C-4.1 presents a set of data taken for four consecutive disturbances and the type and duration of pulses used.

From this table, it can be seen that the deviation in overhead composition can be as large as .3 wt % MeOH, but a deviation of about .1 wt % MeOH would be average.

The reproducibility of a transient run was investigated by comparing similar open loop cases. Figure C-4.1 compares two similar transient runs. As can be seen the overhead compositions at final steady state are different by about .15% and the bottoms composition differ by 0.5%. From these observations and consideration of the data in Table C-4.1 it can be concluded that the transient data is about as reproducible as the steady state data, having variations of about the same order of magnitude.

The reproducibility of a multivariable feedback control run was also investigated. Figure C-4.2 compares two such runs. Although the initial steady states are different, the controlled behaviour is very similar. The bottoms composition shows similar oscillations with an average offset of about 0.5%. The overhead composition in each case has very little offset and small fluctuations. This would indicate that the controlled behaviour is reproducible despite slight variations

TABLE C-4.1

No.	Pulse Disturbance	Duration (min)	Final Overhead Composition
1	Initial		94.40
2	Feed (+10%)	15	
	Reflux (+5%)	7	94.73
3	Steam (+5%)	7	
	Reflux (-10%)	7	94.78
4	Feed (-10%)	8	
	Reflux (-5%)	9	94.70
5	Feed (+10%)	8	
	Reflux (+10%)	8	94.82
Average Final Overhead Composition -			94.69

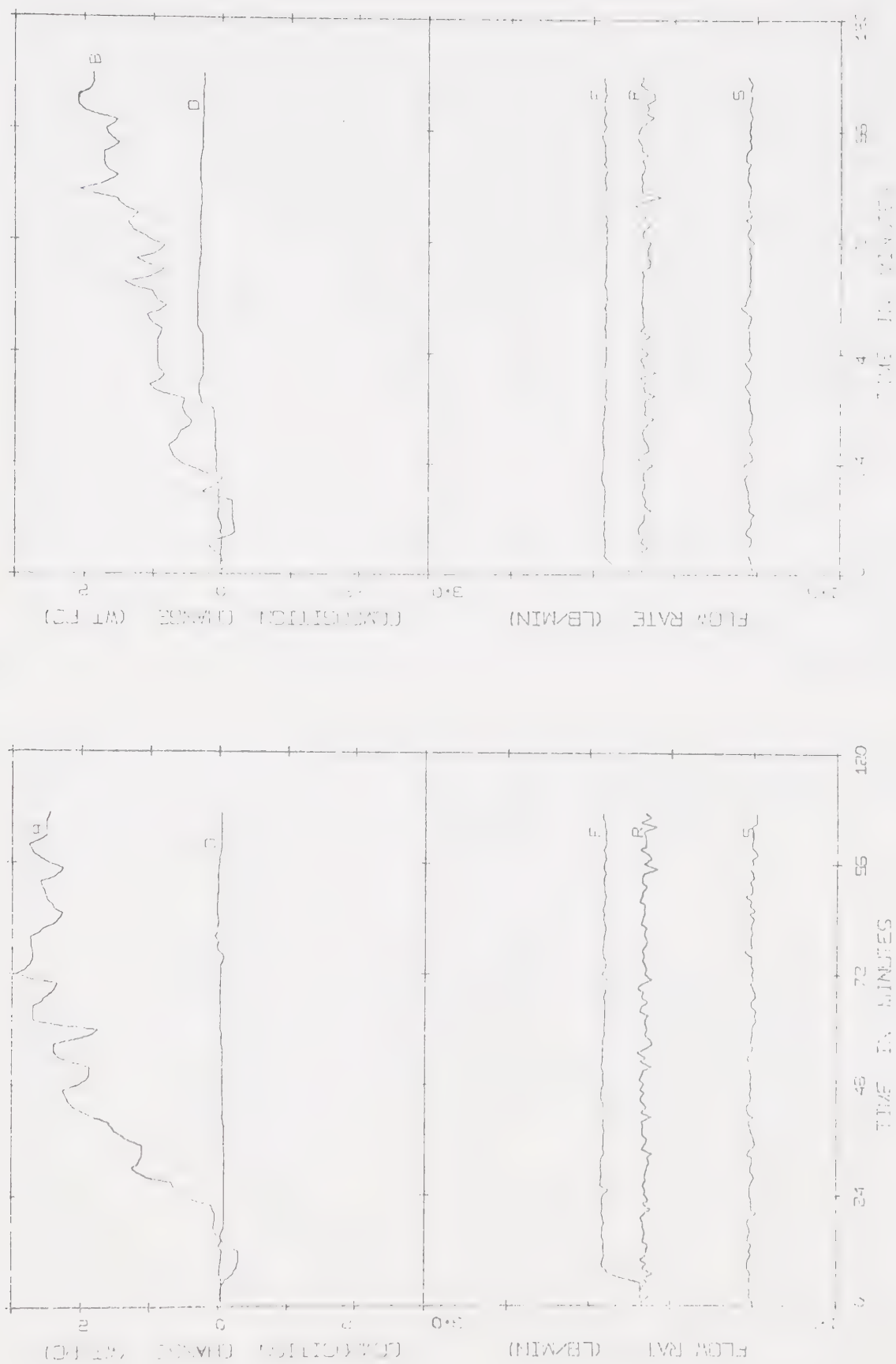


FIGURE C-4.1: COMPARISON OF TWO OPEN LOOP RUNS WITH POSITIVE FEED FLOW STEPS

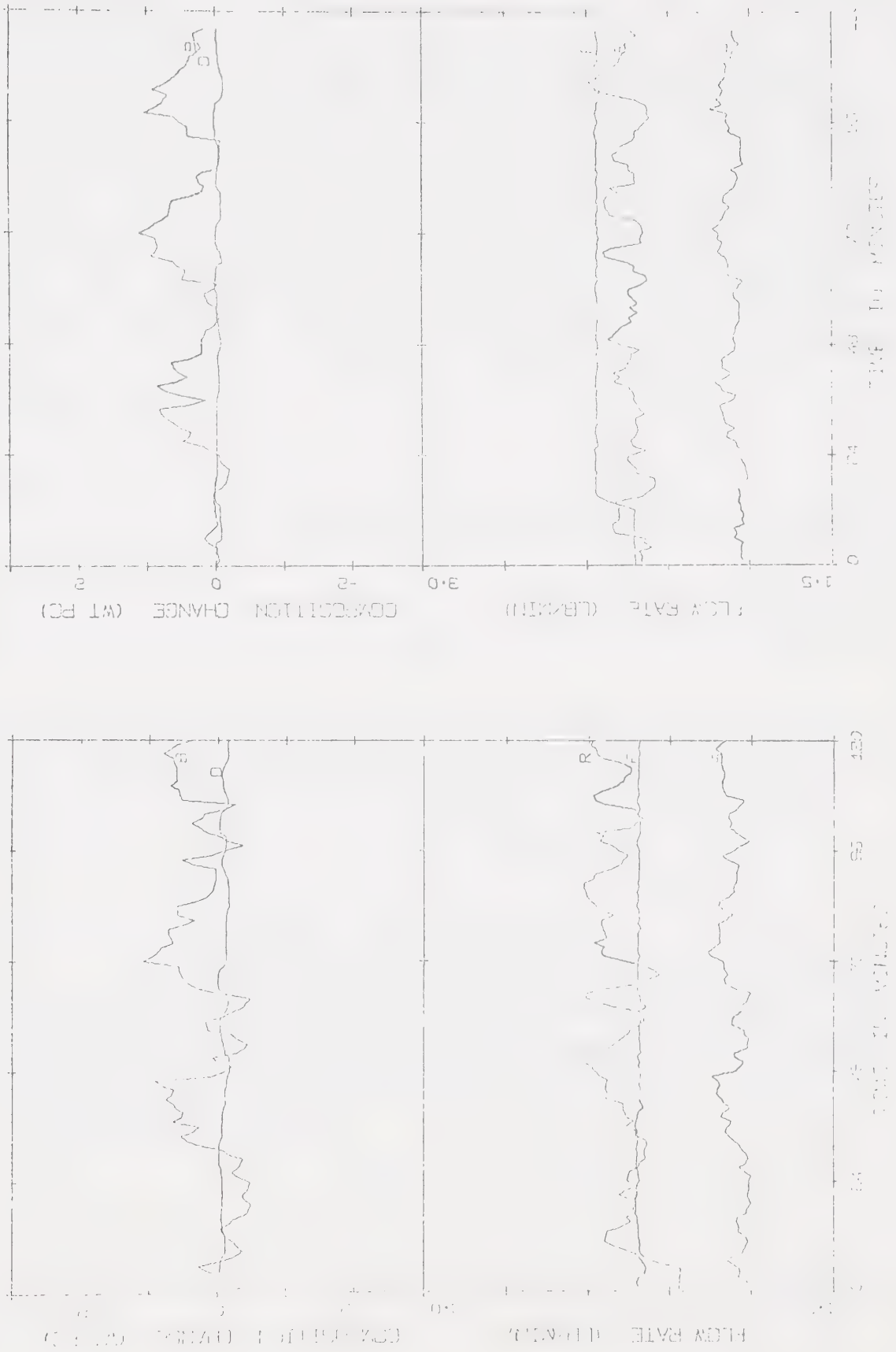


FIGURE C-4.2: COMPARISON OF TWO MULTIVARIABLE FEEDBACK EXPERIMENTAL RUNS

in steady state.

The main difficulty in attempting to reproduce experimental data is in the slight variations in conditions which lead to differing results. Slight differences in tray loading or in steam pressure can cause appreciable differences in transient or final steady state readings. These problems however do not appear to introduce appreciable problems into the control studies, as controlled behaviour is fairly reproducible.

C-5 Model Matrices

The twenty state model, in differential form can be written as:

$$\dot{\underline{x}} = \underline{A} \underline{x} + \underline{B} \underline{v}$$

The coefficient matrices for this formulation are presented in Table C-5.1, and were calculated from the steady state data previously presented.

C-6 Noise for Simulation Studies

The simulation studies presented in Chapter VI of this work include experimentally measured noise in the bottoms composition. This noise was determined at an experimental steady state and the case used is presented in Figure C-6-1.

TABLE C-5.1 MODEL COEFFICIENT MATRICES

MODEL $DX/DT = A*X + B*U$

MATRIX A (COLUMNWISE)

-0.1381E 01	0.5015E 01	0.0000E 00	0.0000E 00	0.0000E 00	0.0000E 00
0.0000E 00	0.0000E 00	0.0000E 00	0.0000E 00	0.0000E 00	0.0000E 00
0.0000E 00	0.0000E 00	0.0000E 00	0.0000E 00	0.0000E 00	0.0000E 00
0.0000E 00	0.0000E 00	0.0000E 00	0.0000E 00	0.0000E 00	0.0000E 00
0.2150E 00	-0.5988E 01	0.5325E 01	0.0000E 00	0.0000E 00	0.0000E 00
0.0000E 00	0.0000E 00	0.0000E 00	0.0000E 00	0.0000E 00	0.0000E 00
0.0000E 00	0.0000E 00	0.0000E 00	0.0000E 00	0.0000E 00	0.0000E 00
0.0000E 00	0.0000E 00	0.0000E 00	0.0000E 00	0.0000E 00	0.0000E 00
0.0000E 00	0.8435E 00	-0.4613E 01	0.3967E 01	0.0000E 00	0.0000E 00
0.0000E 00	0.0000E 00	0.0000E 00	0.0000E 00	0.0000E 00	0.0000E 00
0.0000E 00	0.0000E 00	0.0000E 00	0.0000E 00	0.0000E 00	0.0000E 00
0.0000E 00	0.0000E 00	0.0000E 00	0.0000E 00	0.0000E 00	0.0000E 00
0.0000E 00	0.0000E 00	0.9079E 00	-0.2336E 01	0.1410E 01	0.0000E 00
0.0000E 00	0.0000E 00	0.0000E 00	0.0000E 00	0.0000E 00	0.0000E 00
0.0000E 00	0.0000E 00	0.0000E 00	0.0000E 00	0.0000E 00	0.0000E 00
0.0000E 00	0.0000E 00	0.0000E 00	0.0000E 00	0.0000E 00	0.0000E 00
0.0000E 00	0.0000E 00	0.0000E 00	0.9848E 00	-0.1999E 01	0.0000E 00
0.1031E 01	0.0000E 00	0.0000E 00	0.0000E 00	0.0000E 00	0.0000E 00
0.0000E 00	0.0000E 00	0.0000E 00	0.0000E 00	0.0000E 00	0.0000E 00
0.0000E 00	0.0000E 00	0.0000E 00	0.0000E 00	0.0000E 00	0.0000E 00

0.0000E 00	0.0000E 00	0.0000E 00	0.0000E 00	0.4587E 00
-0.1764E 01	0.1322E 01	0.0000E 00	0.0000E 00	0.0000E 00
0.0000E 00	0.0000E 00	0.0000E 00	0.0000E 00	0.0000E 00
0.0000E 00	0.0000E 00	0.0000E 00	0.0000E 00	0.0000E 00
0.0000E 00	0.0000E 00	0.0000E 00	0.0000E 00	0.0000E 00
0.5326E 00	-0.3365E 01	0.2850E 01	0.0000E 00	0.0000E 00
0.0000E 00	0.0000E 00	0.0000E 00	0.0000E 00	0.0000E 00
0.0000E 00	0.0000E 00	0.0000E 00	0.0000E 00	0.0000E 00
0.0000E 00	0.0000E 00	0.0000E 00	0.0000E 00	0.0000E 00
0.0000E 00	0.0000E 00	0.0000E 00	0.0000E 00	0.0000E 00
0.0000E 00	0.5858E 00	-0.5208E 01	0.2925E 01	0.0000E 00
0.0000E 00	0.0000E 00	0.0000E 00	0.0000E 00	0.0000E 00
0.0000E 00	0.0000E 00	0.0000E 00	0.0000E 00	0.0000E 00
0.0000E 00	0.0000E 00	0.0000E 00	0.0000E 00	0.0000E 00
0.0000E 00	0.0000E 00	0.0000E 00	0.0000E 00	0.0000E 00
0.0000E 00	0.0000E 00	0.6017E 00	-0.1511E 02	0.1391E 02
0.0000E 00	0.0000E 00	0.0000E 00	0.0000E 00	0.0000E 00
0.0000E 00	0.0000E 00	0.0000E 00	0.0000E 00	0.0000E 00
0.0000E 00	0.0000E 00	0.0000E 00	0.0000E 00	0.0000E 00
0.0000E 00	0.0000E 00	0.0000E 00	0.0000E 00	0.0000E 00
0.0000E 00	0.0000E 00	0.0000E 00	0.3777E 00	-0.7494E 01
0.0000E 00	0.0000E 00	0.0000E 00	0.0000E 00	0.0000E 00
0.0000E 00	0.0000E 00	0.0000E 00	0.0000E 00	0.0000E 00
0.0000E 00	0.0000E 00	0.0000E 00	0.0000E 00	0.0000E 00
0.0000E 00	0.0000E 00	0.0000E 00	0.0000E 00	0.0000E 00
0.0000E 00	0.0000E 00	0.0000E 00	0.0000E 00	0.0000E 00
-0.1265E 00	0.0000E 00	0.0000E 00	0.0000E 00	0.0000E 00
0.0000E 00	0.0000E 00	0.0000E 00	0.0000E 00	0.0000E 00

-0.1976E 00	0.0000E 00	0.0000E 00	0.0000E 00	0.0000E 00	0.0000E 00
0.0000E 00	0.0000E 00	0.0000E 00	0.0000E 00	0.0000E 00	0.0000E 00
0.1064E 00	-0.1250E 00	0.0000E 00	0.0000E 00	0.0000E 00	0.0000E 00
0.0000E 00	0.0000E 00	0.0000E 00	0.0000E 00	0.0000E 00	0.0000E 00
0.0000E 00	-0.2545E 01	0.0000E 00	0.0000E 00	0.0000E 00	0.0000E 00
0.0000E 00	0.0000E 00	0.0000E 00	0.0000E 00	0.0000E 00	0.0000E 00
0.0000E 00	0.1075E 00	-0.1234E 00	0.0000E 00	0.0000E 00	0.0000E 00
0.0000E 00	0.0000E 00	0.0000E 00	0.0000E 00	0.0000E 00	0.0000E 00
0.0000E 00	0.0000E 00	-0.7825E 01	0.0000E 00	0.0000E 00	0.0000E 00
0.0000E 00	0.0000E 00	0.0000E 00	0.0000E 00	0.0000E 00	0.0000E 00
0.0000E 00	0.0000E 00	0.1085E 00	-0.1010E 00	0.0000E 00	0.0000E 00
0.0000E 00	0.0000E 00	0.0000E 00	0.0000E 00	0.0000E 00	0.0000E 00
0.0000E 00	0.0000E 00	0.0000E 00	-0.5102E 01	0.0000E 00	0.0000E 00
0.0000E 00	0.0000E 00	0.0000E 00	0.0000E 00	0.0000E 00	0.0000E 00
0.0000E 00	0.0000E 00	0.0000E 00	0.8989E-01	-0.9900E-01	0.0000E 00
0.0000E 00	0.0000E 00	0.0000E 00	0.0000E 00	0.0000E 00	0.0000E 00
0.0000E 00	0.0000E 00	0.0000E 00	0.0000E 00	-0.8206E 01	0.0000E 00
0.0000E 00	0.0000E 00	0.0000E 00	0.0000E 00	0.0000E 00	0.0000E 00
0.0000E 00	0.0000E 00	0.0000E 00	0.0000E 00	0.0000E 00	0.8950E-01
-0.2000E 00	0.0000E 00	0.0000E 00	0.0000E 00	0.0000E 00	0.0000E 00
0.0000E 00	0.0000E 00	0.0000E 00	0.0000E 00	0.0000E 00	0.0000E 00
-0.3269E 01	0.0000E 00	0.0000E 00	0.0000E 00	0.0000E 00	0.0000E 00
0.0000E 00	0.0000E 00	0.0000E 00	0.0000E 00	0.0000E 00	0.0000E 00
0.1821E 00	-0.2564E 00	0.0000E 00	0.0000E 00	0.0000E 00	0.0000E 00

0.0000E 00	0.0000E 00	0.0000E 00	0.0000E 00	0.0000E 00
0.0000E 00	-0.3588E 00	0.0000E 00	0.0000E 00	0.0000E 00
0.0000E 00	0.0000E 00	0.0000E 00	0.0000E 00	0.0000E 00
0.0000E 00	0.2358E 00	-0.2500E 00	0.0000E 00	0.0000E 00
0.0000E 00	0.0000E 00	0.0000E 00	0.0000E 00	0.0000E 00
0.0000E 00	0.0000E 00	-0.9018E-01	0.0000E 00	0.0000E 00
0.0000E 00	0.0000E 00	0.0000E 00	0.0000E 00	0.0000E 00
0.0000E 00	0.0000E 00	0.2310E 00	-0.3333E 00	0.0000E 00
0.0000E 00	0.0000E 00	0.0000E 00	0.0000E 00	0.0000E 00
0.0000E 00	0.0000E 00	0.0000E 00	0.0000E 00	0.0000E 00
0.0000E 00	0.0000E 00	0.0000E 00	0.0000E 00	0.0000E 00
0.0000E 00	0.0000E 00	0.0000E 00	0.0000E 00	-0.1000E 00

MATRIX B (COLUMNWISE)

0.0000E 00	0.0000E 00	0.0000E 00	0.0000E 00	-0.5791E 01
0.0000E 00	0.0000E 00	0.0000E 00	0.0000E 00	0.0000E 00
0.0000E 00	0.0000E 00	0.0000E 00	0.0000E 00	0.9900E-01
0.0000E 00	0.0000E 00	0.0000E 00	0.0000E 00	0.3400E-01
0.0000E 00	0.0000E 00	0.0000E 00	0.0000E 00	0.0000E 00
0.0000E 00	0.0000E 00	0.0000E 00	-0.1797E 00	0.0000E 00
0.0000E 00	0.0000E 00	0.0000E 00	0.0000E 00	0.0000E 00
0.0000E 00	0.0000E 00	0.0000E 00	0.3333E 00	-0.3400E-01
0.6333E-01	0.0000E 00	0.0000E 00	0.0000E 00	0.0000E 00
0.0000E 00	0.0000E 00	0.0000E 00	0.0000E 00	0.0000E 00

0.0000E 00	0.0000E 00	0.0000E 00	0.0000E 00	0.0000E 00
0.0000E 00	0.0000E 00	0.0000E 00	0.0000E 00	0.0000E 00
0.0000E 00	0.0000E 00	0.0000E 00	0.0000E 00	0.0000E 00
0.0000E 00	0.0000E 00	0.0000E 00	0.0000E 00	-0.1784E 00
0.0000E 00	0.0000E 00	0.0000E 00	0.0000E 00	0.0000E 00
0.0000E 00	0.0000E 00	0.0000E 00	0.0000E 00	0.0000E 00
0.0000E 00	0.0000E 00	0.0000E 00	0.0000E 00	0.6166E 00
0.0000E 00	0.0000E 00	0.0000E 00	0.0000E 00	0.0000E 00
0.0000E 00	0.0000E 00	0.0000E 00	0.0000E 00	0.0000E 00
0.0000E 00	0.0000E 00	0.0000E 00	0.0000E 00	0.0000E 00

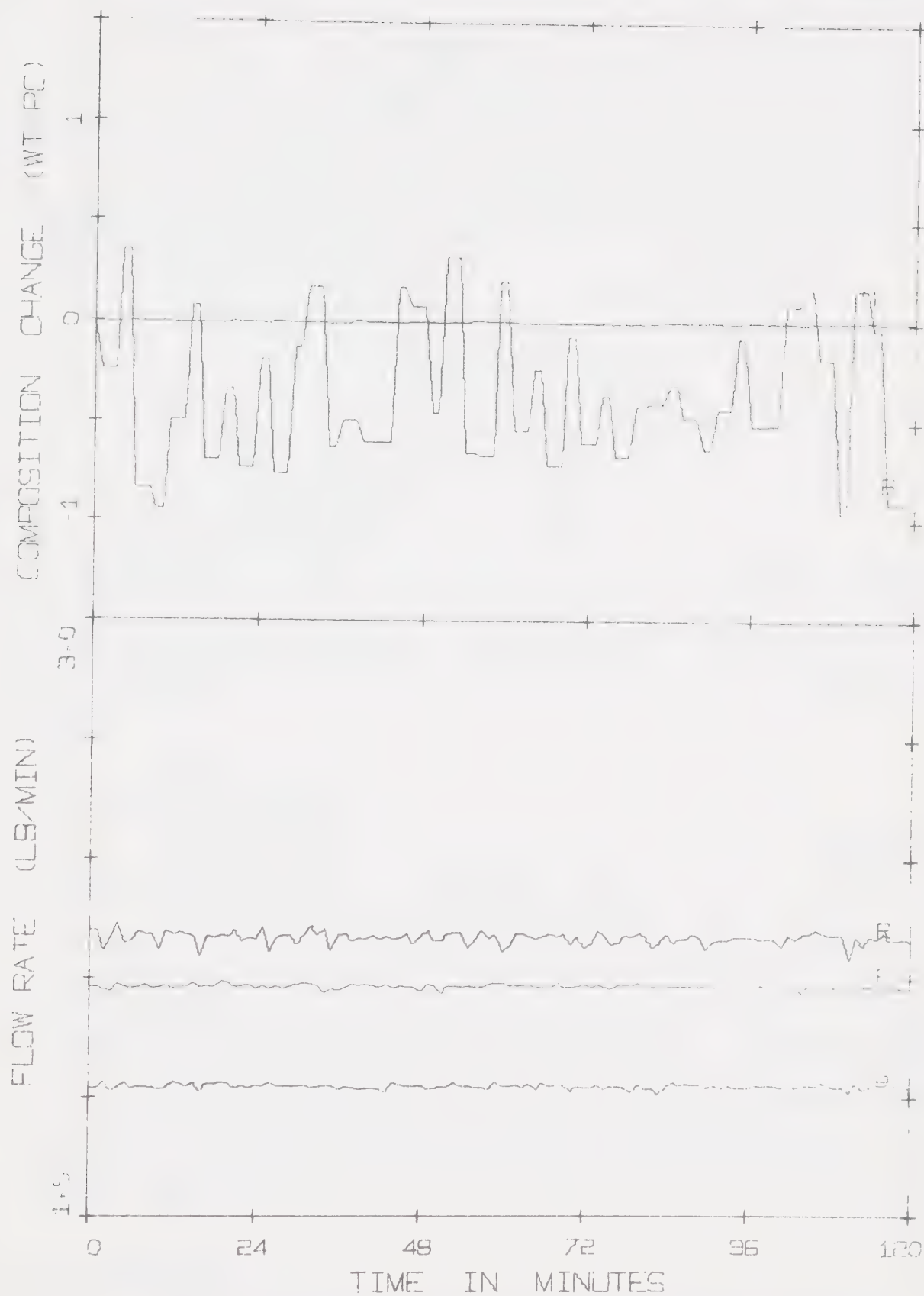


FIGURE C-6.1: EXPERIMENTAL STEADY STATE DATA USED FOR SIMULATION NOISE ESTIMATION

APPENDIX D

COMPUTER PROGRAMS

The programs written and implemented on the IBM 1800 Data Acquisition and Control computer during the course of this study fall into five general categories:

- 1) Standard DDC operation and associated utility programs.
- 2) Steady state data analysis programs.
- 3) Test run data accumulation and control programs.
- 4) Model derivation and reduction programs.
- 5) Miscellaneous utility programs.

These programs are briefly described in the following sections, and these sections have been combined with program listings as a Users' Manual. Table D-1 presents a tabulation of the programs and data files and their uses.

D-1 DDC Utility Programs

The system DDC (Direct Digital Control) program is interfaced to the distillation column so that many variables can be displayed and the feed, steam and reflux flows controlled. Table D-2 is a tabulation of the DDC loop designations. The data accumulation loops are turned on and off by the program RGM40. The data collected is punched to cards with the titles stored in RGM01 by the program RGM41. The program RGM42 is similar to RGM40, but is used to turn the data acquisition and control loops on or off.

D-2 Steady State Programs

In this category of programs there are two sets of programs,

TABLE D-1 - DISTILLATION COLUMN PROGRAMS AND DATA FILES

MAINLINE CORELOADS

BALNC- CORELOAD TO DO MASS AND ENERGY BALANCES AND OUTPUT
DASS - QUEUED CORELOAD FOR STEADY STATE DATA COLLECTION
DATAC- CORELOAD TO GATHER STEADY STATE DATA AND WRITE IT ON
DISK FILE 'PAC01'
DCMOD,DCMD1,DCMD2- BATCH CORELOADS TO CALCULATE MODEL MATRICES
DCRED- BATCH CORELOAD TO PERFORM LEAST SQUARES REDUCTION
CHRTM- INTERRUPT CORELOAD FOR G.C. OPERATION
CRASH- SYSTEM PROGRAM FOR EMERGENCY SHUTDOWN
RGM40- TURN ON/OFF DDC DATA ACCUMULATION LOOPS
RGM41- PUNCH DATA FROM DDC DATA ACCUMULATION LOOPS TO CARDS
RGM42- TURN ON/OFF DDC DATA ACQUISITION AND CONTROL LOOPS
RGM43- TURN ON/OFF EMERGENCY SHUTDOWN ECO
RGM45- START AND STOP BOTTOMS GAS CHROMATOGRAPH
RGM46- TRANSFER DATA FROM DISK FILE 'RGM03' TO 'RGM04'
GM46A- PUNCH DATA FROM 'RGM04' TO CARDS
RGM4A- READ LABELS FOR GM46A INTO 'RGM01'
RGM47- TURN ON BOTTOMS G.C. FOR ONE ANALYSIS CYCLE
RGM50- INTERRUPT CORELOAD FOR CONTROL AND DATA ACCUMULATION
RGM51- BATCH CORELOAD TO READ CONTROL MATRICES INTO 'RGM03'

CONT'D

TABLE D-1 - CONT'D

RGM52- QUEUED CORELOAD TO START AND STOP 'RGM50' TIMER

RGM53- PROGRAM TO PLOT DATA AS PUNCHED OUT BY 'GM46A'

SSDAT- BATCH CORELOAD TO DO STEADY STATE ANALYSIS

DATA FILES

PAC01- DATA FILE FOR 'DASS', 'DATA0', 'BALNC' (15 SECTORS)

RGM01- LABELS FOR DATA STORED IN 'RGM04' AND PUNCHED OUT
BY 'GM46A'

RGM03- DATA FILE FOR 'RGM50', 'RGM52' (17 SECTORS)

RGM04- DATA FILE FOR 'RGM46', 'GM46A' (16 SECTORS)

TABLE D-2 DISTILLATION COLUMN DDC LOOPS

DATA ACQUISITION AND CONTROL LOOPS

0601 - FEED FLOW
0602 - REFLUX FLOW
0603 - STEAM FLOW
0604 - OVERHEAD COMPOSITION
0605 - TOP PRODUCT FLOW
0606 - BOTTOM PRODUCT FLOW
0607 - BOTTOM PRODUCT COMPOSITION
0610 - REBOILER TEMPERATURE
0611 - TRAY 1 TEMPERATURE
0612 - TRAY 2 TEMPERATURE
0613 - TRAY 3 TEMPERATURE
0614 - TRAY 4 TEMPERATURE
0615 - TRAY 5 TEMPERATURE
0616 - TRAY 6 TEMPERATURE
0617 - TRAY 7 TEMPERATURE
0618 - TRAY 8 TEMPERATURE
0619 - CONDENSER TEMPERATURE
0620 - REFLUX TEMPERATURE
0621 - FEED TEMPERATURE
0622 - COOLING WATER INLET TEMPERATURE
0623 - COOLING WATER OUTLET TEMPERATURE

DATA ACCUMULATION LOOPS

0201 - G.C. DATA ACQUISITION
0202 - G.C. DATA ACCUMULATION
0210 - FEED FLOW
0211 - REFLUX FLOW
0212 - STEAM FLOW
0213 - TOP PRODUCT FLOW
0214 - BOTTOM PRODUCT FLOW
0215 - TOP PRODUCT COMPOSITION
0216 - REBOILER TEMPERATURE
0217 - BOTTOM PRODUCT COMPOSITION
0218 - FEED TEMPERATURE
0219 - REFLUX TEMPERATURE
0220 - TRAY 1 TEMPERATURE
0221 - TRAY 2 TEMPERATURE
0222 - TRAY 3 TEMPERATURE
0223 - TRAY 4 TEMPERATURE
0224 - TRAY 5 TEMPERATURE
0225 - TRAY 6 TEMPERATURE
0226 - TRAY 7 TEMPERATURE
0227 - TRAY 8 TEMPERATURE
0228 - CONDENSER TEMPERATURE

one which reads the data from the column at steady state, and the other which uses the steady state data to calculate all unmeasurable variables. The first function is performed by the programs DASS, DATAC and BALNC. The first is a teletype queued coreload and is used to enter certain information and start the data gathering. Adequate description is printed on the teletype before each input request. DASS queues DATAC which gathers the required data for a predetermined length of time and writes the data to disk file PAC01. When enough data has been gathered DATAC queues BALNC which performs mass and energy balances using the data in the disk file and outputs the balances and variable averages. The programs are queued to V-Core and output in to the line printer.

The second function outlined above is performed by the batch process program SSDAT. It does an iterative mass and energy balance on each stage given the input liquid flow, the output vapour flow and the liquid composition. This allows each stage to be solved in turn from the top of the column. The subroutine REGFL uses a false position search to solve the stage equations.

D-3 Data Accumulation and Control Programs

There are many programs in this category and each will be mentioned in turn, in approximately the order in which they would be used during a test run. The hardware timer which repetitively queues the accumulation and control program, RGM50, is started and stopped by RGM52. The type of control and steady state data are also set by this program. The control matrices are read into the disk file RGM03 by the program RGM51. The model order, feedback, feedforward and integral control matrices are supplied to the program. The steady state data

and control matrices stored in RGM03 can be listed on the printer by using the program RGM54.

As mentioned previously, the accumulation and control action is carried out by the program RGM50. The possible options are:

- 1) data accumulation only
- 2) porportional feedback control
- 3) proportional feedback & feedforward control
- 4) proportional & integral feedback control
- 5) proportional & integral feedback & feedforward control.

The data is accumulated in the file RGM03. The data in this file is sorted rewritten into disk file RGM04 by the program RGM46. The data in RGM04 can then be punched onto cards by GM46A, along with a title read from RGM01 and the number of data points stored for each variable. The data can then be plotted on the digital plotter for visual inspection by using the program RGM53.

D-4 Model Derivation and Reduction Programs

The terms in the coefficient matrices of the model as presented in Chapter III of this work consist of steady state operating data. These matrices were calculated from the steady state data by the programs DCMOD, DCMD1, and DCMD2. The input required is outlined in the program comment statements, and the discrete form of the model equation is punched onto cards.

The twenty state model was reduced to a fourth and to a second order system. The GEMSCOPE system [54] was used to obtain the fourth order model. The second order system was obtained by using the program DCRED in which the subroutine LSRED used the least squares method of Anderson [2] to reduce the model. The input data is the original

model, the disturbance to be used and the states to be retained. The subroutine LSRED was written in general form to allow its adaption to any order model and set of disturbances.

D-5 Miscellaneous Utility Programs

There are several programs associated with the distillation column which don't fall into the above categories. The following is a brief description of these programs.

CRASH/CRAS1: The CRASH system (Computerized Remote Automatic Shutdown) is a system of software and hardware which is used to shut down pilot plant equipment in emergency situations. It is connected to the distillation column and is used as a monitor over periods of operator absence. For a complete description of the system, variable limits and required input see the CRASH/CRAS1 Dacs Centre System Documentation (R.G. McGinnis Nov. 1971).

RGM43: This program is used in conjunction with the CRASH system and is used to set the shutdown ECO on or off. After CRASH has caused a shutdown, the ECO is reset by this program, so the pumps can be restarted. The program can also be used to simulate the effect of a CRASH shutdown.

RGM45/CHRTM/RGM47: This system of programs is used to control the operation of the bottoms gas chromatograph on the distillation column. It initiates sampling, collects the data, and calculates the composition. For a listing and description of the programs and hardware and their use see the 'Gas Chromatograph Operating Manual' (Revised Nov. 1971).

B30030